MSc Thesis – Electrical Engineering

The Observable Field

On the estimation of the available power for antennas in reception

Arturo Fiorellini Bernardis 4512626

Delft University of Technology

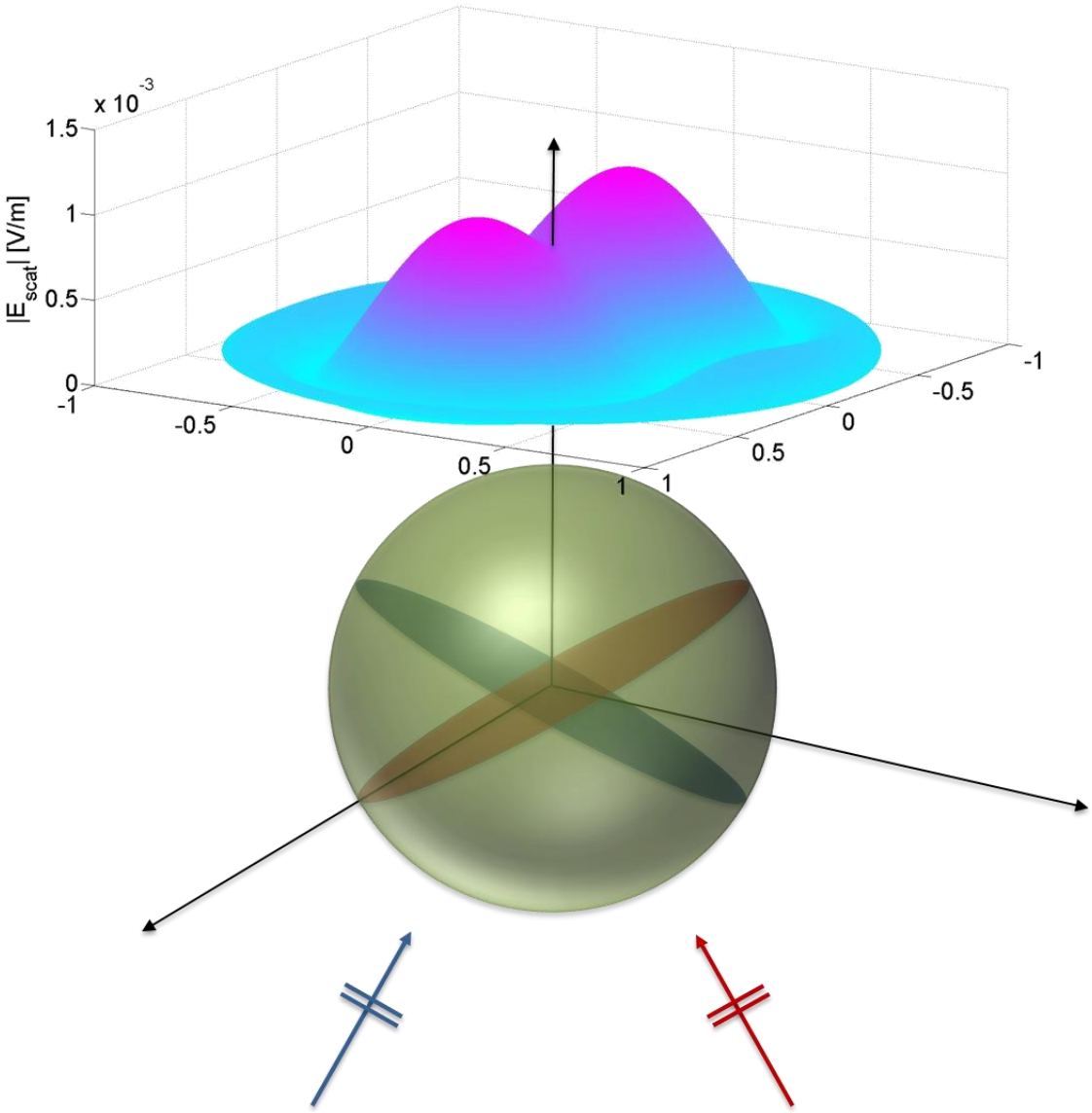

TU Delft Delft University of Technology
THz Sensing Group

Challenge the future

The Observable Field: On the estimation of the available power for antennas in reception (June 10, 2017)

AKNOWLEDGEMENT

To my family; to my dad, to my mom, and to Alvi. You were, and still are, the starting point. Needless to say, none of this would make any sense without you. Thanks for the money as well, that is also quite important, I am not going to lie. And to my grandmother, for nothing will ever stop you.

To Professor Neto, for the opportunity I have been given. Thank you, for your patient guidance and for the inestimable knowledge of yours. I would have never expected to learn this much in such a little time; I am certain this is only the beginning.

To Professor Llombart, for keeping me down to earth. Thank you, for always having the right answer. You are one of the smartest, and toughest, people I know.

To the whole THz Sensing Group, for who you are. I know how it is elsewhere, I am aware of how lucky I am to have worked next to you. You are capable of great things, and still you are always there when I am looking for help.

To my best friends, to my brothers from another mother, for reminding me that life is beautiful; although, maybe, a little bit too often. Also, thank you for all the humble pies you made me eat; you know they will never be enough.

To my girlfriend, for I always imagined it. You do not exist; yet. However, this is quite an important turn for me, and you are one of the most important persons in my life. I know you are somewhere out there.

The Observable Field

On the estimation of the available power for antennas in reception

This thesis is submitted in partial fulfillment of the requirements for the degree of

MASTER OF SCIENCE
in
ELECTRICAL ENGINEERING

by

Arturo Fiorellini Bernardis

The work presented in this thesis was performed at:
Tera-Hertz Sensing Group
Department of Microelectronics
Faculty of Electrical Engineering, Mathematics and Computer Science
Delft University of Technology

DELFT UNIVERSITY OF TECHNOLOGY

DEPARTMENT OF ELECTRICAL ENGINEERING

The undersigned hereby certify that they have read and recommend to the Faculty of Electrical Engineering, Mathematics and Computer Science for acceptance a thesis entitled "**The Observable Field: On the estimation of the available power for antennas in reception**" by **Arturo Fiorellini Bernardis** in partial fulfillment of the requirements for the degree of Master of Science.

Dated: June 21st, 2017

Chairman:

_____

prof.dr. Andrea Neto

Committee Members:

_____

dr. Nuria Llombart Juan

_____

dr.ir. Rob Remis

Table of Contents

I) INTRODUCTION

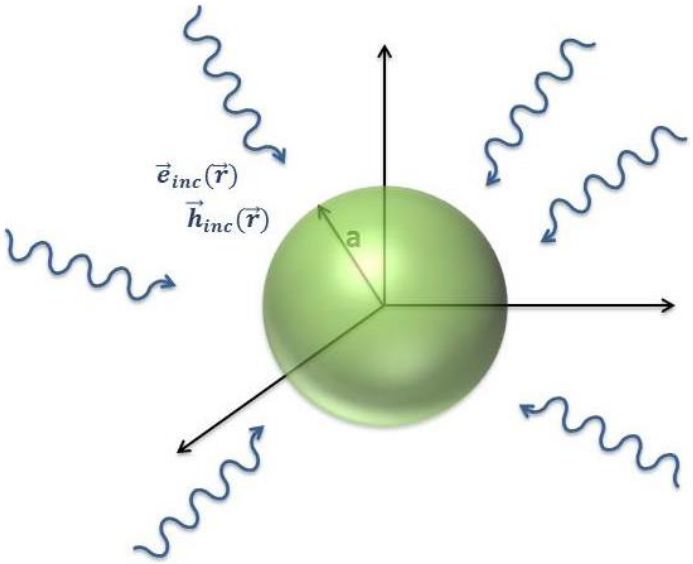

Fig 1. 1) Incident field impinging on an antenna (sphere of radius $\boldsymbol{a}$)

How antennas absorb a generic incident electro-magnetic field impinging on it is a mechanism that is still not perfectly known. Thanks to reciprocity, the means we analyze antennas in reception by is a set of techniques developed for antennas in transmission. In spite of this fact, some aspects, like scattering and absorption, are being investigated in order to define procedures to facilitate optimal designs through numerical software, e.g. how to define currents or boundaries. However, other aspects, which seem to be significantly important, still lack of a proper understanding; one of these is the power available to an antenna given whichever field impinging on it.

One of the most clarifying works on this topic is from 2009 by Kwon and Pozar [9]. To address the power available to an antenna enclosed in a generic volume they expand the incident field as an infinite summation of spherical TE and TM vector modes. Thanks to this field representation they express the incident field and the perturbation introduced by the antenna in terms of spherical waves. They then split the incident field in 2 different terms: one that is significantly different from zero in the antenna domain (the low order 'LO' modes field), and a remaining part (the high order 'HO' modes field), which is instead negligible in

the surroundings of the antenna (please, note that the fact that the LO field is the portion of the incident field which is different from zero in the antenna domain does not mean the it is not present in the far field region). The LO field is the maximum portion of the incident field the antenna can interact with and absorb, it defines the available power, and it is evaluated as the sum of a finite number of modes; this number will depend on the dimension of the antenna volume in terms of wavelength. The available power is estimated considering an ideal lossless, load-matched antenna.

Implicitly in this spherical mode representation is the definition of an 'observable' component of the incident field, which is the largest portion that can be absorbed by the antenna. Based on this assumption the purpose of this work is designated, and it is the exploitation of the opportunity to identify in the total incident field the maximum part the antenna can interact with; the remaining fraction of the field is what cannot be absorbed. The characterization of the Observable field will depend on the field representation adopted, *e.g.* it corresponds to the low order field if a spherical modes expansion is applied.

$$\vec{e}_{inc}(\vec{r}) = \vec{e}_{obs}(\vec{r}) + \vec{e}_{rem}(\vec{r}) \tag{1.1}$$

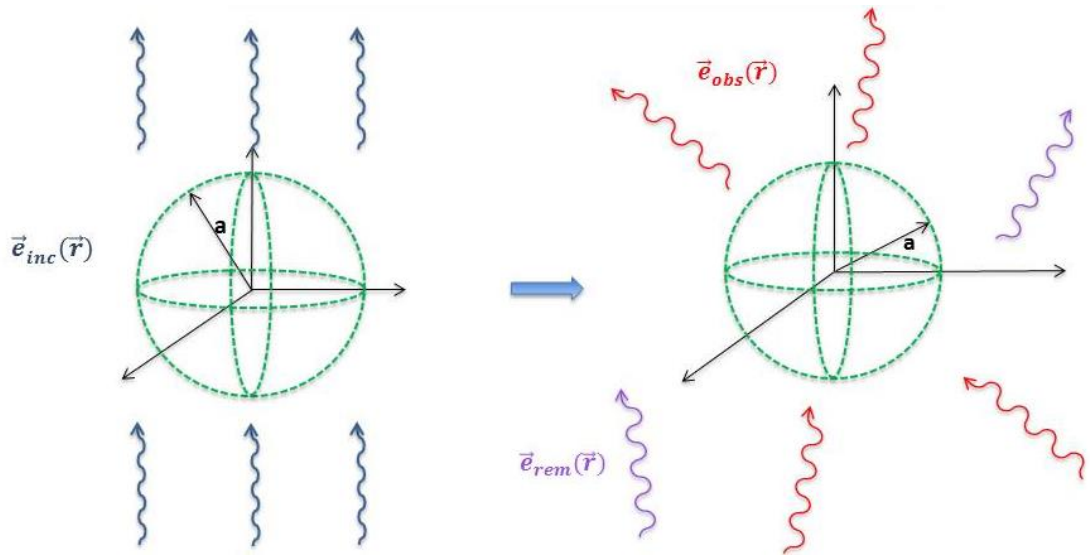

Fig 1. 2) Representation of the observable field and of the antenna domain (the antenna is not present now)

In order to estimate the available power given by the observable component of the incident field it is necessary, as it will be clear in the following, to express the observable field as the sum of an inward propagating component, that converges from large distance r_∞ towards the

antenna domain, plus an outward propagating component, that diverges from the antenna domain to r_∞.

$$\vec{e}_{obs}(\vec{r}) = \vec{e}_{obs}^{inw}(\vec{r}) + \vec{e}_{obs}^{outw}(\vec{r}) \tag{1.2}$$

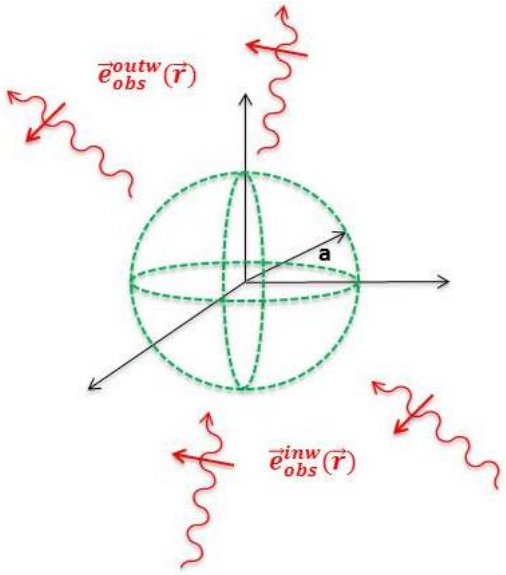

Fig 1. 3) Observable field component as the sum of an inward plus an outward propagating wave

In the far field region r_∞ we express the two inward and outward propagating components as the product between an angular distribution and a spherical spreading.

$$\vec{e}_{obs}^{\frac{inw}{outw}}(\vec{r}_\infty) = \vec{V}_{obs}^{\frac{inw}{outw}}(\theta,\phi)\frac{e^{\pm jkr_\infty}}{r_\infty}; \quad |\vec{r}_\infty| > \frac{2(2a)^2}{\lambda} \quad Vel \quad |\vec{r}_\infty| \gg a \tag{1.3}$$

The usage of the letter $\vec{V}$ for the angular distribution points out the fact that it is a Voltage quantity. If no perturbation is present, as in this case where the antenna is not there yet, the inward propagating wave is equal to the outward propagating one: the field converges to the antenna region and, if nothing is there, it diverges from it. The relationship between the two depends on the reference system, the kind of coordinates that are adopted and the polarization of the field. Using a spherical coordinates system centered in the antenna domain, and having the electric field represented as TE and TM spherical vector modes oriented along the unit vectors $\hat{\theta},\hat{\phi} = f(\theta,\phi)$, it is possible to define the outward components as:

$$\vec{V}^{outw}_{obs-TM}(\theta,\phi) = V^{outw}_{obs-TM}(\theta,\phi)\hat{\theta} \tag{1.4}$$

$$\vec{V}^{outw}_{obs-TE}(\theta,\phi) = V^{outw}_{obs-TE}(\theta,\phi)\hat{\phi} \tag{1.5}$$

And their relation with the inward propagating components as:

$$V^{outw}_{obs-TM}(\theta,\phi)\hat{\theta} = V^{inw}_{obs-TM}(\pi-\theta,\pi+\phi)\hat{\theta} \tag{1.6}$$

$$V^{outw}_{obs-TE}(\theta,\phi)\hat{\phi} = -V^{inw}_{obs-TE}(\pi-\theta,\pi+\phi)\hat{\phi} \tag{1.7}$$

This highlights the fact that the polarization is unperturbed if the antenna is absent.

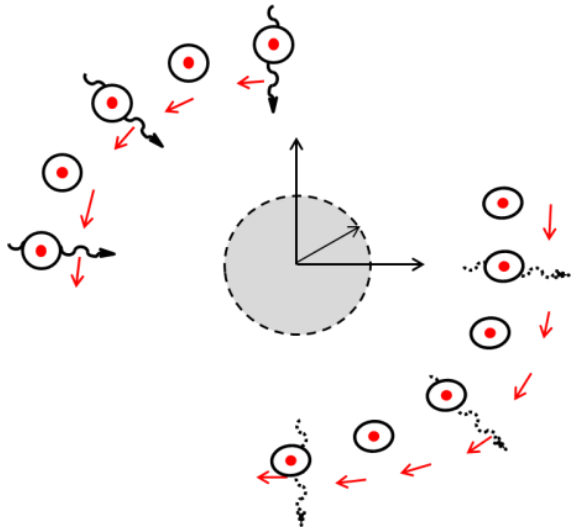

Fig 1. 4) *vector nature of the Observable field, ($\hat{\boldsymbol{\theta}}$ polarized example). The observable field converges toward the origin, and then emerges to diverge, maintaining the unaltered ray like vector orientation.*

The magnetic field derivation is straight forward. At large distance from the center of the reference system the spherical waves can be locally approximated as plane waves, and the following, well-known rule applies:

$$\vec{h}_{obs}(\vec{r}_\infty) = \frac{1}{\zeta}\hat{k} \times \vec{e}_{obs}(\vec{r}_\infty) \tag{1.8}$$

II) STATE OF THE ART: THE SPHERICAL MODES REPRESENTATION OF THE INCIDENT FIELD

II.a) The spherical modes procedure

The incident field, at any observation point, can be expanded as an infinite summation of spherical vector modes:

$$\vec{e}_{inc}(\vec{r}) = \sum_{n=0}^{\infty} \vec{E}_n\,(r, \theta, \phi) \tag{2.1}$$

The spherical modes functions are defined with respect to the center of the reference system and depend on the antenna electrical dimensions. Each spherical modes function can be expressed either as a TE or TM mode and split into an inward and an outward propagating component. Inward and outward propagating components are related as in (1.4), (1.5), (1.6), (1.7). The number of modes used to represent the field depends on the observation point $\vec{r}$ and on the source location $\vec{r}'$. If the observation point is close to the origin of the reference system, and if the sources are located at large distance from it, only a few harmonics are necessary. However, the further from the origin the observation point is, the more modes will be needed. This becomes clear when looking at the radial dependence of the scalar free space Green's function $g(\vec{r}, \vec{r}')$, when expressed as a summation of spherical functions:

$$g(\vec{r}, \vec{r}') = \frac{e^{-jk|\vec{r}-\vec{r}'|}}{4\pi|\vec{r}-\vec{r}'|} = \sum_{m=0}^{\infty}\sum_{n=0}^{\infty} C_{mn} L_{mn}(\theta, \theta', \phi, \phi')\, d_n(\vec{r}, \vec{r}') \tag{2.2}$$

C_{mn} are functions that depends only on the indices (m, n), L_{mn} are the Legendre's polynomials which depend on the angular coordinates, and d_n takes into account the radial dependence. Assuming that the sources are located at large distance from the origin we can express d_n as a function of the spherical Bessel's j_n and Hankel's h_n^2 functions of integer order:

$$d_n(\vec{r},\vec{r}') = \frac{j_n(kr)h_n^2(kr')}{krr'} \tag{2.3}$$

Moreover, if the observation point is close to the source, the expression turns into:

$$\lim_{r\to 0} d_n(r,r') = \begin{cases} \frac{h_0^2(kr')}{r'} & for\ \ n=0 \\ 0 & \forall\ \ n>0 \end{cases} \tag{2.4}$$

Finally, if the condition $|\vec{r}'| \gg |\vec{r}|$ is verified, thus if the source location is much further away than the observation point, the number of modes is independent from the source location itself $\vec{r}'$.

II.b) *The low order field*

The final aim of this procedure is to define the available power. Thus, we need to derive the portion of the incident field the antenna can interact with: the observable field, once again. If the adopted field representation is the spherical modes expansion, the observable field will coincide with the low order modes field. Let us stress again the fact that the observable component of the incident field is the only portion which is significantly different than zero in the antenna region.

$$\vec{e}_{LO}(\vec{r}) = \sum_{n=0}^{N} \vec{E}_n(r,\theta,\phi), \qquad \vec{e}_{HO}(\vec{r}) = \sum_{n=N+1}^{\infty} \vec{E}_n(r,\theta,\phi) \tag{2.5}$$

$$N = ka = 2\pi\frac{a}{\lambda} \tag{2.6}$$

N is such that $\vec{e}_{HO}(\vec{r}) \to 0$ in the antenna domain, which from now on will be considered a sphere of radius a. This means:

$$\vec{e}_{inc}(r \in V_{ant}) \simeq \vec{e}_{LO}(\vec{r}) \qquad V_{ant}: |\vec{r}| \le a \tag{2.7}$$

Now, in the case of a plane wave incident from broadside, the incident field is written as:

$$\vec{e}_{inc}(\vec{r}) = \vec{E}_{inc}(r,\theta,\phi)e^{jkz}, \quad \vec{h}_{inc}(\vec{r}) = \vec{H}_{inc}(r,\theta,\phi)e^{jkz} \quad \forall\, \vec{r} \tag{2.8}$$

The low order field depends on N, which means that it depends on the antenna length in terms of wavelength. Here are the plots of the LO field at $z \to 0$ scanned on the E-plane for a plane wave incident from broadside with $\vec{E}_{inc}(r,\theta,\phi) = 1\,\hat{\theta}\ [V/m]$ for three significant cases: $a = 0.01\lambda,\ \ a = \lambda,\ \ a = 10\lambda$

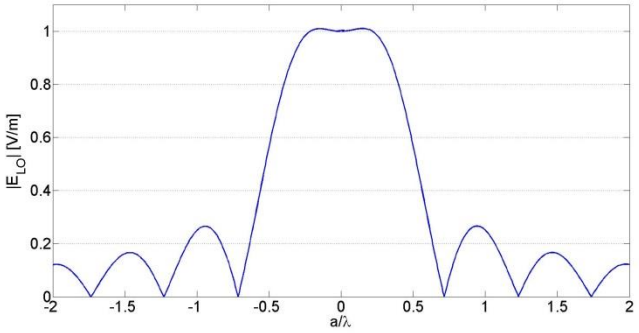

a $- a = 0.01\lambda$

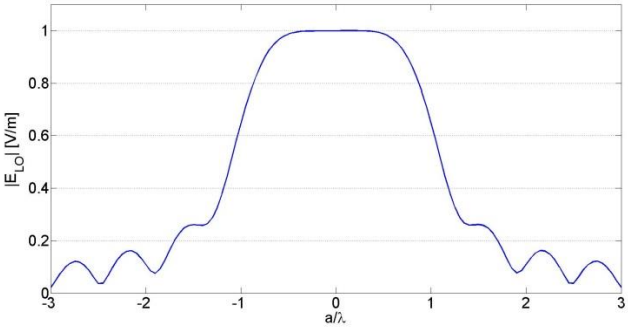

b $- a = \lambda$

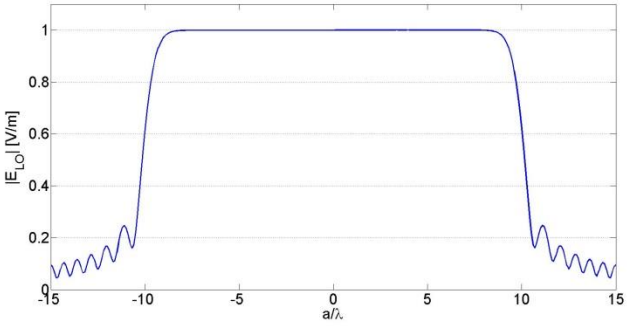

c $- a = 10\lambda$

Fig 2. 1) Electric field scanned in the E-plane, for $\boldsymbol{z = 0}$, for three cases: Fig 2.1a) $\boldsymbol{a = 0.01\lambda}$, Fig 2.1b) $\boldsymbol{a = \lambda}$, Fig 2.1c) $\boldsymbol{a = 5\lambda}$

It is apparent that the spherical modes representation introduces a spatial filtering action that selects only the central portion of the incident field around the antenna domain. Please, note

that considering the first antenna its domain is small in terms of wavelengths: it only comprises the region $a/\lambda = [-0.01 \rightarrow 0.01]$, and the field amplitude remains close to the incident field value much further away; this phenomenon can also be seen through the effective area concept. Instead, as far as relatively large antennas are concerned the spherical modes expansion constitutes a good approximation of the incident field itself on the antenna domain, then it starts decaying.

II.c) *The fields far away from the antenna*

As already stated, the fact that the LO field is the only part of the incident field which is significantly different than zero in the antenna region does not mean that it is zero in the far field region as well. The LO field is defined over the entire space indeed. For observation points far away from the center of the reference system the radial dependence of the modes tends to the spherical spreading $e^{\pm jkr_\infty}/r_\infty$, and the electric and magnetic fields tend to be orthogonal and transversely polarized. This allows the summation in amplitude and phase of every mode, leading to the construction of a single outward (or inward) propagating spherical wave. It is immediate to verify that at $\vec{r}_\infty$ we can express the LO field as in (1.3), thus an inward/outward component defined as the product between an angular distribution and a spherical spreading function. In general, the remaining field, which is in this representation the HO field, is not zero at $\vec{r}_\infty$, given the fact that the LO field does not represent the whole incident field:

$$\vec{e}_{LO}(\vec{r}_\infty) \neq \vec{e}_{inc}(\vec{r}_\infty) \quad \rightarrow \quad \vec{e}_{HO}(\vec{r}_\infty) \neq 0 \tag{2.9}$$

In order to clarify this concept, the far field pattern of the LO field, normalized to its maximum value and expressed in dB, is plotted for the same antennas that were analyzed previously. 3 antennas of radius $a = 0.01\lambda$, $a = \lambda$, $a = 10\lambda$, far field at $\vec{r}_\infty > 2(2a)^2/\lambda$, scanned for $\theta = (-\pi \rightarrow \pi)$, $\phi = 0$ (E-plane):

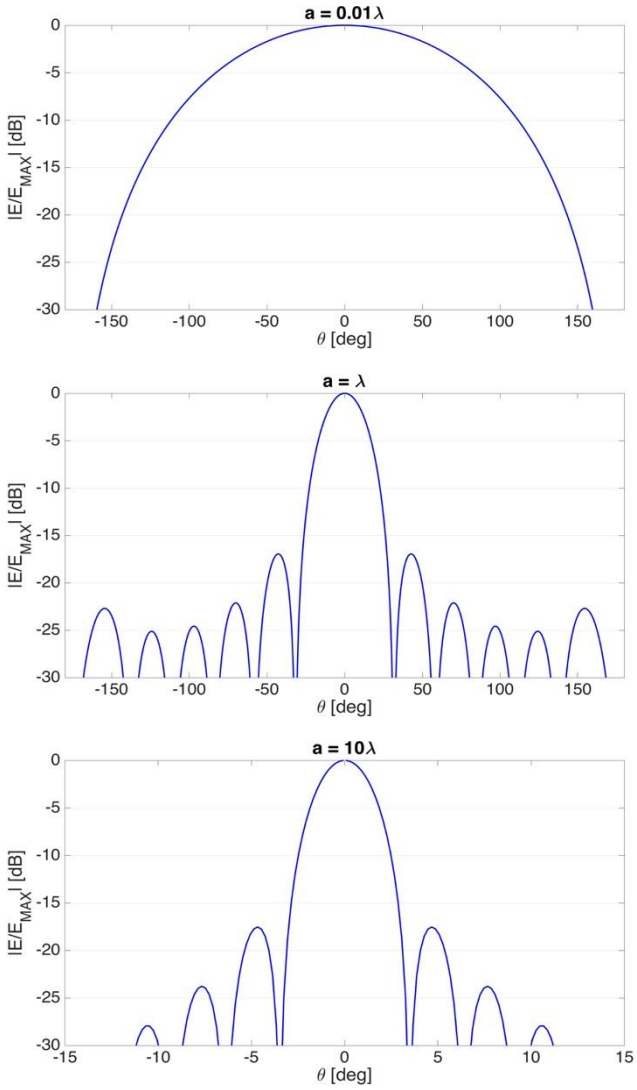

Fig 2. 2) *Observable fields patterns, for three different dimensions of the antenna domain for normal incidence plane waves*: Fig 2.2a) $\boldsymbol{a = 0.01\lambda}$, Fig 2.2b) $\boldsymbol{a = \lambda}$, Fig 2.2c) $\boldsymbol{a = 5\lambda}$

II.d) The available power estimated by the spherical modes procedure

The easiest way to calculate the available power is to consider the Poynting vector in the far field region, where the field can be locally approximated as a superposition of plane waves; this means that the flux that crosses a generic surface in the far field S_∞ needs to be evaluated (if $|\vec{r}_\infty| > 2(2a)^2/\lambda$) the available power is independent on the radius of the sphere it will be evaluated at). It is well known that the total flux of a field crossing a closed surface in absence of any perturbation is zero: this is because the inward propagating component, that contributes to a positive flux, leaves then the surface as an outward propagating component, contributing

in an equal but opposite way. [9] clarified that due to this reason only the inward propagating component has to be taken into account when calculating the available power:

$$P_{ava} \equiv P_{inw} = \frac{1}{2\zeta} \iint_{S_\infty} \left| \vec{e}_{LO}^{inw}(\vec{r}_\infty) \right|^2 d\vec{r}_\infty \tag{2.10}$$

When analyzing the case of a single plane wave impinging from broadside, the effective area A_{eff} represents a useful parameter to quantify the available power and then compare it when different procedures are used:

$$A_{eff} = \frac{P_{ava}}{\frac{1}{2\zeta} \left| \vec{E}_{PW}(\vec{r}) \right|^2} \tag{2.11}$$

The effective area given a plane wave impinging from broad side ($\theta_{inc} = 0, \phi_{inc} = 0$) estimated with the spherical modes expansion is plotted as a function of the physical area, when both are normalized to λ^2:

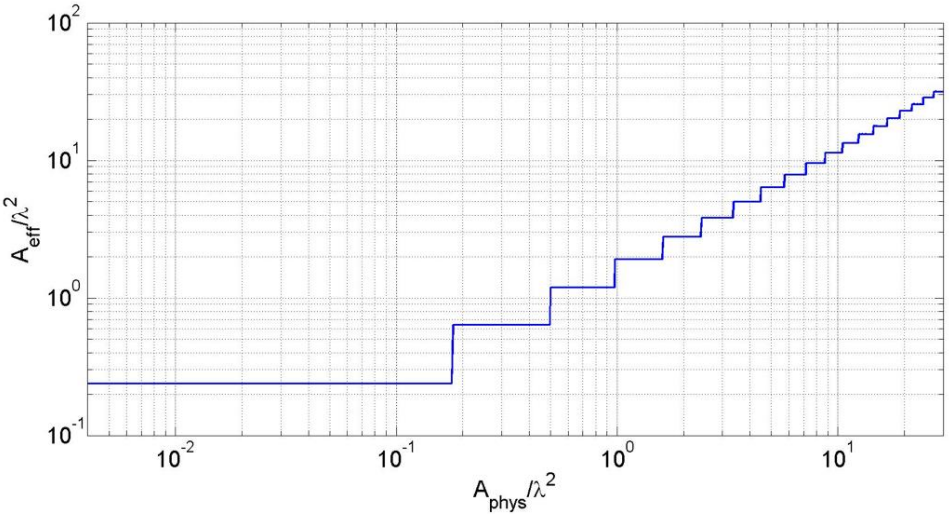

Fig 2. 3) *Effective area as a function of the physical area estimated by the spherical modes expansion, both normalized to the wavelength squared.* $\boldsymbol{N}$ *chosen as* $\boldsymbol{N = round(ka)}$

This kind of stepped function highlights the uncertainty error introduced by the spherical modes description: they quantize a process that is continuous instead. The approximation error becomes negligible for extremely small or extremely large antennas in terms of wavelength, where the steps are either not present or negligible; while for antennas whose dimension is in the range between some fraction to some units of λ the uncertainty is

significant. This quantized behavior depends on the choice of $N = ka$, which is, in general, not an integer number; moreover, there is no rule that defines how one should choose N (the observable fields estimated by $N = round(ka)$, $N = round(ka) + 1$ or $N = round(ka) - 1$ present significant differences when working with antenna of dimensions around λ).

II.e) *The heuristic extension*

The antenna community tried to overcome this issue by means of an interpolation of the results predicted by the spherical modes procedure. A simple formula that accounts for the effective area for really large and really small antennas in terms of wavelength has been proposed. It is well known that for really directive antennas the effective area tends to equate the physical area, while for extremely small antennas the spherical modes procedure predicts the effective area of a Huygens' source: the heuristic formula simply interpolates these two results [12].

$$A_{eff}^{heu} = \frac{3}{4\pi}\lambda^2 + A_{phys} \tag{2.12}$$

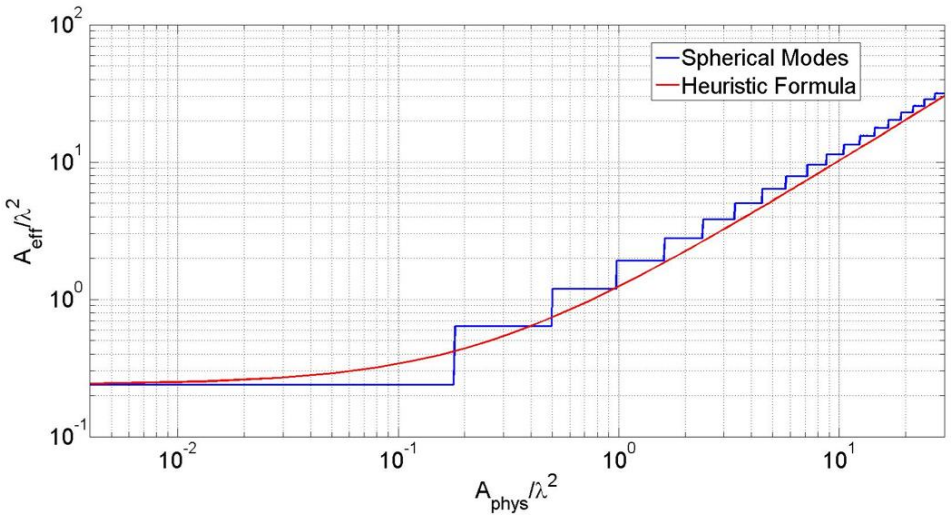

Fig 2. 4) *Effective area as a function of the physical area estimated by the spherical modes expansion and by the heuristic formula, both normalized to the wavelength squared.* $\boldsymbol{N}$ *chosen as* $\boldsymbol{N = round(ka)}$

However, even if the curve predicted by the heuristic formula seems to have solved the quantization problem, there is *de facto* no reason to believe that the results it gives are more

accurate; they should be compared to actual measurements. Moreover, the extension to more realistic cases where the incident field can be described as a superposition of multiple plane waves is not possible, since their phase is not considered by this procedure at all.

III) *THE IDEAL CURRENTS METHOD*

A new procedure, meant to estimate the observable component of the incident field overcoming the stumbling block given by the quantization introduced by the spherical modes expansion, is here presented. The field is hereby split into two components once again: an observable component, and a remaining component $\vec{e}_{inc}(\vec{r}) = \vec{e}_{obs}(\vec{r}) + \vec{e}_{rem}(\vec{r})$. Now, a new methodology is needed to evaluate $\vec{e}_{obs}(\vec{r})$ given whatever $\vec{e}_{inc}(\vec{r})$. In order to have a quick and immediate insight into this procedure let us first consider the case of a single plane wave impinging on a focusing system

III.a) The ideal antenna in a focusing system

When a plane wave excites a focusing system, within the system itself the field $\vec{e}_i(\vec{r})$ can be represented as a spherical wave that converges to its focus, and then diverges; the center of the reference system will be placed at the focus. Once again then, the field is represented as the sum of an inward and an outward propagating spherical waves (keep in mind that this is the field inside the focusing system, not the incoming plane wave):

$$\vec{e}_i(\vec{r}) = \vec{e}_i^{inw}(\vec{r}) + \vec{e}_i^{outw}(\vec{r}) \tag{3.1}$$

The ideal lossless, load matched antenna is a device that absorbs the whole inward propagating component, cancelling the outward propagating one (an intuitive parallelism can be made with the concept of a perfect absorber, even if the mechanism is different); the ideal antenna will convert the EM energy in a guided wave. The cancellation of $\vec{e}_i^{outw}(\vec{r})$ happens via scattering: the incident field will excite a set of currents on the antenna, that radiate a field which will be equal and opposite to the first.

$$\vec{e}_{tot}^{outw}(\vec{r}) = \vec{e}_i^{outw}(\vec{r}) + \vec{e}_{scat}^{id}(\vec{r}) = 0 \tag{3.2}$$

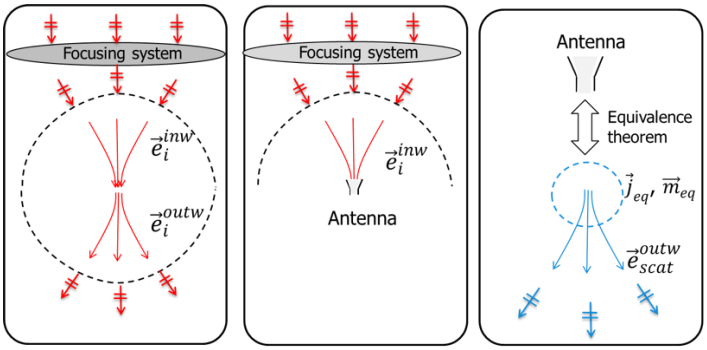

Fig 3. 1) *Field picture in an ideal focusing system,* Fig 3.1 b) *Incident field as sum of inward and outward propagating waves.* Fig 3.1b) *the ideal antenna captures all the inward incident field.* Fig 3.1 c) *The scattered field radiated by the currents of the ideal antenna is equal and opposite to the outward component of the incident field.*

Please note that the '*outw*' superscript is omitted in $\vec{e}_{scat}^{id}(\vec{r})$, since the field scattered by an antenna is always propagating outward its domain. Now, note that within a focusing system excited by a plane wave, the incident field can coincide with the observable field. Indeed, in this particular case the field is no more a plane wave, and it is possible to define a set of sources that can radiate it.

$$\vec{e}_i(\vec{r}) = \vec{e}_{obs}(\vec{r}) \quad \rightarrow \quad \vec{e}_{rem}(\vec{r}) = 0 \tag{3.3}$$

The available then will be:

$$P_{ava} = P_{rx}^{id} = P_i^{inw} \tag{3.4}$$

$$P_i^{inw} = P_i^{outw} = P_{scat}^{id} \tag{3.5}$$

III.b) Plane wave incidence

In case of plane wave incidence $\vec{e}_{inc}(\vec{r}) = \vec{E}_{inc}^{PW}(\vec{r})e^{j\vec{k}_{in}\cdot\vec{r}}$, the first thing to be taken into account is that it does not exist a set of sources able to radiate such a field. This is because the spatial domain of a plane wave is infinite, and so should be the distribution of the currents. Thus, the ideal antenna will never be able to absorb the whole $\vec{e}_{obs}^{inw}(\vec{r})$, and the definition of the observable component of the incident field is not straightforward.

$$\vec{e}_{inc}(\vec{r}) \neq \vec{e}_{obs}(\vec{r}) \quad \rightarrow \quad \vec{e}_{rem}(\vec{r}) \neq 0 \tag{3.6}$$

The observable field will be now specified as the largest portion of the incident field the antenna can interact with. The proposal is to define the observable field as equal and opposite to the field scattered by the ideal antenna given a plan wave impinging on it, so that they cancel out leading to $\vec{e}_{tot}^{outw}(\vec{r}) = 0$.

$$\vec{e}_{obs}^{outw}(\vec{r}) \equiv -\vec{e}_{scat}^{ideal}(\vec{r}) \tag{3.7}$$

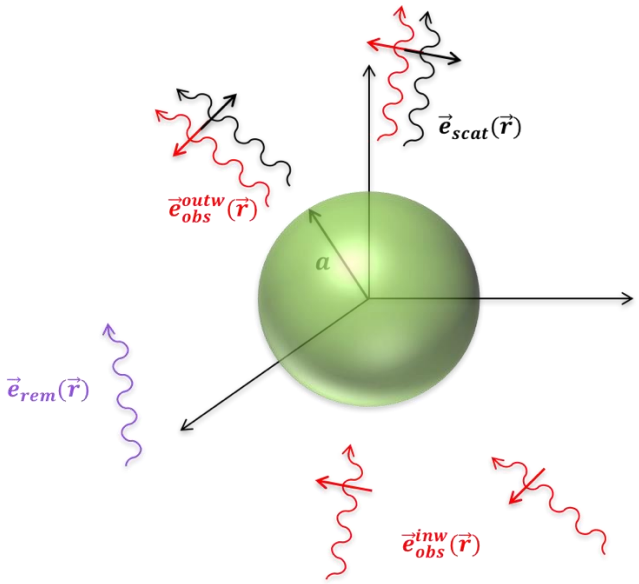

Fig 3. 2) *Observable field as the field equal and opposite to the one scattered by an ideal antenna given a generic incident field.*

We call the scattered field '*ideal*' to underline the fact that it radiates a power which is equal to the received one: the maximum possible power in the given antenna volume. Once again, when dealing with plane wave incidences it is possible, and useful, to define the effective area:

$$P_{rx}^{id} = \frac{1}{2\zeta}\left|\vec{E}_{inc}^{PW}(\vec{r})\right|^2 A_{eff} = P_{scat}^{id} \tag{3.8}$$

The effective area will be the parameter used to compare the procedure introduced by this work to the spherical modes representation. The point now is the definition of a set of sources that scatter $\vec{e}_{scat}^{ideal}(\vec{r})$: the 'Ideal Currents'.

III.c) *The Ideal Currents*

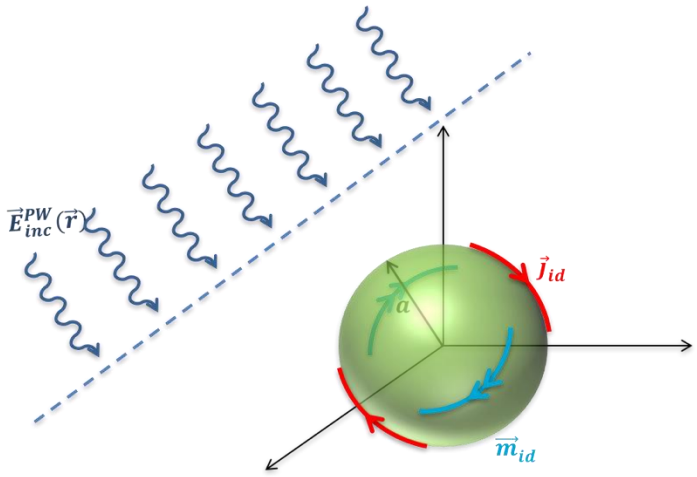

Fig 3. 3) *Ideal currents on the antenna volume induced by the incident field*

We define the 'Ideal Currents' by means of the equivalence theorem. This theorem says that, given whatever kind of field at any observation point, this can be represented by a set of sources that radiate it. In the case of a plane wave it is apparent that these currents' spatial domain must be infinitely extended in order to satisfy the condition: indeed, they are defined over the hemisphere of the antenna volume illuminated by the incident field and over an infinite plane orthogonal to the plane wave propagation direction $\hat{k}_{in}$ and crossing the antenna in the middle. The mathematical derivation of the currents is performed through the physical optics (PO) approximation, then they are amplified by a constant factor that accounts for the power budget of the system (the scattered power will thus be equal to the received power); this amplifying factor definition will be explained soon. Now, thanks again to the equivalence theorem we can represent the radiation of the currents distributed on the illuminated hemisphere of the antenna volume through another set of planar distributed sources that will generate the same field: they will be defined over the cross section of the antenna orthogonal to $\hat{k}_{in}$ (please, note that the current will be different now, but it is their radiation what matters). These are precisely the sources we're interested in.

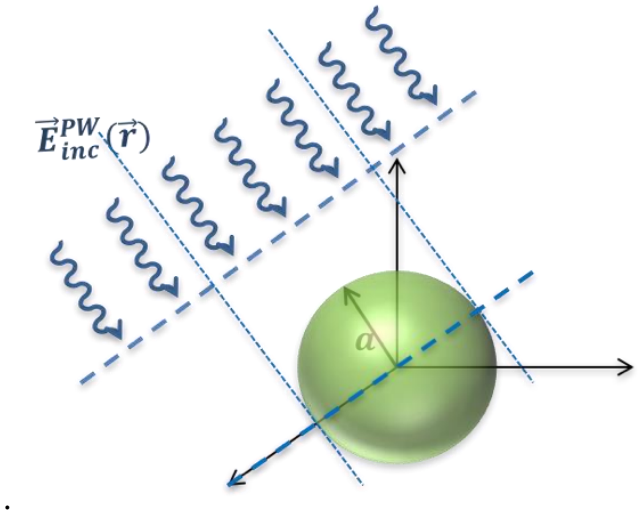

Fig 3. 4) *Definition of the domain orthogonal to* $\hat{k}_{in}$

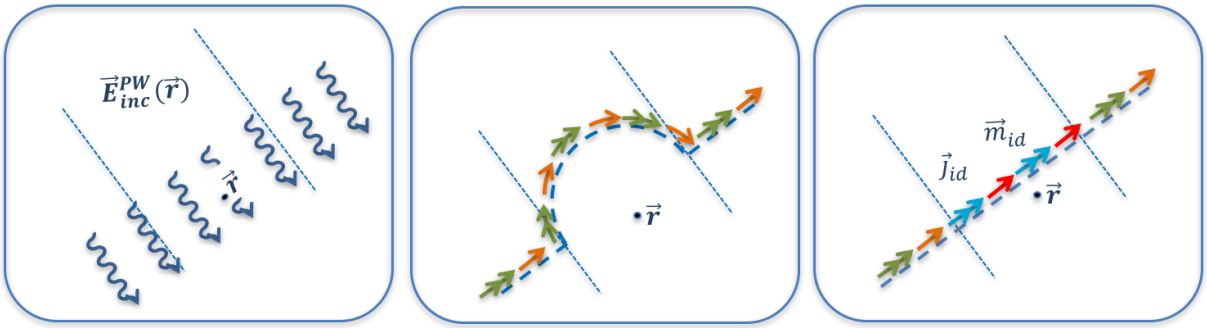

Fig 3. 5) *1D cut of the procedure of the evaluation of the ideal currents:* Fig 3.5a) *plane wave and observation point.* Fig 3.5b) *distribution of the currents over an infinitely extended planar domain including the surface of the hemisphere illuminated by the incident field.* Fig 3.5c) *substitution of the current on the hemisphere surface with the ideal currents distribute over a planar distribution (antenna cross section orthogonal to* $\hat{k}_{in}$*)*

The Ideal Currents value will depend on the antenna domain electrical length, they will be multiplied by the amplifying factor and distributed over the whole cross section. From now on, the plane wave will be considered impinging from underneath the antenna (from $\theta_{in} = 180°$), so that its scattered field and the outward component of the observable field will be defined with the maximum directivity towards the positive hemi-axis z^+. The ideal currents are thus defined as in Appendix A:

$$\vec{J}_{id}(\vec{r}') = C_{amp}\hat{z} \times \vec{h}_{inc}(\vec{r})\chi(\vec{r}', a), \quad \vec{m}_{id}(\vec{r}') = -C_{amp}\hat{z} \times \vec{e}_{inc}(\vec{r})\chi(\vec{r}', a) \tag{3.9}$$

$$\chi(\vec{r}', a) = [\rho: 0 \to a, \phi: 0 \to 2\pi] \tag{3.10}$$

$$C_{amp} = \frac{A_{eff}}{A_{phys}} \tag{3.11}$$

$\chi(\vec{r}', a)$ represents the spatial domain of the sources distribution. Note that this kind of approximation (physical optics approximation) represents a spatial truncation: the currents cannot go from a certain value to 0 instantaneously at the edge of the antenna domain. This kind of spatial truncation is somehow comparable to the modes truncation introduced by the spherical modes expansion when selecting the LO field. Due to the PO approximation, the electric and magnetic current will always be one orthogonal to the other, determining a distribution of Huygens' sources. A Huygens' source is indeed constituted by an elementary electric dipole orthogonal to a magnetic one; for the sake of clarity its far field pattern is plotted:

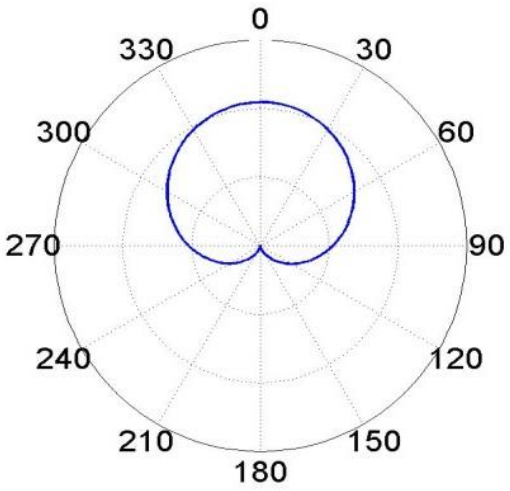

Fig 3. 6) *Far field radiation pattern of a Huygens' source*

III.d) The amplification factor

Given a uniform distribution of Huygens' sources, where in this particular case the sources are the ideal currents excited by a plane impinging orthogonally to the antenna domain (please, keep in mind that the currents are defined with the PO approximation and then amplified by a constant factor), the scattered power results (Appendix G):

$$P_{scat}^{id} = \frac{1}{2\zeta}\frac{A_{phys}^2}{A_{eff}}\left|E_{inc}^{PW}(\vec{r})\right|^2 C_{amp}^2 \tag{3.12}$$

The received power from an ideal antenna will be instead:

$$P_{rx}^{id} = \frac{1}{2\zeta} \left| E_{inc}^{PW}(\vec{r}) \right|^2 A_{eff} \tag{3.13}$$

This two powers have to be equal. Imposing this condition the value of the amplifying factor is eventually obtained:

$$P_{scat}^{id} = \frac{1}{2\zeta} \frac{A_{phys}^2}{A_{eff}} \left| E_{inc}^{PW}(\vec{r}) \right|^2 C_{amp}^2 = \frac{1}{2\zeta} \left| E_{inc}^{PW}(\vec{r}) \right|^2 A_{eff} = P_{rx}^{id} \tag{3.14}$$

$$C_{amp} = \frac{A_{eff}}{A_{phys}} \tag{3.15}$$

III.e) The far field radiation

It is well known that the radiation of the ideal currents can be calculated by the convolution integral between the free space spatial Green's function $\tilde{g}^{fc}(\vec{r})$ and the currents themselves:

$$\vec{e}_{rad}(\vec{r}) = \tilde{g}^{ej}(\vec{r},\vec{r}') * \vec{j}_{id}(\vec{r}') + \tilde{g}^{em}(\vec{r},\vec{r}') * \vec{m}_{id}(\vec{r}') \tag{3.16}$$

$$\vec{e}_{rad}(\vec{r}) = \int_0^a \int_0^{2\pi} \left[\tilde{g}^{ej}(\vec{r},\vec{r}') \vec{j}_{id}(\vec{r}') + \tilde{g}^{em}(\vec{r},\vec{r}') \vec{m}_{id}(\vec{r}') \right] d\vec{r}' \tag{3.17}$$

$$\vec{h}_{rad}(\vec{r}) = \tilde{g}^{hm}(\vec{r},\vec{r}') * \vec{m}_{id}(\vec{r}') + \tilde{g}^{hj}(\vec{r},\vec{r}') * \vec{j}_{id}(\vec{r}') \tag{3.18}$$

$$\vec{h}_{rad}(\vec{r}) = \int_0^a \int_0^{2\pi} \left[\tilde{g}^{hj}(\vec{r},\vec{r}') \vec{j}_{id}(\vec{r}') + \tilde{g}^{hm}(\vec{r},\vec{r}') \vec{m}_{id}(\vec{r}') \right] d\vec{r}' \tag{3.19}$$

However, in the far field region asymptotical considerations can be made in order to render the calculations much easier (see Appendix A for the detailed derivation). Eventually, the expression one obtains for the electric field in the far field region (remember that in the far field region the radiation can be locally considered a plane wave, thus the derivation of the magnetic field is immediate) is:

$$\vec{e}_{rad}(\vec{r}_\infty) = C_{amp}\frac{jk}{4\pi}\{Airy(ksin\theta, a)\}\left[\hat{r}_\infty \times \left(\vec{E}_0 \times (\hat{r}_\infty + \hat{z})\right)\right]\frac{e^{-jkr_\infty}}{r_\infty}$$
$$= C_{amp}V_{PO}^{outw}\left(a, \vec{r}, \vec{k}_{in}\right)\frac{e^{-jkr_\infty}}{r_\infty} \quad (3.20)$$

$$V_{PO}^{outw}\left(a, \vec{r}, \vec{k}_{in}\right) = Airy(ksin\theta, a)\vec{H}(\vec{r}_\infty, \vec{k}_{in}) \quad (3.21)$$

$Airy(ksin\theta, a)$ represents spectrum of the sources. It is an Airy distribution indeed, given by the fact that the sources are symmetrical in ϕ' over the antenna cross section S_{in}; the resulting radiation follows in the spatial domain the spectral behavior of the Airy pattern, ending up having a minimum in the direction where the plane wave is impinging from, and a maximum in the direction of propagation of the scattered field. The Airy distribution sets the directivity of the pattern as well: the higher the radius a, the higher the directivity. $\vec{H}(\vec{r}_\infty, \vec{k}_{in})$ instead, reflects the spectral behavior of a Huygens' source. $V_{PO}^{outw}\left(a, \vec{r}, \vec{k}_{in}\right)$ expresses the angular distribution of the pattern indeed.

The same result can be obtained using the spectral representation of the Green's function. Following the steps reported in Appendix C one eventually obtains:

$$\vec{f}_{rad}(\vec{r}) = \frac{1}{4\pi^2}\int_{-\infty}^{+\infty}\int_{-\infty}^{+\infty}\tilde{G}_{fs}^{fc}(k_x, k_y) \cdot \tilde{\vec{C}}_{id}(k_x, k_y)e^{-jk_x(x-x')}e^{-jk_y(y-y')}e^{-jk_z|z-z'|}dk_x dk_y \quad (3.22)$$

where $\vec{f}_{rad}(\vec{r})$ is either the electric or the magnetic field and $\tilde{\vec{C}}_{id}(k_x, k_y)$ is the spectrum of either the electric or the magnetic current; the subscript $'fs'$ means 'free space', while the superscript $'fc'$ indicates that the Green's function expresses the field $\vec{f}_{rad}(\vec{r})$ radiated by the source $\tilde{\vec{C}}_{id}(k_x, k_y)$. Also on the spectral integral asymptotical consideration can be made when analyzing the field at $\vec{r}_\infty$, which lead to the final result (detailed steps in Appendix C):

$$\vec{f}_{rad}(\vec{r}_\infty) = -jk_z\,\widetilde{GF}_{fs}^{fc}(k_0 sin\beta_s, \alpha_s)\tilde{\vec{C}}_a(k_0 sin\beta_s, \alpha_s)\frac{e^{-jkr_\infty}}{2\pi r_\infty} \quad (3.23)$$

Please, note that the latter expression is exactly equal to (3.20); only the notation is different. Now, from the asymptotical evaluation of the radiation in the far field region it is evident that

we're dealing with a spherical wave. Remember that the ideal scattered field is what it has just been calculated, and that is equal and opposite to the outward propagating component of the observable field. The assumption we made previously is then verified: we can represent at $\vec{r}_\infty$ the observable field as the sum of an inward and an outward propagating spherical wave. The 3 procedures to estimate the far field radiation have been implemented using Matlab, and their plot superposed in order to verify them; a perfect agreement is obtained:

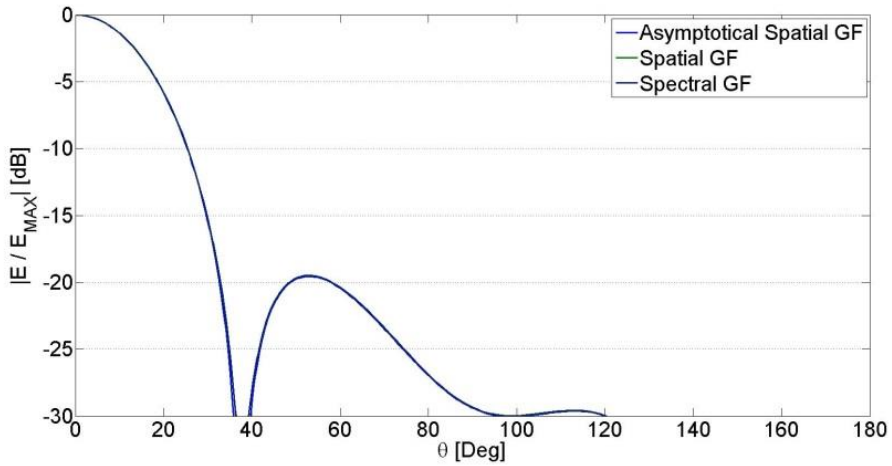

Fig 3. 7) *Comparison of the far field radiation pattern given by the three methodologies. Antenna of radius* $\boldsymbol{a = \lambda}$*. The plots were normalized to their maximum value, expressed in dB for a scan* $\boldsymbol{\theta = 0 \rightarrow \pi, \phi = 0}$.

When analyzing really large, or really small, antennas in terms of wavelength it is possible to make a few assumptions (please, refer to Appendix D) and derive an analytical formulation for the broadside radiation of the ideal currents. This was used in order to verify the validity of the Matlab script: the case of an extremely small antenna ($a = 0.01\lambda$) was considered, and a perfect agreement between the analytical prediction and the numerical evaluation of any of (3.16), (3.20), (3.22), (3.23) was found. From (3.20) we obtain:

$$\left|\vec{e}_{rad}\left(\vec{r}_\infty,\ \hat{k}_{in}\right)\right| = \mathrm{C_{amp}} \cdot \left|-\vec{V}_{PO}^{outw}\left(a,\ \vec{k}^{in}, \vec{k}\right)\frac{e^{-jkr_\infty}}{r_\infty}\right| = C_{amp} \cdot \frac{\pi a^2}{\lambda}\frac{1}{r_\infty} = 7.9482 \cdot 10^{-5}\left[\frac{V}{m}\right] \tag{3.24}$$

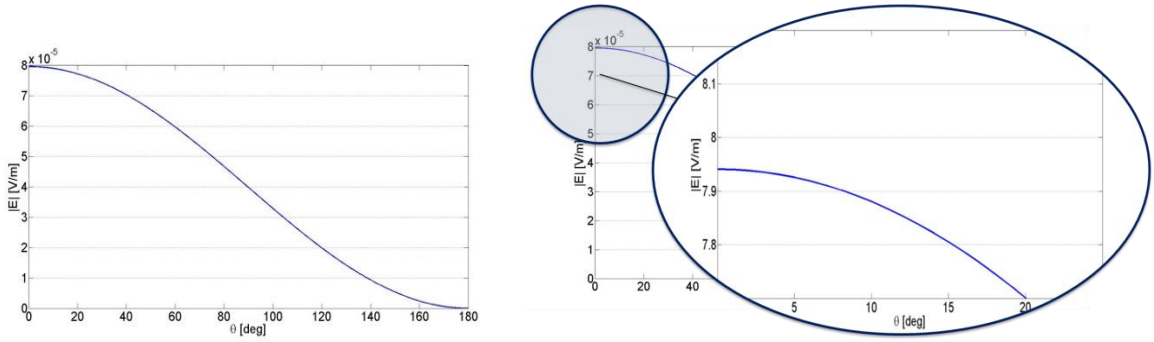

Fig 3. 8) *Broad side radiation validation for the following data:* $|\boldsymbol{E_{PW}}| = \mathbf{1}\,\boldsymbol{V\backslash m},\ \boldsymbol{a} = \mathbf{0.01}\boldsymbol{\lambda},\ \boldsymbol{r_{obs}} = \mathbf{3000}\boldsymbol{\lambda},\ \boldsymbol{\lambda} = \mathbf{1}\,\boldsymbol{m}$

It should be noted that in the case of an extremely small antenna the two sources distributions can be considered two orthogonal elementary dipoles:

$$\vec{J}_{id}(\vec{r}') = C_{amp}\hat{z} \times \vec{h}_{inc}(\vec{r})\delta(\vec{r}') \tag{3.25}$$

$$\vec{m}_{id}(\vec{r}') = -C_{amp}\hat{z} \times \vec{e}_{inc}(\vec{r})\delta(\vec{r}') \tag{3.26}$$

In this case we can consider the system to be exactly a Huygens' source. This is evident from the pattern of Fig.15, where the field is plotted linearly as function of the observation angle θ (instead that using a polar plot as in Fig.13).

III.f) Far field patterns comparison: Ideal Currents Vs Spherical Modes

It is fundamental to assess whether or not this work's procedure has a scientific dignity. In order to do this, the far field patterns of the field estimated by the spherical modes and radiated by the ideal currents are compared. Three antennae are analyzed ($a = 0.01\lambda,\ a = \lambda,\ a = 5\lambda$); the field is scanned on the E-plane ($\phi = 0,\ \theta = -\pi \rightarrow \pi$). The fields estimated by the two different methodologies are expressed in dB and superposed one on top of the other. When the antennae are small or large in terms of wavelength the two procedures give the same result for the value of the broadside radiation, thus for these two antennae ($a = 0.01\lambda,\ a = 5\lambda$) the patterns are normalized to their maximum value, which is, as already stated, the same; this is not the case for the medium antenna. The results given by the spherical modes are always plotted with a red line, while the ones given by the ideal currents with a blue line. We can see that for the small antenna the results are perfectly superposed, and for the large

antenna there is a really good agreement down to $-23dB$; increasing even more the radius of the antenna would lead to a better and better agreement for the far field patterns. For the medium antenna instead, the results are different, and the absolute value (without any normalization) is plotted. Note that for the most directive antenna case ($a = 5\lambda$) the scan is interrupted at $\theta = \pm 25°$, since no value of the patterns is higher than $-30dB$ after that threshold. The input data are $|E_{PW}| = 1\ V\backslash m,\ \ r_{obs} = 3000\lambda,\ \ \lambda = 1\ m$.

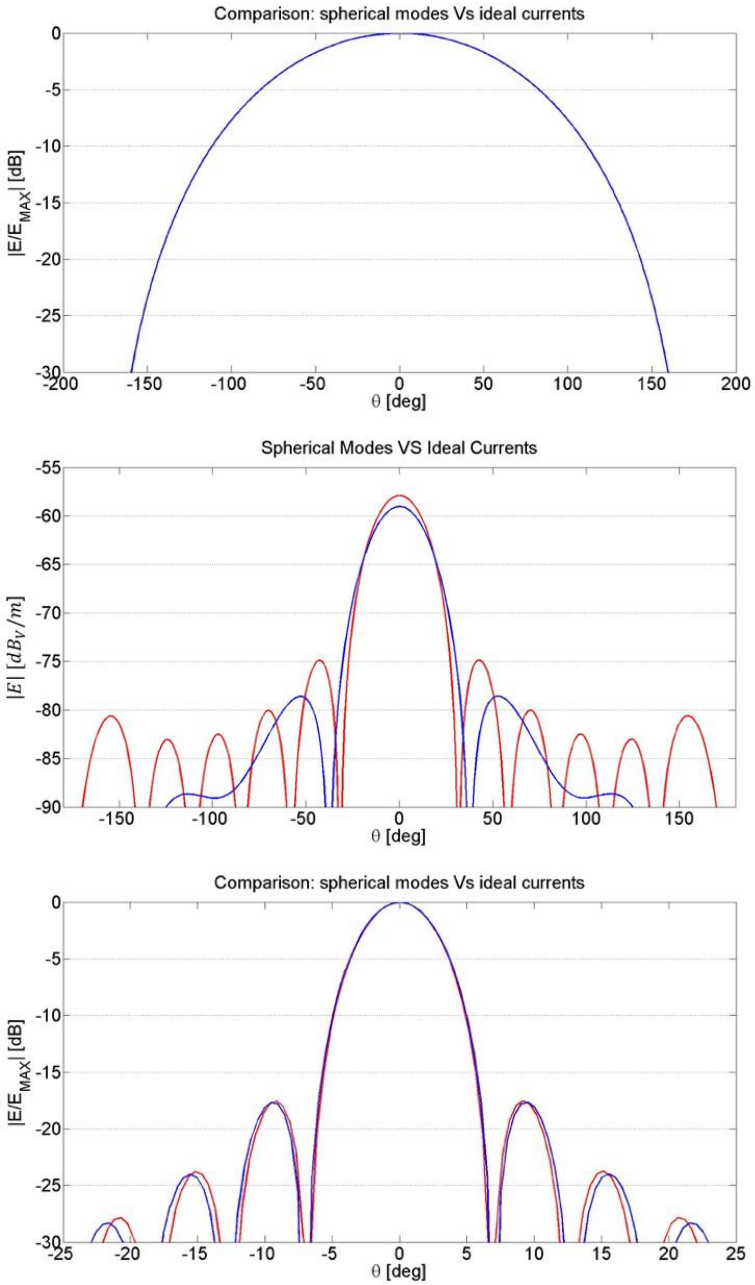

Fig 3. 9) *Far field pattern comparison: Ideal currents (blue line) Versus Spherical Modes (red line).* Fig 3.9a) *antenna of* $\boldsymbol{a = 0.01\lambda}$. Fig 3.9b) *antenna of* $\boldsymbol{a = \lambda}$. Fig 3.9c) *antenna of* $\boldsymbol{a = 5\lambda}$

III.g) *Available power and comparison between Ideal Currents and Spherical Modes*

Once again, what we are looking for is the field the ideal antenna should scatter to cancel the outward propagating component of the observable part of the incident field. Keep in mind that $\vec{e}_{obs}^{inw}(\vec{r}) = \vec{e}_{obs}^{outw}(\vec{r})$, $\vec{e}_{scat}^{id}(\vec{r}) = -\vec{e}_{obs}^{outw}(\vec{r})$. This means that the inward and the outward component of the observable field carry the same amount of power, thus the power carried by the field radiated by the ideal current, that is the power the antenna absorbs, has equal amplitude as well, which is:

$$|P_{ava}| = \left|P_{rx}^{id}\right| = \left|P_{obs}^{inw}\right| = |P_{obs}^{outw}| = |P_{scat}^{id}| \tag{3.27}$$

The available power has been calculated using the Poynting vector in the far field region. Since in this zone the field can be locally approximated as a plane wave, the flux of the Poynting vector given by the ideal scattered field is of simple expression, so that the available power calculation becomes an integration over the angular distribution of the inward or outward component of the observable field (or of the field radiated by the ideal currents, of course); the only thing that changes is the sign of P_{ava}.

$$\begin{aligned} P_{ava} &= \frac{1}{2} Re\left\{\iint_{S(\vec{r}_\infty)} \left(\vec{e}_{scat}^{id}(\vec{r}_\infty) \times \vec{h}_{scat}^{id\ *}(\vec{r}_\infty)\right) \cdot d\vec{S}(\vec{r}_\infty)\right\} \\ &= \int_0^{2\pi} \int_0^{\pi} \frac{1}{2\zeta} \left|\vec{E}_{scat}^{id}(r_\infty, \Theta, \Phi)\right|^2 r_\infty^2 sin\Theta d\Theta d\Phi \end{aligned} \tag{3.28}$$

Please, note that now the available power depends in a continuous way on the antenna dimension. Thus, the spatial truncation introduced by the Ideal Currents method does not compromise the continuous nature of the reception mechanism, which is what the Spherical Modes expansion does instead. Given the fact that the incident field is a plane wave coming from underneath ($\theta_{inc} = \pi$) and orthogonally to the plane where the ideal sources are induced, we can define an effective area, whose expression is:

$$A_{eff} = \frac{\lambda^2}{4\pi} D_{max} \tag{3.29}$$

For the derivation of A_{eff} see Appendix B. D_{max} is the directivity of the antenna in the direction of maximum radiation, which in this case is $\theta = 0, \forall\, \phi$. The effective area has been calculated and then compared to the other two estimated by the spherical modes procedure and the heuristic formula:

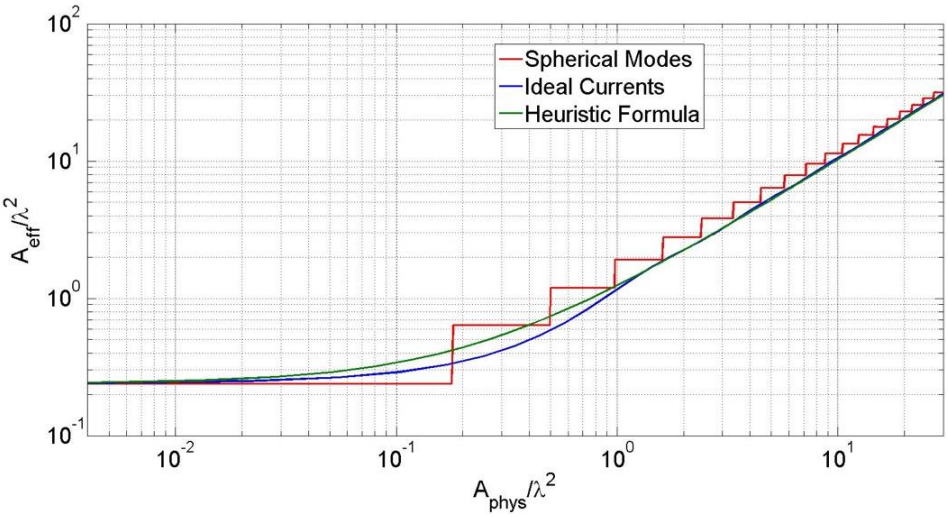

Fig 3. 10) *Effective area as a function of the physical area, normalized to* $\boldsymbol{\lambda^2}$*: comparison between the three methods.*

All the methodologies tend to give the same results for really small and really large antennae in terms of wavelength. For really small antennae they all predict an effective area which is the one given by a Huygens' source; for really large antennae the effective area becomes to the limit equal to the physical one. This is obvious for the heuristic formula though: it is constructed exactly to do so. In the region that represents most of the antennae designs we notice the biggest differences between the ideal currents and the spherical modes, especially for antennae of surface around $0.5\lambda^2$. However, the technique proposed in this work gives results that are always comparable to the ones estimated by the spherical modes expansion; also it seems to have solved the quantization problem introduced by the latter one, which is an error, of course. Finally, it is necessary to stress again the fact the curve obtained with the spherical modes is based upon the choice of $N = round(ka)$, but there is no rule that tells us how to choose it: the plot might shift to the left or to the right choosing N in a different way, and the result would have the same dignity.

IV) NEAR FIELD DERIVATION: SPECTRAL INTEGRALS

In the region close to the antenna domain the asymptotical considerations that were made in the previous chapters to derive easier expressions for the field do not apply anymore. This is because the reactive part of both the electric and the magnetic field is still present and its effect is not negligible. When moving to the far field region this component attenuates (this is why it is also called *non-visible* field, it does not reach the far field region), and it is well known that it can be neglected when evaluating the field at distances bigger than the Fraunhofer distance $d_F = 2(2a)^2/\lambda$ (or $d \gg \lambda$ if $a < \lambda$), after which only the *visible* component of the field remains. Let us take a look at the field expressed as a spectral integral as in (3.22):

$$\vec{f}_{rad}(\vec{r}) = \frac{1}{4\pi^2}\int_{-\infty}^{+\infty}\int_{-\infty}^{+\infty} \tilde{G}_{fs}^{fc}(k_x,\, k_y) \cdot \tilde{\vec{C}}_{id}(k_x,\, k_y) e^{-jk_x(x-x')} e^{-jk_y(y-y')} e^{-jk_z|z-z'|} dk_x dk_y \tag{4.1}$$

When calculating the field using the $2D$ spectral Green's function and performing the integration in a cylindrical coordinates system in the two complex variables set $(k_\rho^2 = k_x^2 + k_y^2,\ \alpha)$, where $dk_x dk_y = k_\rho dk_\rho d\alpha$, one can have a quick insight into the visible and non-visible 'behaviors' of the field imagining to perform the integration along the real axis of k_ρ and looking at its exponential dependence $e^{-jkr} = e^{-jk_\rho\rho} e^{-jk_z|z|}$:

$$kr = k_\rho\rho + k_z z; \quad k_z = -j\sqrt{-(k^2 - k_\rho^2)} \tag{4.2}$$

Selecting the expression for k_z this way allows us to set it always with a negative imaginary part, choosing the Riemann space for the solutions of the square root that will be adopted. Integrating over the real axis of k_ρ if $|k_\rho| > k$ then k_z will be imaginary. Expressing:

$$k_z = -jb; \quad e^{-jk_z|z|} = e^{-b|z|} \tag{4.3}$$

the solution decreases exponentially as a function of z, thus it decays with the distance from the reference system where the antenna is allocated at. That solution is precisely the reactive

component of the field, whose effect is considered not negligible for small $\vec{r}$. The field component that does not attenuate (visible) is thus the one obtained cropping the integration at $k_\rho = 0 \to k^-$, the non-visible component the one obtained extending the integration from $k_\rho = k^+ \to \infty$. The attenuation of the reactive component depends on the observation point: the more $\vec{r} \to 0$, and the more $\theta \to \pi/2$, which translates into $z \to 0$, the weaker is the attenuation. Thus, for observation points close to the source (near field region) and/or for $\theta \to \pi/2$, the integrand function, which is in general constituted by highly oscillating complex components, can be of extremely hard numerical evaluation. Appropriate techniques have been implemented to overcome this hurdle.

IV.a) *Spectral integral in cylindrical coordinates: closing it in α*

To derive the whole integral expression for the field in the spectral domain, let us first consider the spatial domain convolution:

$$\vec{e}_{rad}(\vec{r}) = \tilde{g}^{ej}(\vec{r},\vec{r}') * \vec{j}_{id}(\vec{r}') + \tilde{g}^{em}(\vec{r},\vec{r}') * \vec{m}_{id}(\vec{r}') \tag{4.4}$$

$$\vec{h}_{rad}(\vec{r}) = \tilde{g}^{hj}(\vec{r},\vec{r}') * \vec{j}_{id}(\vec{r}') + \tilde{g}^{hm}(\vec{r},\vec{r}') * \vec{m}_{id}(\vec{r}') \tag{4.5}$$

Let us consider for now only the electric field given by the electric current

$$\vec{e}_{rad}(\vec{r}) = \tilde{g}^{ej}(\vec{r},\vec{r}') * \vec{j}_{id}(\vec{r}') = \int_0^a \int_0^{2\pi} \tilde{g}^{ej}(\vec{r},\vec{r}')\vec{j}_{id}(\vec{r}')d\vec{r}' \tag{4.6}$$

Expressing the spatial Green's function as the Fourier anti-transform of its spectral representation:

$$\tilde{g}_{fs}^{ej}(\vec{r},\vec{r}') = \frac{1}{4\pi^2}\int_{-\infty}^{+\infty}\int_{-\infty}^{+\infty} \tilde{G}_{fs}^{ej}(k_x,k_y,z,z')e^{-jk_x(x-x')}e^{-jk_y(y-y')}e^{-jk_z|z-z'|}dk_x dk_y \tag{4.7}$$

$$\vec{e}_{rad}^{ej}(\vec{r}) = \frac{1}{4\pi^2}\int_0^a\int_0^{2\pi}\int_{-\infty}^{+\infty}\int_{-\infty}^{+\infty} \tilde{G}_{fs}^{ej}(k_x,k_y,z,z') \cdot e^{-jk_x(x-x')}e^{-jk_y(y-y')}e^{-jk_z|z-z'|}dk_x dk_y \vec{j}_{id}(\vec{r}')d\vec{r}' \tag{4.8}$$

$$\vec{J}_{id}(\vec{r}') = C_{amp}\hat{z} \times \vec{h}_{inc}(\vec{r})\chi(\vec{r}', a) \tag{4.9}$$

After a few mathematical derivations that can be found in Appendix C one obtains the following expression (from now on, since everything is evaluated in free space, $k = k_0$):

$$\vec{e}_{rad}^{ej}(\vec{r}) = -\frac{1}{8\pi^2}\frac{\zeta}{k_0}\int_0^{\infty}\int_0^{2\pi}\frac{1}{k_z}\tilde{D}_{fs}^{ej}(k_x, k_y, z, z')\tilde{\vec{J}}_{id}(k_\rho, a)e^{-jk_\rho\rho\cos(\alpha-\phi)}e^{-jk_z|z|}k_\rho dk_\rho d\alpha \tag{4.10}$$

$$\tilde{D}_{fs}^{ej}(k_x, k_y, z, z') = \begin{bmatrix} k_0^2 - k_\rho^2\cos^2\alpha & -k_\rho^2 sin\alpha cos\alpha & -k_\rho cos\alpha(\pm k_z) \\ -k_\rho^2 sin\alpha cos\alpha & k_0^2 - k_\rho^2\sin^2\alpha & -k_\rho sin\alpha(\pm k_z) \\ -k_\rho cos\alpha(\pm k_z) & -k_\rho sin\alpha(\pm k_z) & k_0^2 - k_z^2 \end{bmatrix} \tag{4.11}$$

$$\tilde{\vec{J}}_{id}(k_\rho, a) = -\frac{1}{\zeta}\vec{E}_{inc}(\vec{r})2\pi a^2\frac{J_1(a, k_\rho)}{k_\rho a} \tag{4.12}$$

Where J_1 is the Bessel's function of order 1 and so, once again, the whole $\tilde{\vec{J}}_{id}(k_\rho, a)$ expression has the spectral signature of an Airy pattern, thanks to fact that the source distribution is homogeneous over the whole circular cross section of the antenna domain. Similar operations can be made for the electric field radiated by the magnetic source, leading to the following expression:

$$\vec{e}_{rad}^{em}(\vec{r}) = -\frac{j}{8\pi^2}\int_0^{\infty}\int_0^{2\pi}\frac{1}{k_z}\tilde{D}_{fs}^{em}(k_x, k_y, z, z')\tilde{\vec{M}}_{id}(k_\rho, a)e^{-jk_\rho\rho\cos(\alpha-\phi)}e^{-jk_z|z|}k_\rho dk_\rho d\alpha \tag{4.13}$$

$$\tilde{D}_{fs}^{em}(k_x, k_y, z, z') = \begin{bmatrix} 0 & \pm jk_z & -jk_\rho sin\alpha \\ \mp jk_z & 0 & jk_\rho cos\alpha \\ jk_\rho sin\alpha & -jk_\rho cos\alpha & 0 \end{bmatrix} \tag{4.14}$$

$$\tilde{\vec{M}}_{id}(k_\rho, a) = -\hat{z} \times \vec{E}_{inc}(\vec{r})2\pi a^2\frac{J_1(a, k_\rho)}{k_\rho a} \tag{4.15}$$

The sum of the two contributions leads to:

$$\vec{e}_{rad}(\vec{r}) = \frac{1}{4\pi^2}\int_0^{+\infty}\int_0^{2\pi}\Big(\tilde{G}_{fs}^{ej}(k_x,k_y,z,z')\vec{\tilde{J}}_{id}(k_\rho,a) + \tilde{G}_{fs}^{em}(k_x,k_y,z,z')\vec{\tilde{M}}_{id}(k_\rho,a)\Big)e^{-jk_\rho\rho\cos(\alpha-\phi)}e^{-jk_z|z|}k_\rho dk_\rho d\alpha \tag{4.16}$$

Identical mathematical steps can be performed in order to define the radiated magnetic field:

$$\vec{h}_{rad}(\vec{r}) = \frac{1}{4\pi^2}\int_0^{+\infty}\int_0^{2\pi}\Big(\tilde{G}_{fs}^{hj}(k_x,k_y,z,z')\vec{\tilde{J}}_{id}(k_\rho,a) + \tilde{G}_{fs}^{hm}(k_x,k_y,z,z')\vec{\tilde{M}}_{id}(k_\rho,a)\Big)e^{-jk_\rho\rho\cos(\alpha-\phi)}e^{-jk_z|z|}k_\rho dk_\rho d\alpha \tag{4.17}$$

The only thing that changes is the constants in front of the spectral Green's functions. Here they are all four listed:

$$\tilde{G}_{fs}^{ej}(k_x,k_y,z,z') = \frac{-\zeta}{2k_0k_z}\begin{bmatrix} k_0^2-k_\rho^2\cos^2\alpha & -k_\rho^2 sin\alpha cos\alpha & -k_\rho cos\alpha(\pm k_z)\\ -k_\rho^2 sin\alpha cos\alpha & k_0^2-k_\rho^2\sin^2\alpha & -k_\rho sin\alpha(\pm k_z)\\ -k_\rho cos\alpha(\pm k_z) & -k_\rho sin\alpha(\pm k_z) & k_0^2-k_z^2\end{bmatrix} \tag{4.18}$$

$$\tilde{G}_{fs}^{em}(k_x,k_y,z,z') = -\frac{j}{2k_z}\begin{bmatrix} 0 & \pm jk_z & -jk_\rho sin\alpha\\ \mp jk_z & 0 & jk_\rho cos\alpha\\ jk_\rho sin\alpha & -jk_\rho cos\alpha & 0\end{bmatrix} \tag{4.19}$$

$$\tilde{G}_{fs}^{hm}(k_x,k_y,z,z') = \frac{-\frac{1}{\zeta}}{2k_0k_z}\begin{bmatrix} k_0^2-k_\rho^2\cos^2\alpha & -k_\rho^2 sin\alpha cos\alpha & -k_\rho cos\alpha(\pm k_z)\\ -k_\rho^2 sin\alpha cos\alpha & k_0^2-k_\rho^2\sin^2\alpha & -k_\rho sin\alpha(\pm k_z)\\ -k_\rho cos\alpha(\pm k_z) & -k_\rho sin\alpha(\pm k_z) & k_0^2-k_z^2\end{bmatrix} \tag{4.20}$$

$$\tilde{G}_{fs}^{hj}(k_x,k_y,z,z') = \frac{j}{2k_z}\begin{bmatrix} 0 & \pm jk_z & -jk_\rho sin\alpha\\ \mp jk_z & 0 & jk_\rho cos\alpha\\ jk_\rho sin\alpha & -jk_\rho cos\alpha & 0\end{bmatrix} \tag{4.21}$$

Note that thanks to the fact that the Airy pattern does not depend on α the radiation integral can be analytically closed in α, since the only dependence of the integrand function on this variable is found in the dyads of $\tilde{G}_{fs}^{fc}(k_x,k_y,z,z')$. This is extremely convenient, since the numerical evaluation of the integral will be much faster (the integrand function is defined as a function of a single complex variable, not two), effectively reducing the time a numerical

software (Matlab was used for this work) needs to perform it. All the detailed derivations can be found in Appendix E, while here are posted only the forms every one of the nine components of the integrand function depends on α with and their analytical solutions:

$$CC = \int_0^{2\pi} \cos^2\alpha\, e^{-jk_\rho\rho\cos(\alpha-\Phi)}d\alpha = \frac{1}{2}\int_0^{2\pi}(1+\cos(2\alpha))e^{-jk_\rho\rho\cos(\alpha-\Phi)}d\alpha \quad (4.22)$$

$$SS = \int_0^{2\pi} \sin^2\alpha\, e^{-jk_\rho\rho\cos(\alpha-\Phi)}d\alpha = \frac{1}{2}\int_0^{2\pi}(1-\cos(2\alpha))e^{-jk_\rho\rho\cos(\alpha-\Phi)}d\alpha \quad (4.23)$$

$$SC = \int_0^{2\pi} sin\alpha\, cos\alpha\, e^{-jk_\rho\rho\cos(\alpha-\Phi)}d\alpha = \frac{1}{2}\int_0^{2\pi}\sin(2\alpha)\, e^{-jk_\rho\rho\cos(\alpha-\Phi)}d\alpha \quad (4.24)$$

$$C = \int_0^{2\pi} cos\alpha\, e^{-jk_\rho\rho\cos(\alpha-\Phi)}d\alpha \quad (4.25)$$

$$S = \int_0^{2\pi} sin\alpha\, e^{-jk_\rho\rho\cos(\alpha-\Phi)}d\alpha \quad (4.26)$$

The integral expressions at the right hand side have analytical results, with the form:

$$\int_0^{2\pi} \begin{matrix} cos \\ sin \end{matrix} (N\alpha)\, e^{-jk_\rho\rho\cos(\alpha-\Phi)}d\alpha = j^{-N}2\pi \begin{matrix} cos \\ sin \end{matrix} (N\Phi)J_N(k_\rho\rho) \quad (4.27)$$

Where J_i are the Bessel's functions of order i. The results are:

$$CC = \pi\left(J_0(k_\rho\rho) - \cos(2\Phi)\,J_2(k_\rho\rho)\right) \quad (4.28)$$

$$SS = \pi\left(J_0(k_\rho\rho) + \cos(2\Phi)\,J_2(k_\rho\rho)\right) \quad (4.29)$$

$$SC = -\pi\sin(2\Phi)\,J_2(k_\rho\rho) \quad (4.30)$$

$$C = -j2\pi\, cos\Phi\, J_1(k_\rho\rho) \quad (4.31)$$

$$S = -j2\pi\, sin\Phi\, J_1(k_\rho\rho) \quad (4.32)$$

The Green's function is a 3×3 matrix, and each of the radiated fields are two, electric and magnetic, is given by the contribution of both the electric and magnetic source, which means that the expression to close are 36 in total. All the expressions for every component of the

electric field are reported in Appendix E; the other ones for the magnetic field differ only for the constant of the Green's functions.

IV.b) Deformation path

Closing the integral in α means that the propagation of the field radiated by the ideal currents is now defined by means of a spectral integration of complex argument k_ρ; the function to be integrated is composed by oscillating terms described through Bessel functions of various order. The expression of the Bessel function is rather complicated, but its asymptotical evaluation for large input arguments can be expressed as a sum of exponential functions that depend on $k_\rho \rho$. It is well known that thanks to the Euler's formula one could express exponential functions as the sum of sinusoidal functions; these functions' value increases extremely fast when the imaginary part of their argument becomes larger. The point is that now it is clear that the integrand function is constituted by highly oscillating function of complex argument. For this reason, the path one will perform the integration on has to be chosen appropriately, otherwise the numerical evaluation of the expression would become impossible.

First thing to consider is that the integrand function depends on:

$$\vec{f}_{rad}(\vec{r}) \propto \frac{1}{k_z}; \quad k_z = -j\sqrt{-\left(k_0^2 - k_\rho^2\right)} \tag{4.33}$$

Performing the integration, which depends now only on k_ρ, we end up having a space of solutions of k_ρ that verify $k_z = 0$, and that make the integrand function explode. That space of solutions is called branch cut, and must be avoided in the integration path. The starting point of the branch cut is precisely on the real axis and it is $k_\rho = k_0$. Also, the path must not be crossed: this is because we are dealing with a multivalued function (the square root), and we have to choose to work with only one set of the positive or negative solutions it gives. If the branch cut is crossed by the integration path the function changes (same absolute value but opposite sign), and this makes its evaluation much more complicated [13].

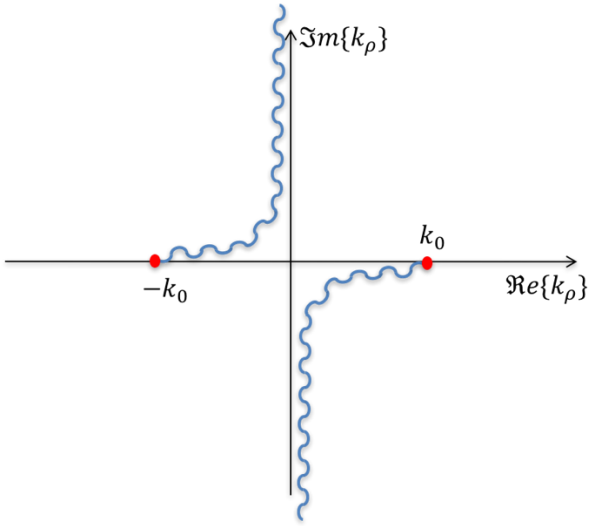

Fig 4. 1) $\boldsymbol{k_\rho}$complex plane and branch cut of $\boldsymbol{k_z = 0}$

The deformation path used for this procedure introduces a new real variable $x > 0 \in \mathcal{R}e$. This variable is used to define the integration path in k_ρ, which is now expressed as:

$$k_\rho = x + \varepsilon j x e^{-\frac{x^2}{2k_0^2}} - j\gamma; \quad x = [0 \to +\infty); \quad \varepsilon, \gamma > 0 \in \mathcal{R}e \tag{4.34}$$

Thanks to the definition of (x, ε, γ), there is now no solution such that $k_\rho = k_0$. The differential has now to be changed in the integrand function due to the variables substitution. It results:

$$dk_\rho = \frac{\partial k_\rho}{\partial x} dx = 1 + \varepsilon j e^{-\frac{x^2}{2k_0^2}} \left(1 - \frac{x^2}{k_0^2}\right) \tag{4.35}$$

ε and γ are two constants that can be modified to adjust the integration path to the characteristics of the radiation problem. In this case they are $\varepsilon = 0.15, \gamma = 0.2$. Due to $\gamma > 0$ the path has been shifted towards the negative region of the imaginary axis of k_ρ: this is because the higher the imaginary part of $\Im m(k_\rho)$ is, the more the integrand function tends to explode, leading to an impossible numerical evaluation. This is clear when looking at the exponential term:

$$e^{-jk_\rho \rho} = e^{-j(Re + jIm)\rho} = e^{-jRe\rho} e^{Im\rho} \tag{4.36}$$

$$e^{Im\rho} \to \infty \quad if \quad Im \uparrow \tag{4.37}$$

The deformation path here applied is meant to avoid any kind of singularity, which in this case is represented only by the branch cuts, and it is qualitatively depicted here on the k_ρ complex plane:

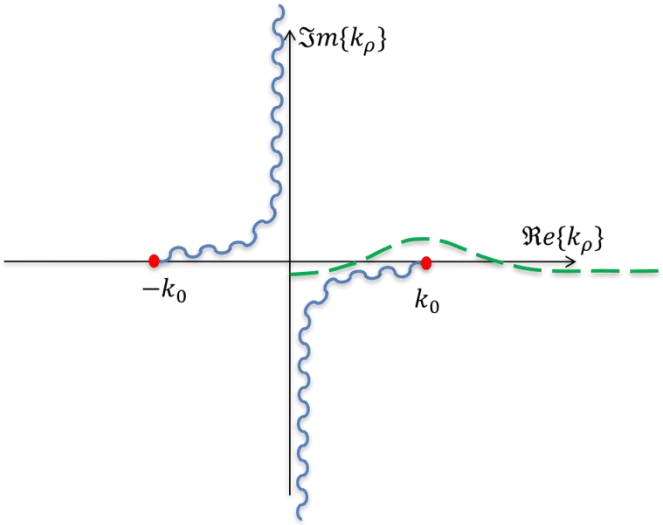

Fig 4. 2) $\boldsymbol{k_\rho}$complex plane and branch cut of $\boldsymbol{k_z = 0}$ and deformation path

Sometimes, it can be helpful to express wave propagations phenomena in cylindrical coordinates systems using a linear combination of Bessel's functions of the first and second kind. These linear combinations' results are also known as Hankel's functions. This substitution can be applied by means of the following integral identity, which renders the convergence, that sometimes can be extremely slow, of the integrand function faster thanks to the integration path that now goes from $-\infty$ to $+\infty$:

$$\int_0^\infty J_i(k_\rho\rho)k_\rho dk_\rho = \frac{1}{2}\int_{-\infty}^{+\infty} H_i^{(2)}(k_\rho\rho)k_\rho dk_\rho \tag{4.38}$$

Both the techniques have been used to test the accuracy of the Matlab scripts. They give the same results in about the same computational time.

Finally, under certain conditions it is possible to mathematically derive the best possible path to perform the integration on, the detailed steps are reported in Appendix F.

IV.c) *Near field Poynting vector: sphere enclosing the antenna*

The Poynting vector theorem states that in absence of lossless (one of the initial hypothesis of the ideal currents procedure was having a losses load-matched antenna indeed) the power available to the antenna can be evaluated by means of the real part of the Poynting vector flux, integrated on a whichever closed surface enclosing the antenna. Having already the value of the available power, the near field procedure has been validated upon this info: both the electric and the magnetic field were calculated over a sphere in the near field region, specifically at $r_{sph} = 1.5a \ \forall a$, varying the antenna radius as $a = 0.01\lambda \rightarrow 5\lambda$. The Poynting vector has been evaluated in two ways: using the fields calculated stopping the spectral integration at $k_\rho = k_0$, which means that only their visible component was accounted for, and using the fields obtained performing the integration until the full convergence of the integrand function, using the techniques before explained, retaining thus their whole spectrum. The plots show that only one of the two operations, namely the Poynting vector obtained using the field calculated by means of a full spectral integration, gives the correct results.

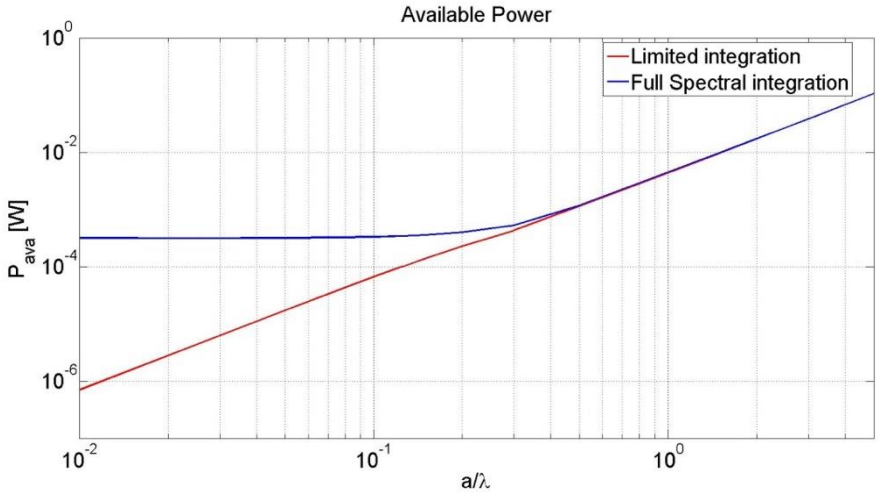

Fig 4. 3) Available power as a function of the antenna domain obtained integrating the Poynting vector flux over a sphere in the near field of the antenna ($\boldsymbol{r_{sph} = 1.5a}$), using the electric and magnetic fields calculated either by means of a full spectral integration or chopping the integration at $\boldsymbol{k_\rho = k_0}$

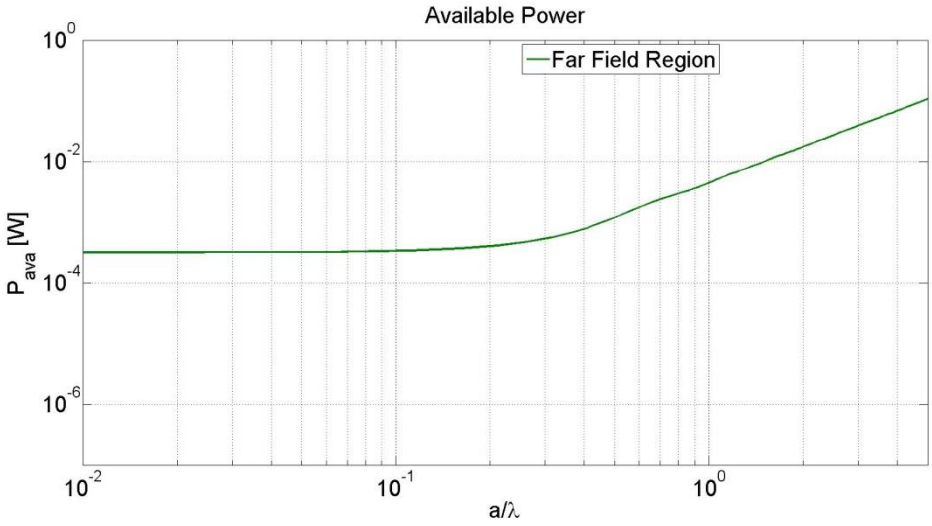

Fig 4. 4) Available power estimated integrating the Poynting vector flux over a sphere in the far field region.

IV.d) Near field Poynting vector: reaction integral on the antenna domain

The fact that retaining only the visible part of the near electric and the magnetic fields to calculate the Poynting vector did not give the expected result was surprising, since it's the component of the fields that is used in the far field region to perform the same operation (it is in fact the only existing component there). Thus, in order to have a confirmation of the results, the available power in the near field region was calculated by means of a reaction integral performed on the antenna domain, considering only the visible spectrum of the Poynting vector. Starting from the Poynting theorem:

$$\frac{1}{2}Re\left\{\iint_S (\vec{e}\times\vec{h}^*)\cdot d\vec{S}\right\}+\frac{1}{2}\omega\iiint_V\left(\mu|\vec{h}|^2+\varepsilon|\vec{e}|^2\right)dV = -\frac{1}{2}Re\left\{\iiint_V(\vec{e}\cdot\vec{j}^*+\vec{h}^*\cdot\vec{m})dV\right\} \tag{4.39}$$

$$\text{Hp: lossless antenna} \rightarrow \frac{1}{2}\omega\iiint_V\left(\mu|\vec{h}|^2+\varepsilon|\vec{e}|^2\right)dV = 0 \tag{4.40}$$

$$\frac{1}{2}Re\left\{\iint_S (\vec{e}\times\vec{h}^*)\cdot d\vec{S}\right\} = -\frac{1}{2}Re\left\{\iiint_V(\vec{e}\cdot\vec{j}^*+\vec{h}^*\cdot\vec{m})dV\right\} \tag{4.41}$$

This is: the real part of the result obtained performing a reaction between the fields and the sources integrated over the volume V must be equal to the real part of the integration of the flux of the Poynting vector over whichever surface enclosing the antenna. The latter result is

already available, thus, in order to verify what the definition of visible is the result of the reaction integral must be compared to it.

In this case we have surface currents, thus the reaction is expressed as a surface integral without any loss of meaning. The chosen surface where to perform the reaction over is a cylinder, centered in the antenna domain. Then, its height has been shrunk until the flux across the lateral surface was negligible: the surface for the integration becomes the antenna cross section itself, where the currents are defined.

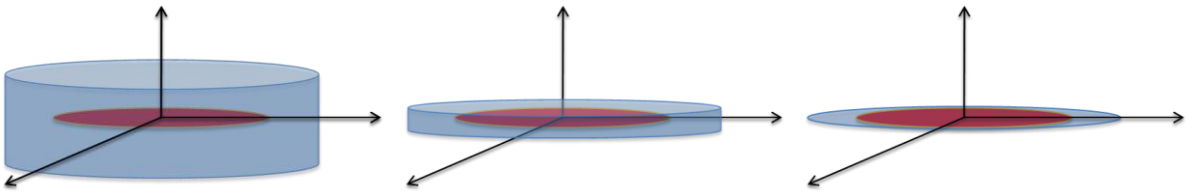

Fig 4. 5) Cylinder chosen as the surface where to perform the reaction integral; height progressively reduced to obtain a negligible contribute from the lateral surface

Expressing the radiated field as the convolution between the spatial Green's functions and the sources, and the Green's function as the anti-Fourier's transform of its spectral representation:

$$P_{rad} = -\frac{1}{2} Re\left(\int_0^{2\pi} \int_0^{a} \left(\vec{e}(\rho,\phi) \cdot \vec{j}_{id}{}^{*}(\rho,\phi) + \vec{h}^{*}(\rho,\phi) \cdot \vec{m}_{id}(\rho,\phi) \right) \rho d\rho d\phi \right) \tag{4.42}$$

$$\vec{e}(\rho,\phi) = \tilde{g}^{ej}(\rho,\ \rho',\phi,\ \phi') * \vec{j}_{id}(\rho',\phi') + \tilde{g}^{em}(\rho,\ \rho',\phi,\ \phi') * \vec{m}_{id}(\rho',\phi') \tag{4.43}$$

$$\vec{h}(\rho,\phi) = \tilde{g}^{hm}(\rho,\ \rho',\phi,\ \phi') * \vec{m}_{id}(\rho',\phi') + \tilde{g}^{hj}(\rho,\ \rho',\phi,\ \phi') * \vec{j}_{id}(\rho',\phi') \tag{4.44}$$

$$\vec{g}^{fc}(\rho,\rho',\phi,\phi') = \frac{1}{4\pi^2} \iint_{-\infty}^{\infty} \tilde{G}^{fc}(k_x,k_y) e^{-jk_x x} e^{jk_x x'}\ e^{-jk_y y} e^{jk_y y'} dk_x dk_y \tag{4.45}$$

After a few mathematical steps the following expression is found (for the detailed derivation please refer to Appendix G):

$$P_{rad} = -\frac{1}{8\pi^2} Re \iint_{-\infty}^{\infty} \left(\frac{G_{xx}^{ej}(k_\rho,\alpha)}{\zeta} + \zeta \left(G_{yy}^{hm}(k_\rho,\alpha) \right)^{*} \right) \frac{1}{\zeta} \left| E_x(k_\rho,\alpha) \right|^2 k_\rho dk_\rho d\alpha \tag{4.46}$$

Thanks to the fact that we are dealing with a uniform distribution of Huygens' sources, which once again are identified as an electric and a magnetic dipole one orthogonal to the other, the mixed terms that emerge in Appendix G (the reaction between the magnetic current and the magnetic field given by electric current, as well as the reaction between the electric current and the electric field given by the magnetic current) cancel out. Moreover, please note that due to the complex conjugate product we ended up having an expression with no exponential dependence. This is fundamental and it will be evident proceeding with the derivation:

$$P_{rad} = \frac{1}{2\pi} Re\left\{\int_0^{\infty} \left(\frac{1}{2k_0}\frac{2k_0^2 - k_\rho^2}{k_z}\right)\frac{1}{2\zeta}\left|E_x(k_\rho)\right|^2 k_\rho dk_\rho\right\} \tag{4.47}$$

$$P(k_\rho) = \frac{1}{2\pi}\left(\frac{1}{2k_0}\frac{2k_0^2 - k_\rho^2}{k_z}\right)\frac{1}{2\zeta}\left|E_x(k_\rho)\right|^2 k_\rho \tag{4.48}$$

$$P_{rad} = Re\left\{\int_0^{\infty} P(k_\rho)dk_\rho\right\} = \int_0^{k_0} P(k_\rho)dk_\rho \tag{4.49}$$

Having no exponential dependence implies in fact that considering only the real part of the integral simply means performing the integration for $k_\rho = 0 \rightarrow k_0$, which is the visible spectrum of the Poynting vector in the near field region. We can see now that the result predicted by this expression is precisely equal to the real part of the Poynting vector flux when integrated over a sphere in the far field region and in the near field region, but using the total electric and magnetic fields (not just their visible part).

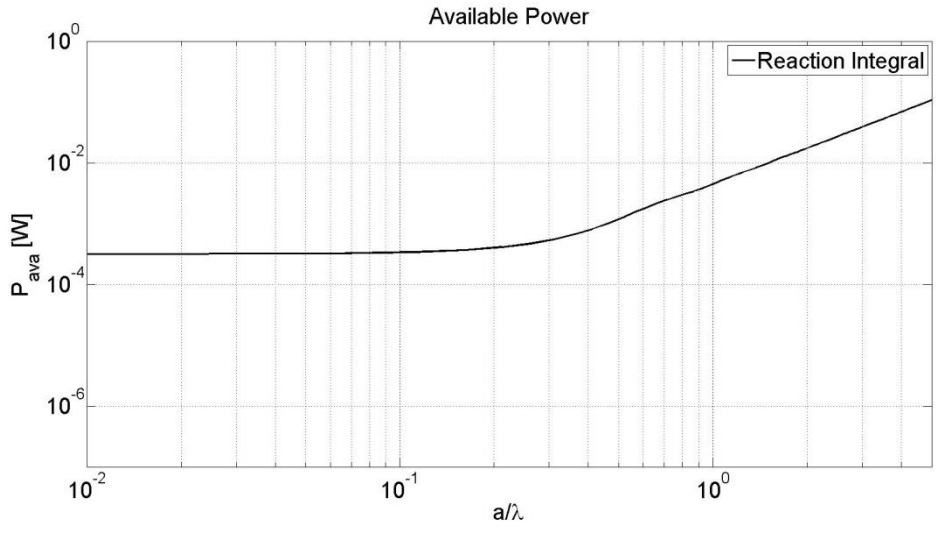

Fig 4. 6) Available power as a function of the antenna domain predicted by the reaction integral.

IV.e) *Interpretation of the definition of 'visible'*

This is where one of the most significant results of this work emerges: it appears that the definition of 'visible' is *de facto* applicable to power rather than to fields. The Poynting vector evaluated in the near field region with the two methods gives of course different results: the correct one, which is perfectly equal to the value estimated using the field in the far field region and the reaction integral on the antenna domain, is the one obtained with the fields calculated by means of a full spectral integration. It seems thus that the definition of visible, which to my knowledge was used to describe the portion of the spectrum of the field that does not attenuate while propagating from the antenna to the far field region, is then applicable to the Poynting vector rather than to the fields themselves. The correct available power is in fact obtained either integrating the flux of the Poynting vector that crosses a sphere in the far field region, or integrating it over a sphere in the near field region using the fields calculated through a full spectral integration, or performing a reaction integral over the antenna domain cropping the integration at $k_\rho = k_0$: while the latter two methods do not use the visible components of the fields, all of them retain only the visible part of the Poynting vector indeed.

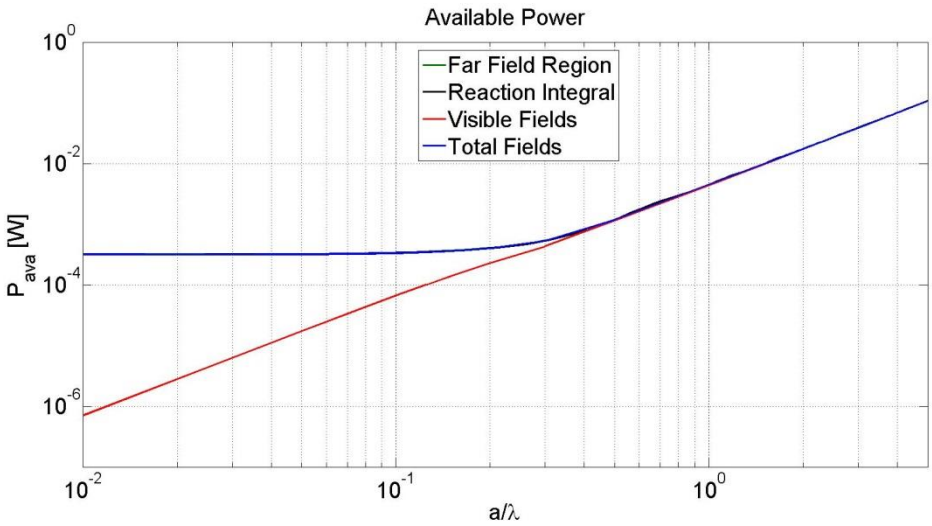

Fig 4. 7) Available power as a function of the antenna domain predicted by the four different methods: comparison.

IV.f) *Near field Poynting vector comparison: Ideal Currents Vs Spherical Modes*

It is interesting to have a comparison of the near field quantities estimated by the two methods, to validate the implementation of the spectral techniques adopted. To do this the Poynting vector was calculated with the two procedures in the near field region. Two antenna dimension are examined: $a = 0.5\lambda, a = 2\lambda$. The absolute value and the direction of real part of the Poynting vector are displayed on a sphere of radius $r_{sph} = 1.5a$. Please, note that the scales on the colorbars relative to the results given by the two methods are different. We can see that for the bigger antenna case the distribution is significantly different, and it reflects the quantization error introduced by the spherical modes expansion: for an antenna of $a = 2\lambda$ it indeed results $N = ka = 4\pi = 12.56$. Having a N value in the middle between two integers is indeed the case with the highest uncertainty, since there is no rule that guides us in the choice between $N = 12$ and $N = 13$. In this case $N = 13$ was chosen. On the other hand, when $a = 0.5\lambda \rightarrow N = \pi = 3.16$. In this case the exact value of N is much closer to its integer approximation given by $N = round(ka)$; however the results are still different:

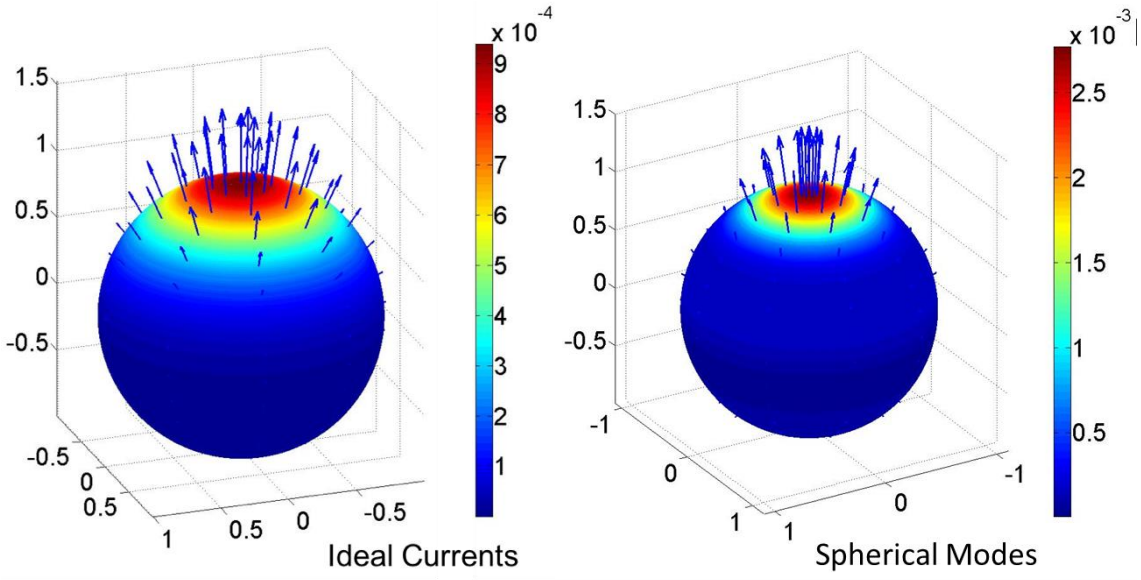

Fig 4. 8) Real part of the Poynting vector (colorbar expressed in [W]) on a sphere of radius $\boldsymbol{a = 1.5\lambda}$ having $\boldsymbol{a = 0.5\lambda}$ enclosing the antenna: Fig 4.8a) Estimated by the Ideal Currents method; Fig 4.8b) Estimated by the Spherical Modes expansion

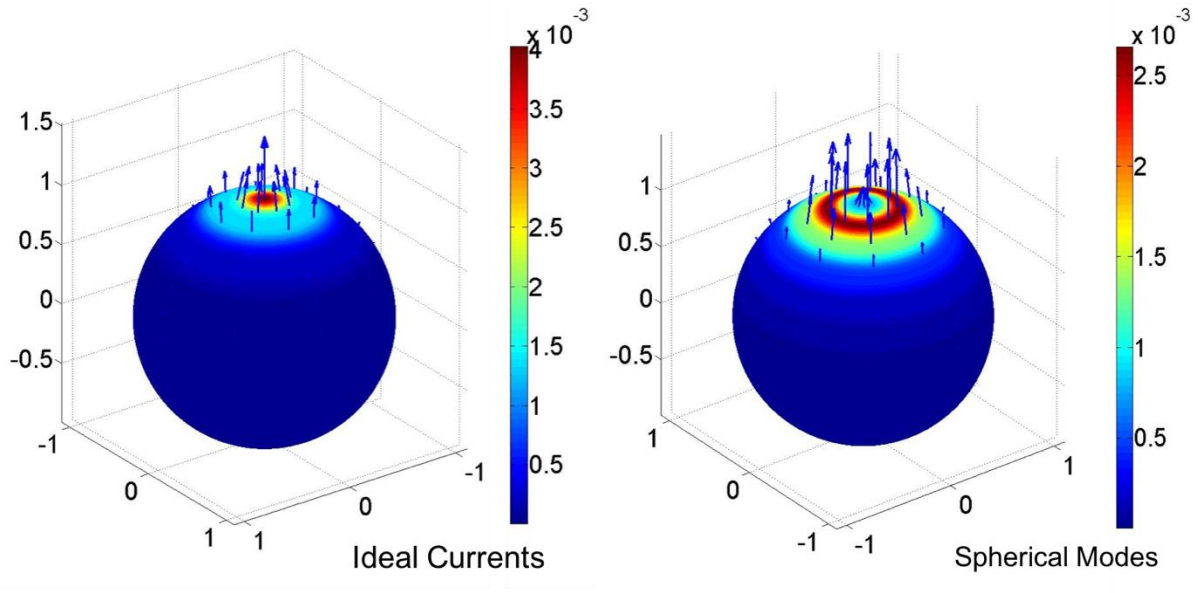

Fig 4. 9) Real part of the Poynting vector (colorbar expressed in [W]) on a sphere of radius $\boldsymbol{a = 1.5\lambda}$ having $\boldsymbol{a = 2\lambda}$ enclosing the antenna: Fig 4.9a) Estimated by the Ideal Currents method; Fig 4.9b) Estimated by the Spherical Modes expansion

Moreover, note how the directivity of the antenna changes between the two procedures and when varying its electrical length.

V) MULTIPLE IMPINGING PLANE WAVES

As far as most of the real case are concerned, the incident field cannot be approximated by a single incident plane wave. Assuming once again that the sources are located at large distance from the reference system, which is centered on the antenna domain, the field can be then expressed as a continuous superposition of plane waves, since Maxwell's equations obey the principle of the superposition of the effects. The final aim of the whole description is to define the power that given an incident field the antenna can absorb, but it is not possible to define an available power for every single plane wave incidence and then simply sum each one of them up. Indeed, the difference with respect to the single plane wave incidence case is that now the relative phase of the plane waves must be taken into account, given the fact that depending on it they can give rise to either constructive or destructive interference. To give a brief and intuitive example, given two equal plane wave impinging from symmetrical directions ($\theta_{in,1} = \theta_{in,2},\ \phi_{in,1} = \phi_{in,2} - \pi$) one would be tempted to define an available power for each one of them, that would be in this case the same, following the procedure defined chapter IV or V; then one would sum them, obtaining a power that will be twice as much. This would lead to huge mistakes though. The electromagnetic fields in general interact with each other, and the available power changes depending on the kind of the interference they establish: it would be zero with a perfect destructive interference, while, in case of constructive interference, it would be four times the power given by a single plane wave. What must be done is to evaluate the total incident field accounting for the relative phase of each plane wave used to describe it, define its observable component and then estimate the available power. As already introduced in chapter *II.d*, this is not something that is achievable by the heuristic formula, since what it would do is precisely a sum of the powers regardless of the relative phase, which is wrong.

V.a) Observable field definition in case of two incident plane waves

Under the assumptions just listed the expression for the total incident field is then:

$$\vec{e}_{inc}(\vec{r}) = \int_0^{2\pi}\int_0^{\pi} \vec{E}_{in}(\theta_{in},\phi_{in}) e^{-jkr(sin\theta_{in}cos\phi_{in}\cos(\phi_{in}-\Phi)+cos\theta_{in}cos\Theta)}\, sin\theta_{in} d\theta_{in} d\phi_{in} \qquad (5.1)$$

In order to define the observable component of the incident field the procedure is a straight forward extension to the one used for the single plane wave incidence case. For each plane wave impinging on the reference system a squinted reference system orthogonal to its direction of propagation is defined, the ideal currents are calculated, and their radiation, which is equal and opposite to the outward component of the observable field, is estimated; then the total field, evaluated accounting for the relative phase, is referred to the main reference system; finally, all the fields with their relative phases are summed up (for the derivation refer to Appendix H). For sake of simplicity, only two waves incoming from symmetrical directions ($\theta_{in,1} = \theta_{in,2} = \bar{\theta},\ \phi_{in,1} = \bar{\phi},\ \phi_{in,2} = \bar{\phi} + \pi$) are taken into account. The ideal currents are of course the PO ones multiplied by the amplification factor C_{amp}, which is defined for every plane wave and is in general different for each one; however, in the case of two equal plane waves incoming from symmetrical directions the effective area is the same, and so is C_{amp}. Once the procedure is properly defined, the extension to a whichever number of plane waves is immediate. A qualitative sketch of the process is the following:

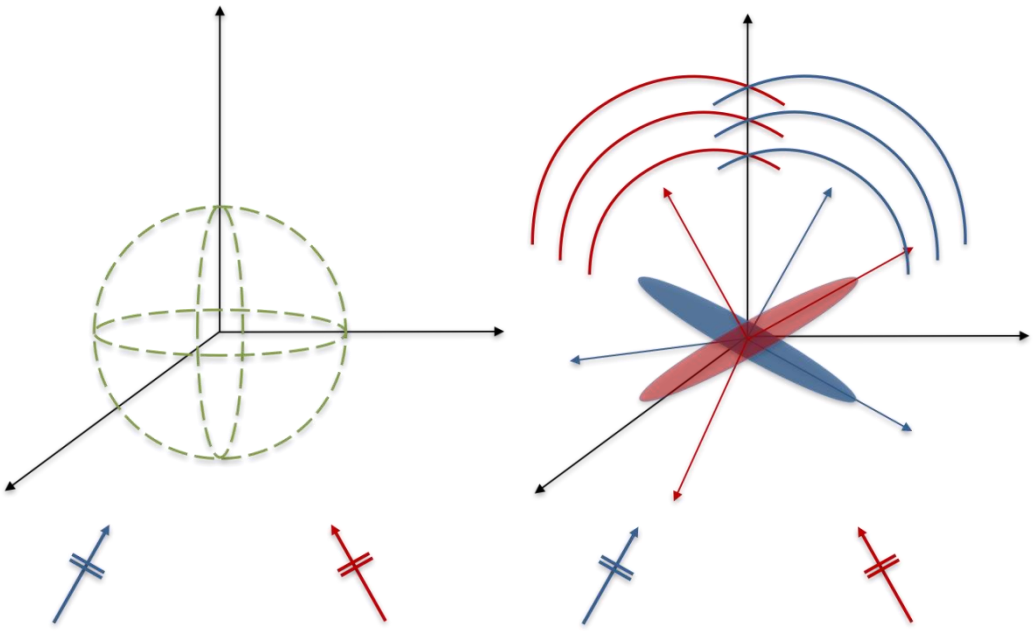

Fig 5. 1) Incoming plane waves and domain where the antenna will be allocated at; Fig 5.1b) squinted domains relative to each plane wave and their ideal radiated field

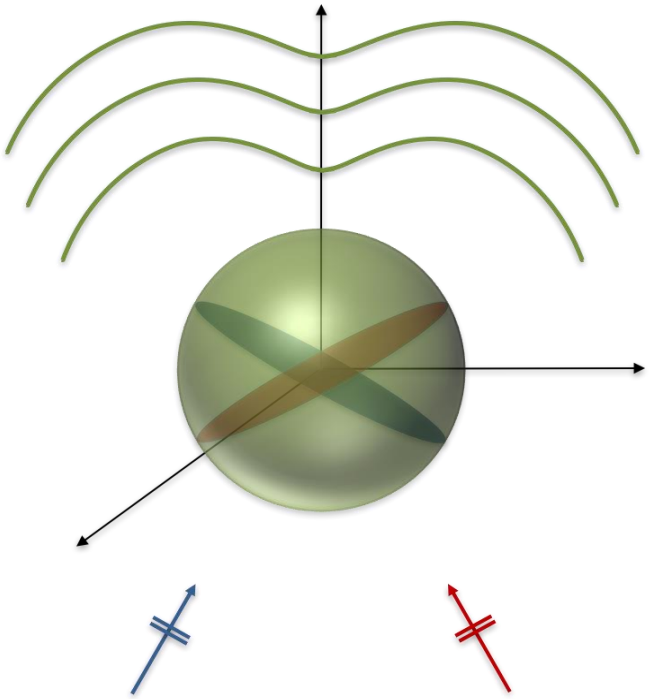

Fig 5. 2) Ideal radiated field in case of multiple impinging plane waves: final configuration with total radiated field.

Once the total field scattered by the ideal currents is evaluated, the calculation of the available power is immediate: it simply is the integration of the real part of the Poynting vector flux over a sphere in the far field region.

$$\vec{e}_{ideal}^{scat}(\vec{r}_\infty) = -\vec{e}_{obs}^{outw}(\vec{r}_\infty) = C_{amp}\int_0^{2\pi}\int_0^{\pi}\vec{V}_{PO}^{outw}(a,\vec{k}^{in},\vec{k})\,sin\beta_{in}d\beta_{in}d\alpha_{in}\frac{e^{-jkr_\infty}}{r_\infty} \tag{5.2}$$

$$P_{ava} = \frac{1}{2\varsigma}\int_0^{2\pi}\int_0^{\pi}\left|C_{amp}\int_0^{2\pi}\int_0^{\pi}\vec{V}_{PO}^{outw}(a,\hat{r}^{in},\vec{k})sin\beta^{in}d\beta^{in}d\alpha^{in}\right|^2 sin\theta d\theta d\phi \tag{5.3}$$

However, before calculating the available power, the ideal scattered field needs to be analyzed.

V.b) *Far field region beams splitting*

As it was already showed in the previous chapters the larger the antenna is in terms of wavelength, the more directive the far field pattern is. This applies also to the multiple plane waves incidence case: the fields radiated by each set of currents on the squinted reference systems will be summed, and the directivity of the total field pattern depends on the antenna electrical length. It is apparent that in the case of two plane waves impinging on a directive antenna from different directions a beam splitting phenomenon will be observed: the main lobe of one of the two scattered field will be summed up with the side lobes of the other one. The more directive the antenna, the more evident this effect. The following plot highlights this aspect: keeping the incident angle constant and varying the antenna dimension one sees that in case of relatively small antennas the directivity is not enough to give rise to two distinct main lobes, while these become more and more visible increasing the antenna dimension. The plot is a cut on the E-plane for $\theta = [0 \rightarrow \pi],\ \phi = 0$, and it is symmetrical for $\theta = [-\pi \rightarrow 0]$; the two plane waves are incoming from $\theta_{in,1} = \theta_{in,2} = 165°,\ \phi_{in,1} = 0°,\ \phi_{in,2} = 180°$. For the largest antenna $a = 5\lambda$ the beam peak occurs almost at 15°, the angle of incident referred to the negative part of the z axis, which means that the main and the side lobes have a really weak interaction due to the high directivity (most of the power is concentrated around the angle of incidence, so that the side lobes present where the other scattered field's main lobe is have a really small amplitude).

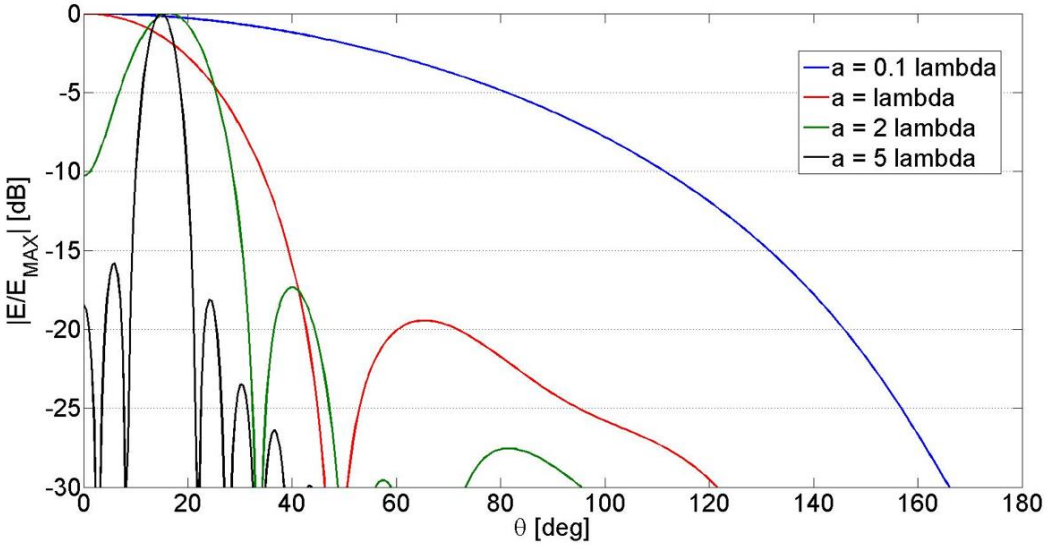

Fig 5. 3) Multiple impinging plane waves: far field pattern plotted for a constant angle of incidence ($\boldsymbol{\theta_{in,1} = \theta_{in,2} = 165°,\ \phi_{in,1} = 0°,\ \phi_{in,2} = 180°}$) varying the antenna electrical length. Electrical field normalized to its maximum amplitude plotted on the E-plane for $\boldsymbol{\theta = [0 \rightarrow \pi],\ \phi = 0}$

V.c) *Far field patterns comparison: Ideal Currents Vs Spherical Modes*

In order to assess whether or not the ideal currents procedure has a scientific dignity the far field pattern has been compared to the one predicted by the spherical modes for different antennae, different angles of incidence and for constructive or destructive interference at the center of the antenna itself.

Three antennae are analyzed ($a = 0.01\lambda, a = \lambda, a = 5\lambda$); field scanned on the E-plane ($\phi = 0, \theta = -\pi \rightarrow \pi$). The fields are expressed in dB and superposed one on top of the other. Since the two plane waves are incoming from symmetrical angles their relative phase ψ gives rise to a perfect destructive interference when it is $\psi = 0$, and to a perfect constructive interference if $\psi = \pi$: this is because the projections along x of the electric field component of the incident waves become either equal ($\psi = \pi$), determining a perfect summation, or opposite ($\psi = 0$), causing the two fields to cancel out. The perfect destructive interference determines a null for $\theta = 0$. Note that for the small antenna ($a = 0.01\lambda$), in the case of a perfect constructive interference ($\psi = \pi$), we basically have the coherent summation of the patterns radiated by two Huygens' sources; since the Huygens' source far field pattern has a single null for $\theta = \pi - \theta_{in}$ that null is now disappeared: it is summed to the radiation of the field scattered by the currents induced by the other incident plane wave. When the antennae are small or large in terms of wavelength the two procedures give the same result for the value of the broadside radiation, thus for these two cases ($a = 0.01\lambda, a = 5\lambda$) the patterns are normalized to their maximum value, which is the same; however, this is not the valid for the medium antenna. The results given by the spherical modes are always plotted with a red line, while the ones given by the ideal currents with a blue line. We can see that for the small antenna the results are perfectly superposed, while for the large antenna there is a really good agreement down to $-20dB$. Increasing the radius of the antenna even more would lead to a better agreement for the far field patterns. For the medium antenna instead, the results are different, and the absolute value (with no normalization) is plotted. Note that for the most directive antenna case ($a = 5\lambda$) the scan is interrupted before $\theta = \pm\pi$, since no value of either the pattern is higher than $-30dB$ after that threshold. The input data are $|E_{PW}| = 1\, V\backslash m,\ r_{obs} = 3000\lambda,\ \lambda = 1\, m.$

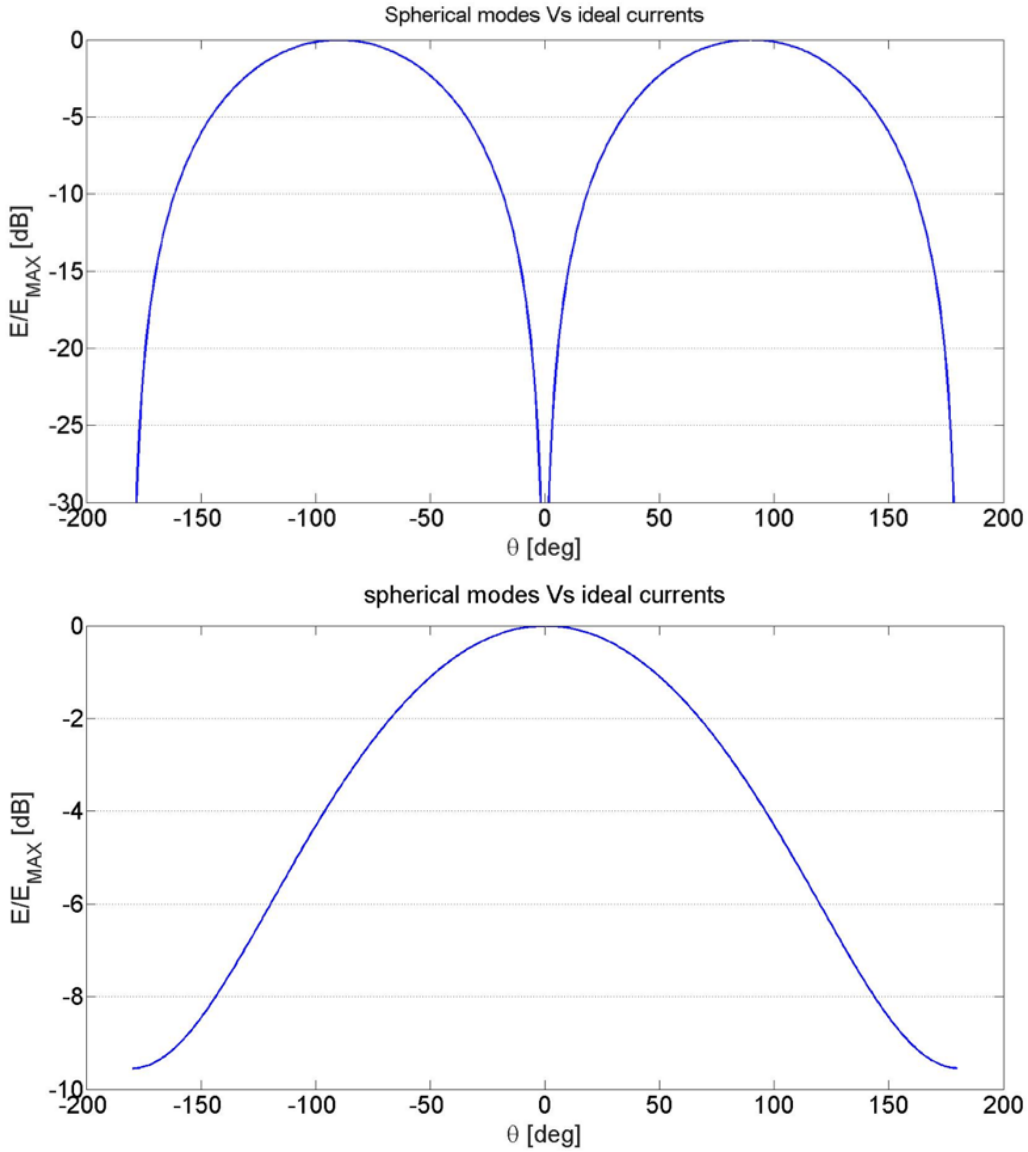

Fig 5. 4) Far field pattern plotted for a constant angle of incidence ($\boldsymbol{\theta_{in,1} = \theta_{in,2} = 120°}$, $\boldsymbol{\phi_{in,1} = 0°}$, $\boldsymbol{\phi_{in,2} = 180°}$), antenna dimension $\boldsymbol{a = 0.01\lambda}$. Electrical field normalized to its maximum amplitude. Blue line: Ideal Currents; red line: Spherical Modes; Fig 5.4a) $\boldsymbol{\psi = 0}$; Fig 5.4b) $\boldsymbol{\psi = \pi}$

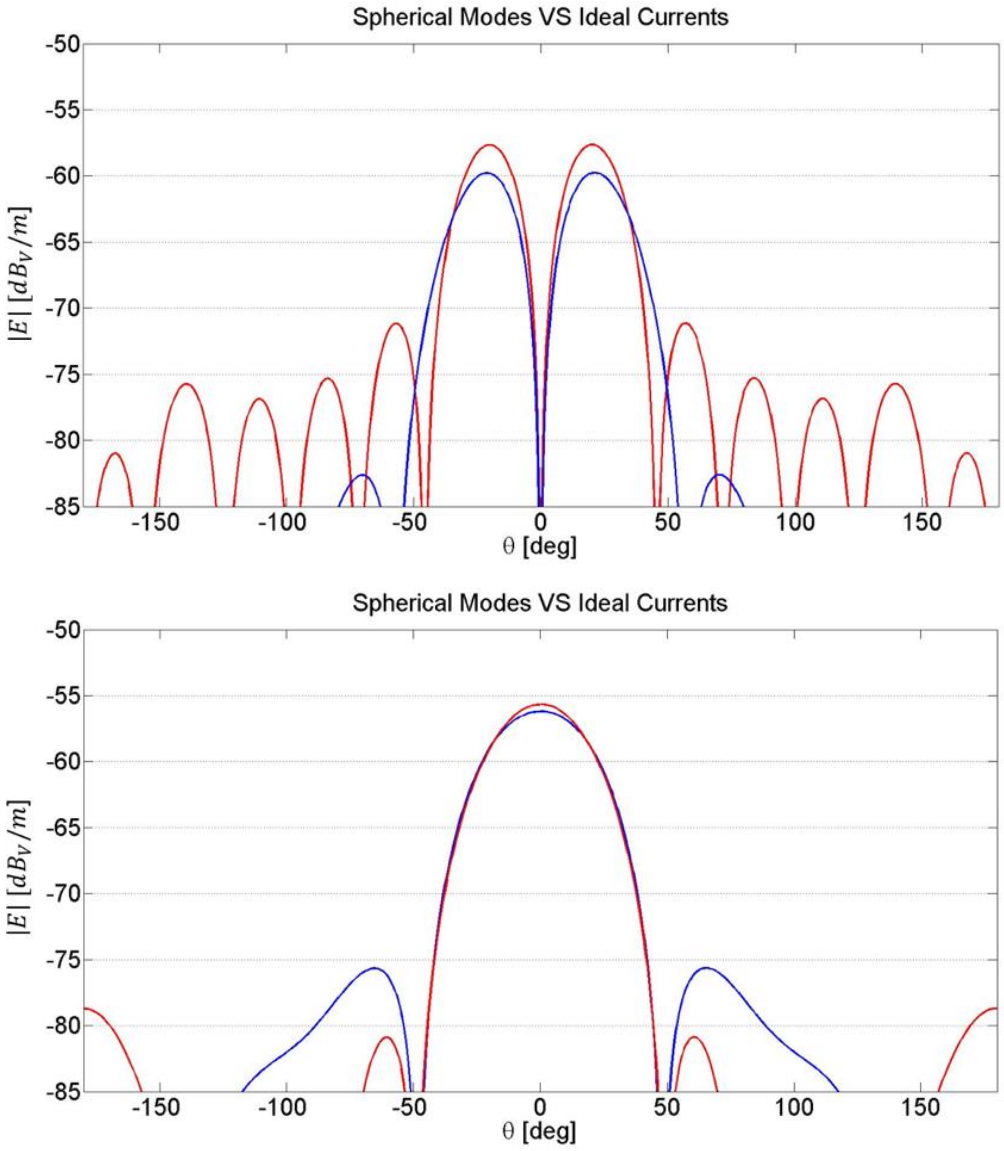

Fig 5. 5) Far field pattern plotted for a constant angle of incidence ($\theta_{in,1} = \theta_{in,2} = 165°,\ \phi_{in,1} = 0°,\ \phi_{in,2} = 180°$), antenna dimension $a = \lambda$. Blue line: Ideal Currents; red line: Spherical Modes; Fig 5.5a) $\psi = 0$; Fig 5.5b) $\psi = \pi$

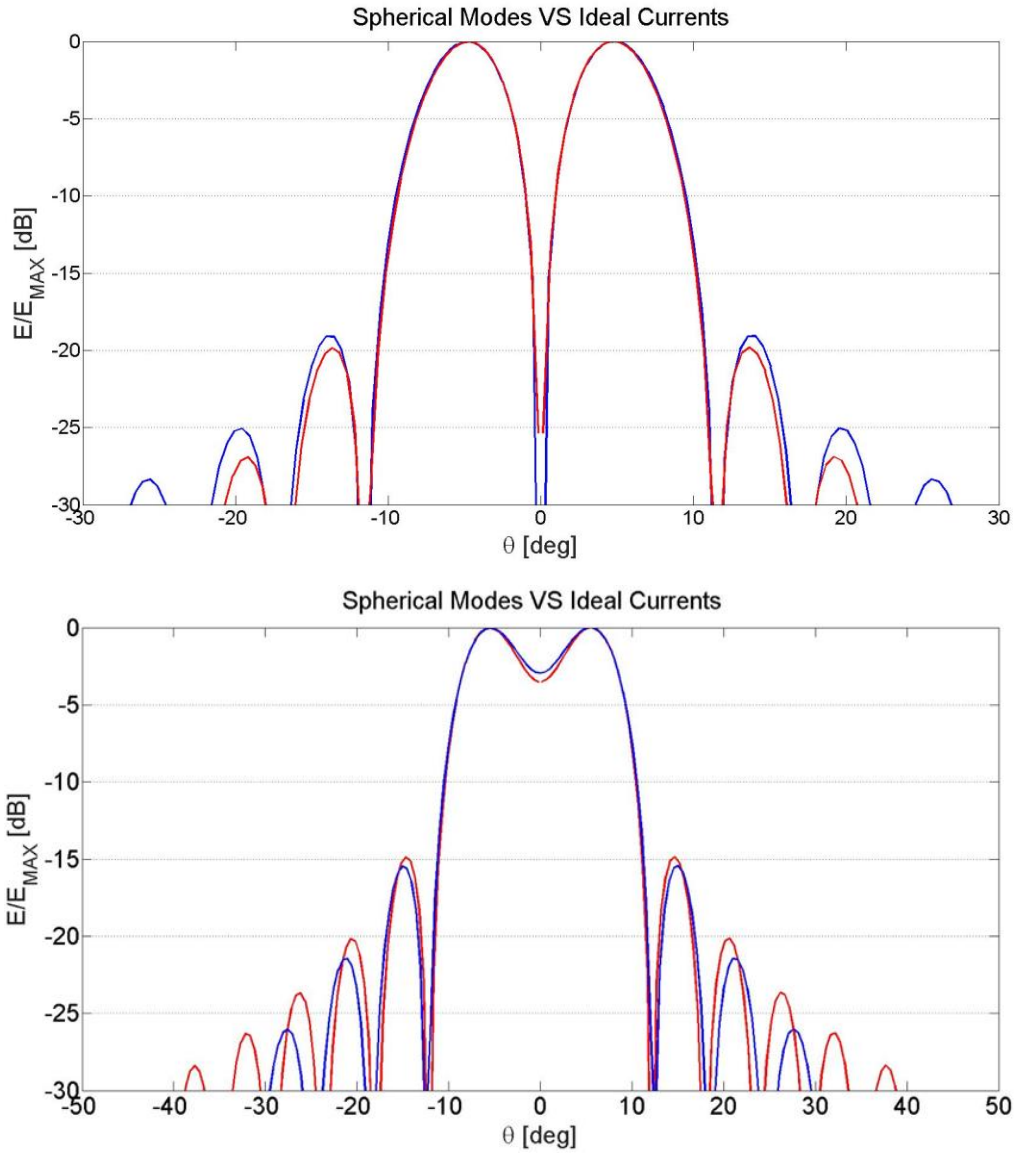

Fig 5. 6) Far field pattern plotted for a constant angle of incidence ($\theta_{in,1} = \theta_{in,2} = 175°,\ \phi_{in,1} = 0°,\ \phi_{in,2} = 180°$), antenna dimension $a = 5\lambda$. Electrical field normalized to its maximum amplitude. Blue line: Ideal Currents; red line: Spherical Modes; Fig 5.6a) $\psi = 0$; Fig 5.6b) $\psi = \pi$

V.d) *Available power as a function of the antenna electrical length*

The power available to the antenna, evaluated retaining the flux of the real part of the Poynting vector over a sphere in the far field region, has been calculated as a function of its electrical length for two incoming plane waves, three different set of incident angles, and for the two cases of perfect constructive or destructive interference at the antenna center.

$$P_{ava} = \frac{1}{2\varsigma}\int_0^{2\pi}\int_0^{\pi}\left|C_{amp}\int_0^{2\pi}\int_0^{\pi}\vec{V}_{PO}^{outw}\left(a,\hat{r}^{in},\vec{k}\right)sin\beta^{in}d\beta^{in}d\alpha^{in}\right|^2 sin\theta d\theta d\phi$$
$$= \int_0^{2\pi}\int_0^{\pi}\frac{1}{2\zeta}\left|\vec{E}_{scat}^{id}(r_\infty,\Theta,\Phi)\right|^2 r_\infty^2 sin\Theta d\Theta d\Phi \qquad (5.4)$$

The result is normalized to the power available to the same antenna in case of a single plane wave incoming form broadside. When the antenna is electrically small the power tends to stay constant for both the interference cases (in-phase or anti-phase); this is due to the fact that the directivity is still low, and the antenna is not able to discern properly the two different patterns given by each of the two incident plane waves. The more the antenna dimension is increased, the more it is able to resolve the two different main lobes, giving rise to beam splitting effects. For small antennas, when the two incoming plane waves give rise to a perfect constructive interference, the power tends to be four times as much the power absorbed from a single plane wave: indeed, the two fields sum up coherently, the total field is thus twice as much, and the power is proportional to its squared value; instead, in the case of a destructive interference the power tends to be zero, since the two incoming plane waves tend to cancel each other. When the angle of incidence referred to the negative part of the z axis increases, the power absorbed by electrically small antennae in case of constructive interference becomes less than four, while the power absorbed in case of destructive interference increases. This is because increasing the θ_{inc} can be seen as a rotation of the far field pattern generated by each plane wave; thus, the two do not sum up (neither they cancel out) in the direction of maximum amplitude. For electrically large antennas, regardless whether the interference is constructive or destructive, and regardless of the angle of incidence, the available power asymptotically tends to be twice as much the power given by a single plane wave. This result is extremely interesting: the interaction between the two ideal scattered fields is so low that they seem to sum up incoherently, that is equivalent to summing the power given by each one of the two in

absence of the other. Finally, note that the sum of the powers given by the two interference cases is always four: the validation is immediate simply applying the principle of the superposition of the effects, for the cases of constructive and destructive interference.

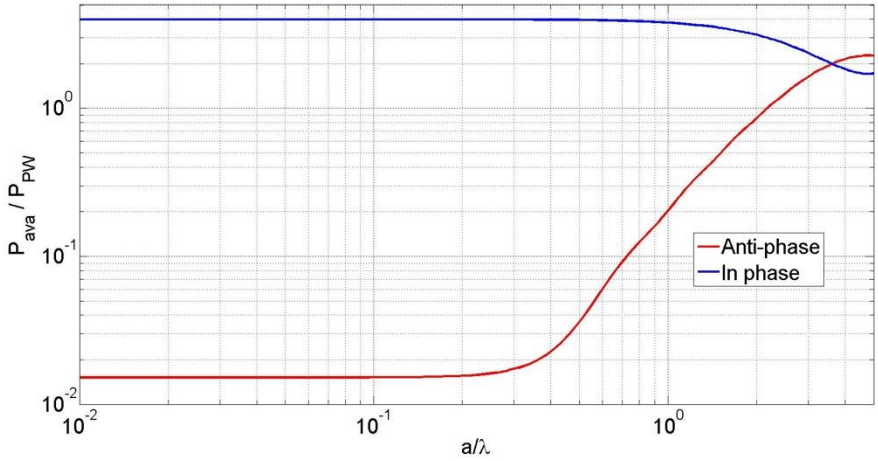

Fig 5. 7) Available power for two incident plane waves plotted as a function of the antenna electrical length and normalized to the power given by the single plane wave incidence case $\theta_{in,1} = \theta_{in,2} = 175°$;

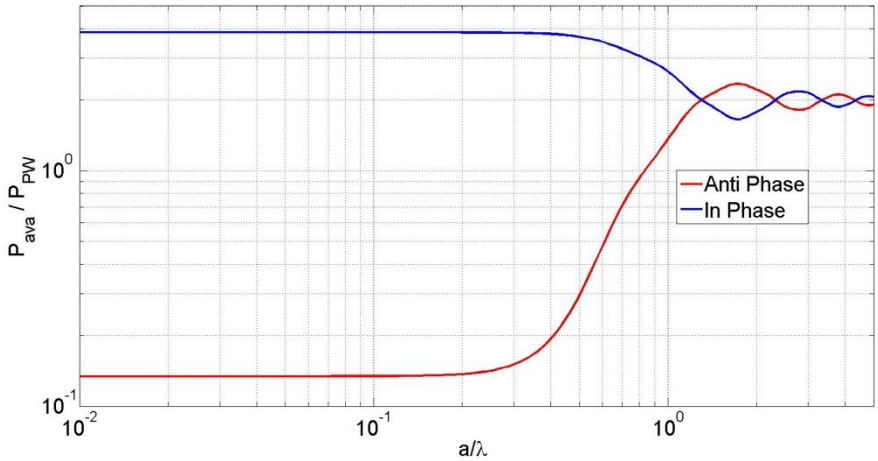

Fig 5. 8) Available power for two incident plane waves plotted as a function of the antenna electrical length and normalized to the power given by the single plane wave incidence case $\theta_{in,1} = \theta_{in,2} = 165°$

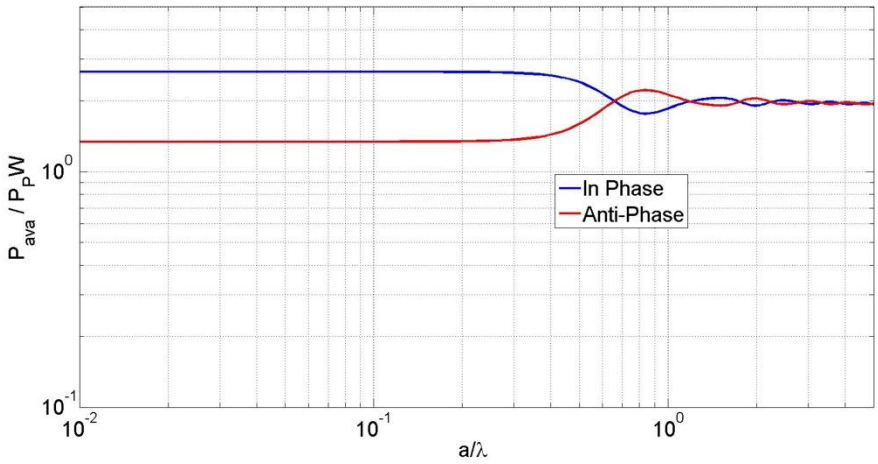

Fig 5. 9) Available power for two incident plane waves plotted as a function of the antenna electrical length and normalized to the power given by the single plane wave incidence case. $\boldsymbol{\theta_{in,1} = \theta_{in,2} = 125°}$

One of the previous cases, namely for $\theta_{in,1} = \theta_{in,2} = 165°$, has been used to compare the Ideal Currents method and the Spherical Modes one. The difference between the two procedures is now even more evident than when opposed to the single plane wave incidence case, and the uncertainty introduced by the quantization process increases. Note that for antenna of radius around $a = \lambda$ the difference is significant: looking at Fig 5.4a, Fig5.4b this is the region where the far field patterns diverged most.

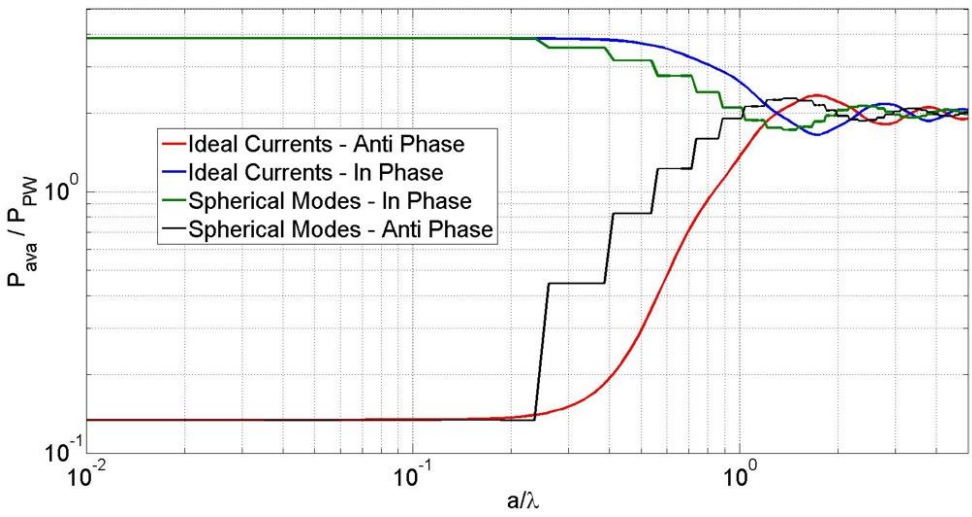

Fig 5. 10) Available power for two incident plane waves plotted as a function of the antenna electrical length and normalized to the power given by the single plane wave incidence case. $\boldsymbol{\theta_{in,1} = \theta_{in,2} = 165°}$. Ideal Currents versus Spherical Modes.

V.e) *Available power as a function of the incident angle*

The available power is now presented as a function of the angle of incidence of the incoming plane waves, namely $\theta_{in,1} = \theta_{in,2} = [180° \rightarrow 90°]$ (or $0° \rightarrow 90°$ when referred to the negative part of the z axis), for both the cases of perfect constructive and destructive interference at the center of the antenna (in phase or in anti-phase). Three different antennae are analyzed: $a = 0.01\lambda, a = \lambda, a = 5\lambda$. The power is normalized to the one evaluated for the single pane wave incidence case, as before. When $\theta_{in} = 180°$ the power is obviously either four times as much or zero, since the fields either perfectly sum up or cancel out each other. When instead $\theta_{in} \rightarrow 90°$ another interesting result emerges: the value of the available power tends once again to be twice as much the one given by a single plane wave incoming from broadside, for both the interference cases. This is because when $\theta_{in} = 90°$ the two plane waves are travelling towards the center of the reference system from exactly opposite directions; if this is the case either one of these two conditions verifies: if the two plane waves are in phase the electric fields sum up while the magnetic fields cancel out, while if they are out of phase the two electric fields cancel out and the magnetic fields add up. As before, it is like the two ideal scattered fields are incoherent, and their power can be summed up independently on from the other.

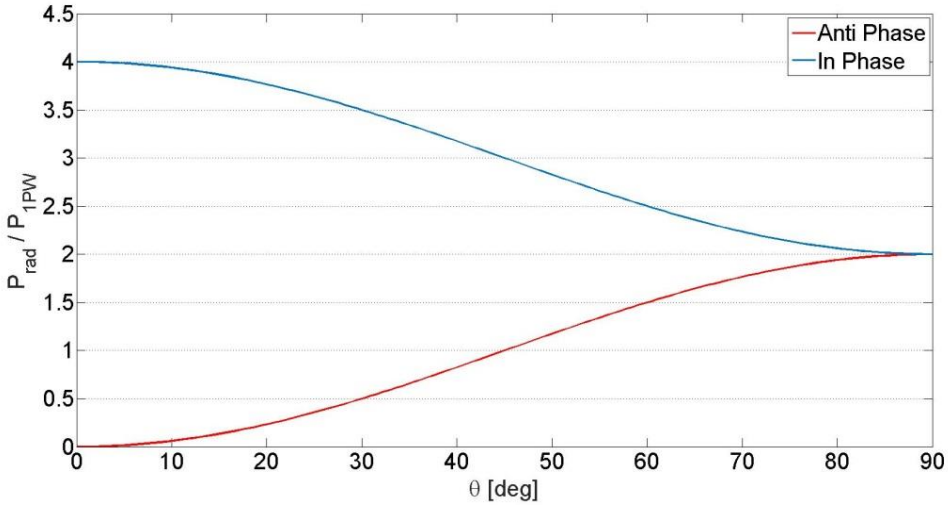

Fig 5. 11) Available power for two incident plane waves plotted as a function of the plane waves incident angle and normalized to the power given by the single plane wave incidence case. $\boldsymbol{a = 0.01\lambda}$

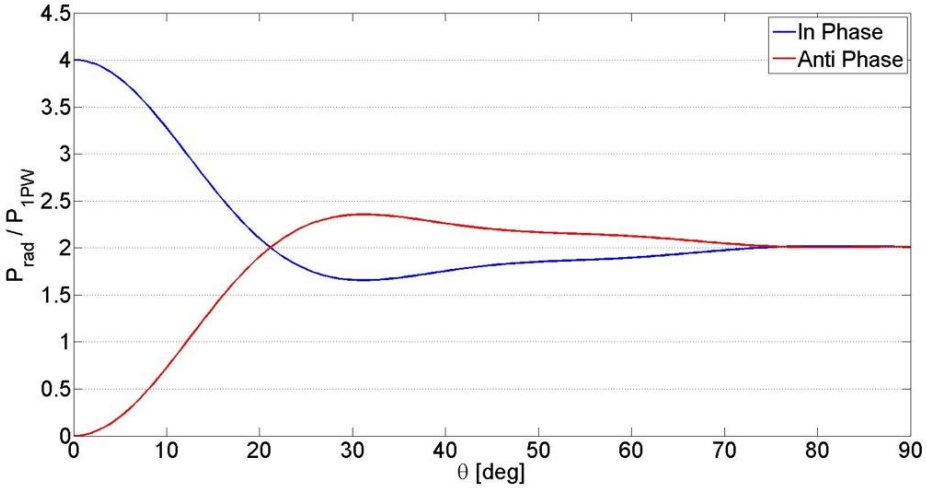

Fig 5. 12) Available power for two incident plane waves plotted as a function of the plane waves incident angle and normalized to the power given by the single plane wave incidence case. $\boldsymbol{a = \lambda}$

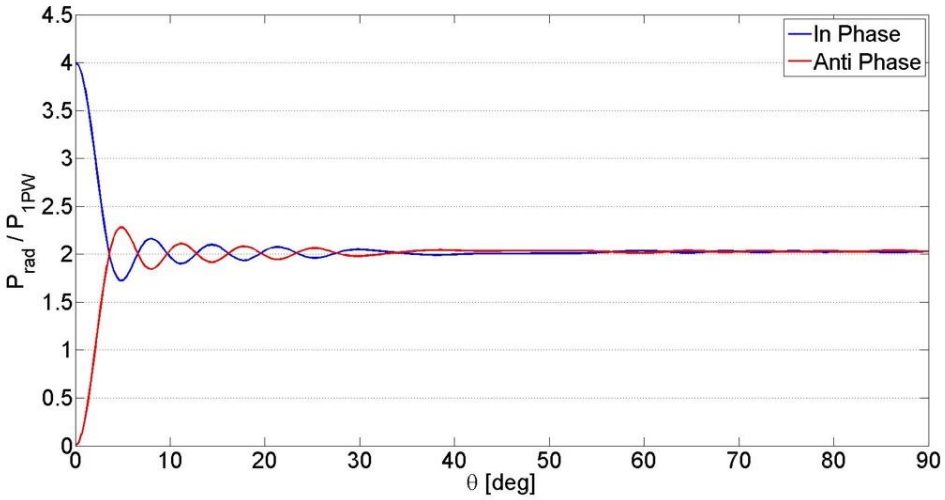

Fig 5. 13) Available power for two incident plane waves plotted as a function of the plane waves incident angle and normalized to the power given by the single plane wave incidence case. $\boldsymbol{a = 5\lambda}$

The biggest differences between the fields estimated by the Ideal Currents method and the Spherical Modes expansion were seen for antennae of radii in the order of $a = \lambda$; thus, for this case a comparison between the two techniques is showed. Note that the quantization effect here is not present, since it depends on $N = ka$, and a is now a fixed parameter. However, the curves relative to the spherical modes expansion are calculate with $N = round(ka) = round(2\pi) = 6$, and the fact that the choice of N is arbitrary has to be stressed again (one could have chosen $N + 1 = 7$ modes and the results would have had the same dignity).

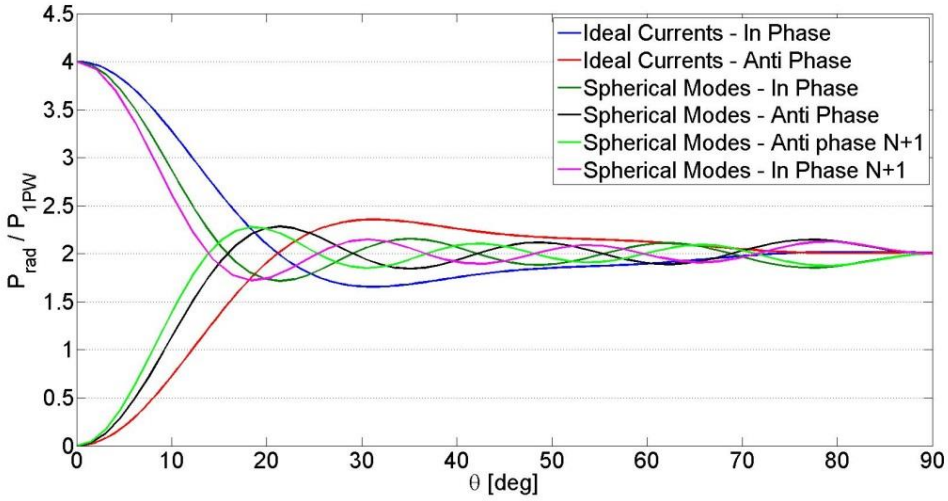

Fig 5. 14) Available power for two incident plane waves plotted as a function of the plane waves incident angle and normalized to the power given by the single plane wave incidence case. Comparison between spherical modes and ideal currents.

VI) CONCLUSIONS

Implicit in the cornerstone article [9] was the definition of the fraction of the incident field able to interact with a generic antenna enclosed in a sphere of radius a. Inspired by it, the novel proposal introduced by this work is to express the incident field as the sum of two distinct components: an 'Observable field', which corresponds to the incident field component the antenna can absorb, and a remaining field, which is substantially zero in the antenna domain. Moreover, the observable field is represented as the sum of two propagating waves: an inward component, that converges towards the antenna domain, and an outward component, that diverges from it. This definition is particularly useful to understand the reception mechanism: the ideal antenna is now considered to be that device absorbing the whole inward propagating component, transforming it into guided waves, and scattering a field that cancels out the outward propagating one. The observable field is identified either as the Lower Order (LO) mode component, by the spherical modes expansion, or as the field whose outward propagating component is equal and opposite to the one radiated by the Ideal Currents. The available power will be associated to the inward component of the observable field.

In order to verify the scientific dignity of the Ideal Currents procedure, the results it predicts have been systematically compared, and then extensively discussed, to the ones given by the Spherical Modes expansion. Both the procedure involve a truncation: spatial truncation around the antenna domain for what concerns the ideal currents, modes truncation based on the antenna domain due to the spherical modes expansion. The available power, expressed in terms of effective area, was taken as the quality parameter to assess whether the procedure was useful: for large and small antennas in terms of wavelength, given a plane wave impinging from broadside, the spherical modes and the ideal currents predict the same values; for the intermediate region, the results are always comparable even if different, but the ideal currents method results are continuous, fact that seems to have solved the quantization error introduced by the modes truncation; moreover, the curve obtained thanks to this work is close to the one given by the heuristic formula. Of course, the estimated available power will have to be compared to real measurements.

Finally, differently from any heuristic formulation that does not account for the relative phase, the procedure has been extended to more generalized cases where the incident field can be approximated as a summation of plane waves. The results have been compared with the

spherical modes technique and then discussed: they are always comparable, although the curves obtained by means of the ideal current technique do not show the controversial quantized behavior belonging to the spherical expansion.

The ideal currents method will be used in the future for the analysis and the design of focusing systems and feeding structures for focal plane arrays.

VII) REFERENCES

[1] C. A. Balanis, Antenna Theory: Analysis and Design, 3rd Edition, John Wiley & Sons, Inc., New Jersey, 2005.

[2] Niamien, M.A.C.; Collardey, S.; Mahdjoubi, K., "A Hybrid Approach for Receiving Antennas: Concepts and Applications," *IEEE Transactions on Antennas and Propagation*, vol.62, no.11, pp.5462-5473, Nov. 2014

[3] Collin, R.E., "Limitations of the Thevenin and Norton equivalent circuits for a receiving antenna," in *Antennas and Propagation Magazine, IEEE* , vol.45, no.2, pp.119-124, April 2003

[4] Andersen, J.B.; Frandsen, A., "Absorption efficiency of receiving antennas," in *IEEE Transactions on Antennas and Propagation*, vol.53, no.9, pp.2843-289, Sept. 2005

[5] C. Sohl, M. Gustafsson, and G. Kristensson, "Physical limitations on broadband scattering by heterogeneous obstacles," J. Phys. A, Math. Theory, vol. 40, pp. 11 165–11 182, 2007.

[6] S. R. Best and B. C. Kaanta, "A Tutorial on the Receiving and Scattering Properties of Antennas," in IEEE Antennas and Propagation Magazine, vol. 51, no. 5, pp. 26-37, Oct. 2009.

[7] Mats Gustafsson, Jørgen Bach Andersen, Gerhard Kristensson, and Gert Frølund Pedersen "Forward Scattering of Loaded and Unloaded Antennas", *IEEE Transactions on Antennas and Propagation*, VOL. 60, NO. 12, DECEMBER 2012 5663

[8] Mats Gustafsson, Member, IEEE, Marius Cismasu, and B. L. G. Jonsson Physical Bounds and Optimal Currents on Antennas , *IEEE Transactions on Antennas and Propagation* VOL. 60, NO. 6, JUNE 2012

[9] Do-Hoon Kwon; Pozar, David M., "Optimal Characteristics of an Arbitrary Receive Antenna," in *IEEE Transactions on Antennas and Propagation* , vol.57, no.12, pp.3720-3727, Dec. 2009

[10] R.F. Harrington. “Time-Harmonic Electromagnetic Fields”, IEEE Press Series on Electromagnetic Wave Theory, Wiley-Interscience, New York, 2001.

[11] E Martini, P-S Kildal, and S Maci ”Degrees of Freedom of the Field and Maximum Directivity” 2016 URSI International Symposium on Electromagnetic Theory (EMTS)

[12] P.-S. Kildal and S. R. Best, “Further investigations of fundamental directivity limitations of small antennas with and without ground planes”, IEEE International Symposium on Antennas and Propagation (IEEE AP-S), San Diego, July 2008

[13] “Radiation and scattering of Waves”, by Leopold Felsen and Nathan Marcuvitz; IEEE Press on Electromagnetic Wave Theory (Book 31); Wiley-IEEE Press (1994)

[14] Do-Hoon Kwon, "On the Radiation Q and the Gain of Crossed Electric and Magnetic Dipole Moments," in Antennas and Propagation, IEEE Transactions on , vol.53, no.5, pp.1681-1687, May 2005

[15] “The Plane Wave Spectrum Representation of Electromagnetic”, by P.C. Clemmow; IEEE Press on Electromagnetic Wave Theory; IEEE Press (1996)

Appendix A

This appendix defines the procedure used to derive the expression for the Ideal Currents, their radiation, and its asymptotical evaluation in the far field region. Let us assume to have a plane wave propagating in z with the electric field polarized along $\hat{\theta}$:

$$\vec{e}_{inc}(\vec{r}) = \vec{E}_{inc} e^{j\vec{k}_i\vec{r}} \tag{A1}$$

Define a set of sources induced by the impinging field on a plane orthogonal to the plane wave propagation direction (z = 0):

$$\vec{m}_{eq}(\vec{r}') = \hat{z} \times \vec{e}_{inc}(\vec{r}) \tag{A2}$$

$$\vec{J}_{eq}(\vec{r}') = -\hat{z} \times \vec{h}_{inc}(\vec{r}) = -\hat{z} \times \left(\frac{1}{\zeta} \hat{k}_{inc} \times \vec{e}_{inc}(\vec{r}) \right) \tag{A3}$$

This set of currents will scatter the incident field, what we need is a field that is equal and opposite its observable component: the Ideal Current will have opposite sign.
Apply the spatial truncation: the ideal currents are defined by means of the PO approximation only on the antenna domain χ, and amplified by a constant factor that depends on the effective area and whose value is explained in Appendix G:

$$\vec{m}_{id}(\vec{r}') = -\hat{z} \times \vec{e}_{inc}(\vec{r}) \chi(\vec{r}', a) C_{amp} \tag{A4}$$

$$\vec{J}_{id}(\vec{r}') = \hat{z} \times \left(\frac{1}{\zeta} \hat{k}_{inc} \times \vec{e}_{inc}(\vec{r}) \right) \chi(\vec{r}', a) C_{amp} \tag{A5}$$

$$\chi(\vec{r}', a) = [\rho' = 0 \div a; \phi' = 0 \div 2\pi] \tag{A6}$$

The far field radiation of this set of currents can be described as the sum of an inward and an outward propagating component. The ideal antenna is that device that absorbs the whole inward component scattering a field that cancels out the outward propagating one.

$$\vec{e}_{rad}(\vec{r}) = \int_0^a \int_0^{2\pi} \left[\tilde{g}^{ej}(\vec{r}, \vec{r}') \vec{J}_{id}(\vec{r}') + \tilde{g}^{em}(\vec{r}, \vec{r}') \vec{m}_{id}(\vec{r}') \right] d\vec{r}' \tag{A7}$$

$$\vec{h}_{rad}(\vec{r}) = \int_0^a \int_0^{2\pi} \left[\tilde{g}^{hj}(\vec{r},\vec{r}')\vec{j}_{id}(\vec{r}') + \tilde{g}^{hm}(\vec{r},\vec{r}')\vec{m}_{id}(\vec{r}')\right] d\vec{r}' \tag{A8}$$

Let us consider only the electric field (the procedure to calculate the magnetic field will be equivalent). Starting from the magnetic and electric vector potentials it is possible to demonstrate that:

$$\vec{e}_{rad}(\vec{r}) = -j\omega\mu \iiint_V \tilde{G}^e(\vec{r},\vec{r}')\vec{j}_{id}(\vec{r}')d\vec{r}' - \iiint_V \tilde{G}^m(\vec{r},\vec{r}')\vec{m}_{id}(\vec{r}')d\vec{r}' \tag{A9}$$

$$\tilde{G}^e(\vec{r},\vec{r}') = \left(\tilde{I} - \frac{\vec{\nabla}\vec{\nabla}}{k^2}\right) g(\vec{r},\vec{r}'); \quad \tilde{G}^m(\vec{r},\vec{r}') = \vec{\nabla} g(\vec{r},\vec{r}') \times \tilde{I} \tag{A10}$$

$$g(\vec{r},\vec{r}') = \frac{e^{-jkR}}{4\pi R}; \quad R = |\vec{r} - \vec{r}'| \tag{A11}$$

Since:

$$\vec{\nabla} g(\vec{r},\vec{r}') = -\left(\frac{1}{R} + jk\right)\frac{e^{-jkR}}{4\pi R}\hat{R} \tag{A12}$$

In the far field $R \gg \lambda$:

$$\vec{\nabla} g(\vec{r},\vec{r}') = -\left(\frac{1}{kR} + j\right) k \frac{e^{-jkR}}{4\pi R}\hat{R} \simeq -jk\frac{e^{-jkR}}{4\pi R}\hat{R} \tag{A13}$$

$$\vec{\nabla} \simeq -jk\hat{R}; \quad \vec{\nabla}\vec{\nabla} = -k^2\hat{R}\hat{R} \tag{A14}$$

this means that:

$$\tilde{G}^e(\vec{r},\vec{r}') = \left(\tilde{I} - \hat{R}\hat{R}\right) g(\vec{r},\vec{r}'); \quad \tilde{G}^m(\vec{r},\vec{r}') = -jk g(\vec{r},\vec{r}')\hat{R} \times \tilde{I} \tag{A15}$$

$$\begin{aligned} \vec{e}_{rad}(\vec{r}) = -jk\zeta \iiint_V \left(\tilde{I} - \hat{R}\hat{R}\right) g(\vec{r},\vec{r}')\vec{j}_{id}(\vec{r}')d\vec{r}' \\ + jk \iiint_V \hat{R} \times \tilde{I} g(\vec{r},\vec{r}')\vec{m}_{id}(\vec{r}')d\vec{r}' \end{aligned} \tag{A16}$$

Also, in the far field, where the vector $\vec{r} - \vec{r}'$ represents the distance from the source to the observation point, the two vectors $\vec{r}, \vec{r}'$ can be considered parallel. Mathematically this is:

$$R = |\vec{r} - \vec{r}'|; \quad \vec{r} \gg \vec{r}' \tag{A17}$$

$$R = \sqrt{(\vec{r} - \vec{r}')(\vec{r} - \vec{r}')} = \sqrt{r^2 - 2\vec{r}\vec{r}' + r'^2} = r\sqrt{1 - \frac{2\vec{r}\vec{r}'}{r^2} + \frac{r'^2}{r^2}} \tag{A18}$$

using Taylor's expansion to the first order

$$R \simeq r\left(1 - \frac{2\vec{r}\vec{r}'}{2r^2} + \frac{r'^2}{2r^2} + \cdots\right) = r - \vec{r}'\hat{r}; \quad |R| \to r; \quad \hat{R} \to \hat{r} \tag{A19}$$

This leads to:

$$\begin{aligned} \vec{e}_{rad}(\vec{r}) = -jk\zeta(\tilde{I} - \hat{r}\hat{r}) \iiint_V \vec{J}_{id}(\vec{r}') \frac{e^{-jk|\vec{r}-\vec{r}'|}}{4\pi|\vec{r} - \vec{r}'|} d\vec{r}' + jk\hat{r} \\ \times \tilde{I} \iiint_V \vec{m}_{id}(\vec{r}') \frac{e^{-jk|\vec{r}-\vec{r}'|}}{4\pi|\vec{r} - \vec{r}'|} d\vec{r}' \end{aligned} \tag{A20}$$

$$\begin{aligned} \vec{e}_{rad}(\vec{r}) \simeq \left[-jk\zeta(\tilde{I} - \hat{r}\hat{r}) \iiint_V \vec{j}(\vec{r}')_{id} e^{jk\vec{r}'\hat{r}} d\vec{r}' + jk\hat{r}\right. \\ \left. \times \tilde{I} \iiint_V \vec{m}_{id}(\vec{r}') e^{jk\vec{r}'\hat{r}} d\vec{r}'\right] \frac{e^{-jkr}}{4\pi r} \end{aligned} \tag{A21}$$

Eventually:

$$\vec{e}_{rad}(\vec{r}) = jk\left[-\zeta(\tilde{I} - \hat{r}\hat{r})\vec{\tilde{J}}_{id}(\vec{k}) + \hat{r} \times \vec{\tilde{M}}_{id}(\vec{k})\right] \frac{e^{-jkr}}{4\pi r} = \vec{E}_{rad}(\vec{r}) \frac{e^{-jkr}}{r} \tag{A22}$$

$$\vec{E}_{rad}(\vec{r}) = \frac{jk}{4\pi}\left[-\zeta(\tilde{I} - \hat{r}\hat{r})\vec{\tilde{J}}_{id}(\vec{k}) + \hat{r} \times \vec{\tilde{M}}_{id}(\vec{k})\right] \tag{A23}$$

Note that this expression underlines the fact the electric field, and so is the magnetic field, is transversely polarized with respect to the direction of propagation of the field. Now, the Fourier's transform of the sources needs to be calculated. First of all, if the plane wave is coming from $\theta_{inc} = 0\ Vel\ \pi \ \rightarrow \ \hat{k}_{inc} = \pm\hat{z}$, and some approximations can be done applying $\boldsymbol{A} \times (\boldsymbol{B} \times \boldsymbol{C}) = (\boldsymbol{AC})\boldsymbol{B} - (\boldsymbol{AB})\boldsymbol{C}$:

$$\vec{J}_{id}(\vec{r}') = -\frac{1}{\zeta}\vec{E}_{inc}(\vec{r}) \tag{A24}$$

$$\vec{J}_{id}(\vec{k}) = \iint_s \vec{J}_{id}(\vec{r}')e^{-jk\vec{r}'\hat{r}}d\vec{r}' = -C_{amp}\frac{1}{\zeta}\vec{E}_{inc}(\vec{r})\iint_s e^{-jk\vec{r}'\hat{r}}d\vec{r}' \tag{A25}$$

$$\begin{aligned}\vec{k}\vec{r}' &= k(sin\Theta cos\Phi\hat{x} + sin\Theta sin\Phi\hat{y} + cos\Theta\hat{z})\rho'(cos\Phi'\hat{x} + sin\Phi'\hat{y}) \\ &= ksin\Theta\rho'\cos(\Phi - \Phi')\end{aligned} \tag{A26}$$

$$FT(\vec{k}) = \int_0^a \int_0^{2\pi} e^{j\vec{k}\vec{r}'}\, dS = \int_0^a \int_0^{2\pi} e^{jksin\theta\rho'\cos(\Phi-\Phi')}\rho' d\rho' d\Phi' \tag{A27}$$

$$FT(\vec{k}) = FT(ksin\theta, a) = 2\pi a^2 \frac{J_1(a, ksin\theta)}{kasin\theta} \tag{A28}$$

Where J_1 is the Bessel's function of order 1, and the whole Fourier's transform is nothing else but the Airy pattern. For the magnetic source the calculation is precisely the same.

$$\vec{J}(\vec{k}) = -C_{amp}\frac{1}{\zeta}\vec{E}_{inc}\{Airy(\vec{k})\} \tag{A29}$$

$$\vec{M}(\vec{k}) = -C_{amp}\hat{z} \times \vec{E}_{inc}\{Airy(\vec{k})\} \tag{A30}$$

Substituting in (A23):

$$\vec{E}_{rad}(\vec{r}) = C_{amp}\frac{jk}{4\pi}\{Airy(\vec{k})\}\left((\tilde{I} - \hat{r}\hat{r})\vec{E}_{inc} - \hat{r} \times (\hat{z} \times \vec{E}_{inc})\right) \tag{A31}$$

$$\vec{E}_{rad}(\vec{r}) = C_{amp}\frac{jk}{4\pi}\{Airy(\vec{k})\}\left(\hat{r} \times \left(\vec{E}_{inc} \times (\hat{r} + \hat{z})\right)\right) \tag{A32}$$

The radiation can be more compactly expressed as in (3.20), (3.21).

Appendix B

This appendix shows how to calculate the antenna effective area, parameter used to estimate the scattered power by the ideal currents. To calculate that we resort first to the time average Poynting vector:

$$\vec{S}_{ave}(\vec{r}) = \frac{1}{2} Re\{\vec{e}_{rad}(\vec{r}) \times \vec{h}_{rad}(\vec{r})^*\} \tag{B1}$$

The Poynting vector is calculated on a sphere located in the far field region, enclosing the antenna and centered in the adopted reference system. We need to calculate the radiation intensity, defined as 'the power radiated from an antenna per unit solid angle'

$$U(\Theta, \Phi) = r^2 S_{ave} = \frac{r^2}{2} Re\{\vec{e}_{\infty}(\vec{r}) \times \vec{h}_{\infty}(\vec{r})^*\} = \frac{r^2}{2\zeta} |\vec{e}_{\infty}(\Theta, \Phi)|^2 \tag{B2}$$

Performing a surface integration of $\vec{S}_{ave}$ would give the total radiated power (integration over any surface enclosing the antenna), so multiplying the Poynting vector by the radius squared we obtain the power density expressed per unitary solid angles.

$$P_{rad} = \int_0^{2\pi} \int_0^{\pi} U(\Theta, \Phi) d\Omega = \int_0^{2\pi} \int_0^{\pi} U(\Theta, \Phi) sin\Theta d\Theta d\Phi \tag{B3}$$

Considering that the average radiated power per unit solid angle is simply the total radiated power divided by the total solid angle, it is immediate to verify that the directivity is:

$$D(\Theta, \Phi) = \frac{U(\Theta, \Phi)}{\frac{P_{rad}}{4\pi}} \tag{B4}$$

Now the maximum effective area of any antenna is related to its maximum directivity through:

Appendix B

$$A_{eff} = \frac{\lambda^2}{4\pi} D_{Max} \tag{B5}$$

Appendix C

This appendix explains how to express the field using the spectral representation of the Green's function and then how to perform an asymptotical evaluation of the radiation in the far field region. Since the further the observation point, the faster the integrand function oscillates (due to its exponential dependence), its numerical evaluation becomes harder and harder to perform. To overcome this problem it is possible to consider the behavior of the function in the far field ($r > 2D^2/\lambda$), that will lead to an expression which is equivalent to (A32). In order to do this we resort to a change of variable to perform an asymptotical evaluation of the far field. The variable change expresses the integrand function as function of (k_ρ, β, α), instead of (k_x, k_y, k_z); Note that both (k_ρ, β, α) are in general complex quantities. Let us first define the radiated electric field using the convolution integral between the spatial Green's functions and the sources (the same steps apply for what concerns the magnetic field):

$$\vec{e}_{rad}(\vec{r}) = \tilde{g}^{ej}(\vec{r},\vec{r}') * \vec{j}_{id}(\vec{r}') + \tilde{g}^{em}(\vec{r},\vec{r}') * \vec{m}_{id}(\vec{r}') \tag{C1}$$

$$\vec{e}_{rad}(\vec{r}) = \iint_{S'} \left[\tilde{g}^{ej}(\vec{r},\vec{r}')\vec{j}_{id}(\vec{r}') + \tilde{g}^{em}(\vec{r},\vec{r}')\vec{m}_{id}(\vec{r}')\right] d\vec{r}' \tag{C2}$$

Now, let us express the spatial Green's function the relates the electric source to the electric field as the 2D anti-Fourier transform of its spectral representation (once again, the derivation is the same for the other components), and then substitute it in (C2):

$$\tilde{g}^{ej}(\vec{r}',\vec{r}) = \frac{1}{4\pi^2}\int_{-\infty}^{+\infty}\int_{-\infty}^{+\infty} \tilde{G}^{ej}(k_x,k_y,z,z') \cdot e^{-jk_x(x-x')}e^{-jk_y(y-y')}e^{-jk_z|z-z'|}\, dk_x dk_y \tag{C3}$$

$$\vec{e}_{rad}(\vec{r}) = \iint_{S'} \frac{1}{4\pi^2}\int_{-\infty}^{+\infty}\int_{-\infty}^{+\infty} \tilde{G}^{ej}(k_x,k_y,z,z') \cdot e^{-jk_x(x-x')}e^{-jk_y(y-y')}e^{-jk_z|z-z'|}\, dk_x dk_y \vec{j}_{id}(\vec{r}')dr' \tag{C4}$$

The integral can be expressed as:

$$\vec{e}_{rad}(\vec{r}) = \frac{1}{4\pi^2}\int_{-\infty}^{+\infty}\int_{-\infty}^{+\infty}\left(\iint_{S'}\vec{J}_{id}(\vec{r}')e^{jk_x x'}e^{jk_y y'}dr'\right) \cdot \tilde{G}^{ej}(k_x,k_y,z,z')e^{-jk_x x}e^{-jk_y y}e^{-jk_z|z-z'|}dk_x dk_y \tag{C5}$$

$$\vec{\tilde{J}}(\vec{k}) = \iint_{S'}\vec{J}_{id}(\vec{r}')e^{jk_x x'}e^{jk_y y'}dr' \tag{C6}$$

It is easy to recognize now the Fourier transform of the current distribution. Let us assume that the source is located at $z' = 0$, the expression turns into:

$$\vec{e}_{rad}(\vec{r}) = \frac{1}{4\pi^2}\int_{-\infty}^{+\infty}\int_{-\infty}^{+\infty}\tilde{G}^{ej}(k_x,k_y,z,z')\vec{\tilde{J}}(\vec{k})e^{-jk_x x}e^{-jk_y y}e^{-jk_z|z|}dk_x dk_y \tag{C7}$$

For this work's configuration, the source are radiating in free space, and the Green's function accounts for it. Adding the magnetic source contribution, and expressing everything in a cylindrical coordinates system:

$$\vec{e}_{rad}(\vec{r}) = \frac{1}{4\pi^2}\int_{0}^{+\infty}\int_{0}^{2\pi}\left(\tilde{G}_{fs}^{ej}(k_x,k_y,z,z')\vec{\tilde{J}}_{id}(k_\rho,a) + \tilde{G}_{fs}^{em}(k_x,k_y,z,z')\vec{\tilde{M}}_{id}(k_\rho,a)\right)e^{-jk_\rho\rho\cos(\alpha-\phi)}e^{-jk_z|z|}k_\rho dk_\rho d\alpha \tag{C8}$$

Now, analyzing for the sake of simplicity only the electric field radiated by the electric current,:

$$\vec{e}_{rad}(\vec{r}) = \frac{1}{4\pi^2}\int_{0}^{+\infty}\int_{0}^{2\pi}\tilde{G}_{fs}^{ej}(k_x,k_y,z,z')\vec{\tilde{J}}_{id}(k_\rho,a)e^{-jk_\rho\rho\cos(\alpha-\phi)}e^{-jk_z|z|}k_\rho dk_\rho d\alpha \tag{C9}$$

$$\tilde{G}_{fs}^{ej}(k_0 sin\beta,\alpha) = -\frac{\zeta}{2k_0 k_z}\tilde{D}_{fs}^{ej}(k_\rho,\alpha) \tag{C10}$$

The chosen change of variable is the following:

$$k_\rho = k_0 sin\beta \tag{C11}$$

$$k_z = \sqrt{k_0^2 - k_\rho^2} = \sqrt{k_0^2 - k_0^2 \sin^2\beta} = \pm k_0 cos\beta \tag{C12}$$

The dyad of this spectral Green's function (4.11) becomes:

$$\tilde{D}_{fs}^{ej}(k_\rho, \alpha) = \begin{bmatrix} k_0^2 - k_0^2 \sin^2\beta \cos^2\alpha & -k_0^2 \sin^2\beta\, sin\alpha cos\alpha & -k_0 sin\beta cos\alpha(\pm k_0 cos\beta) \\ -k_0^2 \sin^2\beta\, sin\alpha cos\alpha & k_0^2 - k_0^2 \sin^2\beta \sin^2\alpha & -k_0 sin\beta sin\alpha(\pm k_0 cos\beta) \\ -k_0 sin\beta cos\alpha(\pm k_0 cos\beta) & -k_0 sin\beta sin\alpha(\pm k_0 cos\beta) & k_0^2 \sin^2\beta - k_0^2 \cos^2\beta \end{bmatrix} \tag{C13}$$

The differential turns into:

$$\frac{dk_\rho}{d\beta} d\beta = k_0 cos\beta d\beta \tag{C14}$$

Substituting (C4), (C5), (C6) in (C2):

$$\vec{e}_{rad}(\vec{r}) = -\frac{1}{8\pi^2}\frac{\zeta}{k_0}\int_0^{\frac{\pi}{2}}\int_0^{2\pi} \frac{1}{k_0 cos\beta} \tilde{D}_{fs}^{ej}(k_0 sin\beta, \alpha)\vec{\tilde{J}}_a(\vec{k}) \cdot e^{-jk_0 sin\beta\, \mathrm{r sin\Theta} \cos(\alpha - \Phi)} e^{-jk_0 r cos\beta |cos\Theta|} k_0^2 sin\beta cos\beta d\alpha d\beta \tag{C15}$$

$$\vec{e}_{rad}(\vec{r}) = -\frac{1}{8\pi^2}\frac{\zeta}{k_0}\int_0^{\frac{\pi}{2}}\int_0^{2\pi} \frac{1}{k_0 cos\beta} \tilde{D}_{fs}^{ej}(k_0 sin\beta, \alpha)\vec{\tilde{J}}_a(\vec{k}) \cdot e^{-jk_0 r(sin\beta\, \mathrm{sin\Theta} \cos(\alpha - \Phi) + cos\beta |cos\Theta|)} k_0^2 sin\beta cos\beta d\alpha d\beta \tag{C16}$$

When evaluating the radiation at large distance from the source this integrand function oscillates really fast. However, it presents much slowly varying points as a function of θ, ϕ (saddle points) that will determine the final result (the integration of the remaining part will give zero, since it adds and subtract continuously really close quantities). Looking into the exponential dependence one derives the first saddle point:

$$\frac{\partial}{\partial\alpha}(sin\beta\, \mathrm{sin\Theta} \cos(\alpha - \Phi) + cos\beta |cos\Theta|) = 0 \tag{C17}$$

$$\frac{\partial}{\partial\alpha}(sin\beta\, \mathrm{sin\Theta} \cos(\alpha - \Phi) + cos\beta |cos\Theta|) = -sin\beta\, \mathrm{sin\Theta} \sin(\alpha - \Phi) = 0 \tag{C18}$$

$$\alpha_s = N\pi + \Phi \tag{C19}$$

The saddle points are numerically periodical, but the result they represent is not always physical. Indeed, we have to describe the propagation of waves, and we're doing it using a spherical coordinates system. This system is defined for $\Theta = [0 \to \pi], \Phi = [0 \to 2\pi]$. This means that also the saddle points we're going to evaluate the field at will have to respect these boundaries. Also, for every observation point we perform an integration in (β, α), which are defined in a spherical coordinate system as well. Moreover, they have to satisfy the domain where the integrand function is defined:

$$\beta \in \left(0 \to \frac{\pi}{2}\ V\ \frac{\pi}{2} \to \pi\right), \alpha \in (0 \to 2\pi) \tag{C20}$$

Thus, the for the two hemisphere $(z < 0, z > 0)$ there is only one possible saddle point for α, and it is:

$$\alpha = \Phi\ (for\ N = 0) \tag{C21}$$

Also, the choice of the N is independent on the observation hemisphere, that depends only on θ. Now, from Balanis, Advanced Engineering Electromagnetics (pag. 963), we know that evaluating a function in its saddle points along a complex integration path leads to the following expression:

$$I(\beta) = \int_C F(z) e^{\beta f(z)} dz \simeq \sqrt{\frac{2\pi}{-\beta f''(z_s)}} F(z_s) e^{\beta f(z_s)} \tag{C22}$$

let's split the integration for the upper and bottom plane.

Positive root:

$$k_z = +k_0 cos\beta \to \left(z > 0, \Theta < \frac{\pi}{2}\right) \tag{C23}$$

the α saddle point is $\alpha_s = \Phi$. Integrating along $d\alpha$ first it is apparent that:

$$F(z) = \frac{1}{k_0 cos\beta} \widetilde{D}_{fs}^{ej}(k_0 sin\beta, \alpha) \vec{\tilde{J}}_a(k_0 sin\beta, \alpha) k_0^2 sin\beta cos\beta \tag{C24}$$

$$e^{\beta f(z)} = e^{-jk_0 r(sin\beta\ \sin\Theta\cos(\alpha-\Phi)+cos\beta|cos\Theta|)} \tag{C25}$$

$$\beta = k_0 r \tag{C26}$$

$$f(z) = -j(sin\beta\ \sin\Theta\cos(\alpha-\Phi) + cos\beta|cos\Theta|) \tag{C27}$$

$$f(z_s) = -j(sin\beta sin\Theta + cos\beta|cos\Theta|) \tag{C28}$$

$$f''(z) = -j(-sin\beta\ \sin\Theta\cos(\alpha-\Phi)) \tag{C29}$$

$$f''(z_s) = jsin\beta\ \sin\Theta \tag{C30}$$

Thus:

$$\vec{e}_{rad}(\vec{r}) \simeq -\frac{1}{8\pi^2}\frac{\zeta}{k_0}\int_0^{\frac{\pi}{2}} \sqrt{\frac{2\pi}{-jk_0 r sin\beta sin\Theta}}\, \widetilde{D}_{fs}^{ej}(k_0 sin\beta, \alpha_s) \cdot \vec{\tilde{J}}_a(k_0 sin\beta, \alpha_s)\, e^{-jk_0 r(cos\beta|cos\Theta|+sin\beta sin\Theta)} (k_0 sin\beta) d\beta \tag{C31}$$

$$\vec{e}_{rad}(\vec{r}) = -\frac{1}{8\pi^2}\frac{\zeta}{k_0}\int_0^{\frac{\pi}{2}} \sqrt{\frac{2\pi}{-jr sin\Theta}}\, \widetilde{D}_{fs}^{ej}(k_0 sin\beta, \alpha_s) \cdot \vec{\tilde{J}}_a(k_0 sin\beta, \alpha_s)\, e^{-jk_0 r(cos\beta|cos\Theta|+sin\beta sin\Theta)} \left(\sqrt{k_0 sin\beta}\right) d\beta \tag{C32}$$

This expression highlights the second saddle point:

$$\frac{\partial}{\partial\beta}(cos\beta|cos\Theta| + sin\beta sin\Theta) = 0 \tag{C33}$$

In this half space ($z - z_c > 0$) we can remove the modulus ($\Theta > \pi/2 \rightarrow cos\Theta > 0$). This way we obtain:

$$\frac{\partial}{\partial\beta}(cos\beta|cos\Theta| + sin\beta sin\Theta) = \frac{\partial}{\partial\beta}\left(k_0 r cos(\beta - \Theta)\right) = -k_0 r sin(\beta - \Theta) = 0 \tag{C34}$$

$$\beta_s = N\pi + \Theta \tag{C35}$$

Now again, since the saddle point must agree with the integral variables boundaries we chose ($\beta \in [0, \pi/2]$) and since in this hemisphere $\Theta \in [0, \pi/2]$ the only possible choice is:

$$\beta_s = \Theta \tag{C36}$$

$$I(\beta) = \int_C F(z) e^{\beta f(z)} dz \simeq \sqrt{\frac{2\pi}{-\beta f''(z_s)}} F(z_s) e^{\beta f(z_s)} \tag{C37}$$

$$F(z) = \tilde{D}_{fs}^{ej}(k_0 sin\beta, \alpha_s) \vec{\tilde{J}}_a(k_0 sin\beta, \alpha_s) \sqrt{k_0 sin\beta} \tag{C38}$$

$$e^{\beta f(z)} = e^{-jk_0 r(cos\beta|cos\Theta| + sin\beta sin\Theta)} \tag{C39}$$

$$f(z) = -jk_0(cos\beta|cos\Theta| + sin\beta sin\Theta) \tag{C40}$$

$$f(z_s) = -jk_0(cos\Theta|cos\Theta| + sin\Theta sin\Theta) \tag{C41}$$

since $z - z_c > 0 \rightarrow |cos\Theta| = cos\Theta$

$$f(z_s) = -jk_0 \tag{C42}$$

$$f''(z) = -jk_0(-cos\beta|cos\Theta| - sin\beta sin\Theta) \tag{C43}$$

$$f''(z_s) = -jk_0(-cos\Theta|cos\Theta| - sin\Theta sin\Theta) \tag{C44}$$

since $z - z_c > 0 \rightarrow |cos\Theta| = cos\Theta$

$$f''(z_s) = jk_0 \tag{C45}$$

so from:

$$\vec{e}_{rad}(\vec{r}) \simeq -\frac{1}{8\pi^2}\frac{\zeta}{k_0}\int_0^{\frac{\pi}{2}} \sqrt{\frac{2\pi}{-jrsin\Theta}}\, \tilde{D}_{fs}^{ej}(k_0 sin\beta, \alpha_s) \cdot \vec{\tilde{J}}_a(k_0 sin\beta, \alpha_s)\, e^{-jk_0 r(cos\beta|cos\Theta| + sin\beta sin\Theta)} \sqrt{k_0 sin\beta}\, d\beta \tag{C46}$$

we obtain:

$$\begin{aligned} &\vec{e}_{rad}(\vec{r}) \\ &\simeq -\frac{1}{8\pi^2}\frac{\zeta}{k_0}\sqrt{\frac{2\pi}{-jrsin\Theta}}\sqrt{\frac{2\pi}{-jk_0 r}}\, \tilde{D}_{fs}^{ej}(k_0 sin\beta_s, \alpha_s)\vec{\tilde{J}}_a(k_0 sin\beta_s, \alpha_s)\sqrt{k_0 sin\beta_s}\, e^{-jk_0 r} \\ &= -\frac{1}{8\pi^2}\frac{\zeta}{k_0}\frac{2\pi}{r}\sqrt{\frac{sin\beta_s}{j^2 sin\Theta}}\, \tilde{D}_{fs}^{ej}(k_0 sin\beta_s, \alpha_s)\vec{\tilde{J}}_a(k_0 sin\beta_s, \alpha_s) e^{-jk_0 r} \end{aligned} \tag{C47}$$

$$\vec{e}_{rad}(\vec{r}) = j\frac{\zeta}{k_0}\,\tilde{D}_{fs}^{ej}(k_0 sin\beta_s, \alpha_s)\vec{\tilde{J}}_a(k_0 sin\beta_s, \alpha_s)\frac{e^{-jk_0 r}}{4\pi r}$$
$$= -jk_z\,\tilde{G}_{fs}^{ej}(k_0 sin\beta_s, \alpha_s)\vec{\tilde{J}}_a(k_0 sin\beta_s, \alpha_s)\frac{e^{-jk_0 r}}{2\pi r} \quad \text{(C48)}$$

Negative root:

$$k_z = -k_0 cos\beta \rightarrow \left(z < 0, \Theta > \frac{\pi}{2}\right) \quad \text{(C49)}$$

$$\vec{e}_{rad}(\vec{r}) = -\frac{1}{8\pi^2}\frac{\zeta}{k_0}\int_0^{\frac{\pi}{2}}\int_0^{2\pi}\frac{1}{k_0 cos\beta}\tilde{D}_{fs}^{ej}(k_0 sin\beta, \alpha)$$
$$\cdot\vec{\tilde{J}}_a(\vec{k})e^{-jk_0 r(sin\beta\,\sin\Theta\cos(\alpha-\Phi)+cos\beta|cos\theta|)}\,k_0^2 sin\beta cos\beta d\alpha d\beta \quad \text{(C50)}$$

First saddle point:

$$\frac{\partial}{\partial\alpha}(sin\beta\,\sin\Theta\cos(\alpha-\Phi)+cos\beta|cos\Theta|) = 0 \quad \text{(C51)}$$

$$\frac{\partial}{\partial\alpha}(sin\beta\,\sin\Theta\cos(\alpha-\Phi)+cos\beta|cos\Theta|) = -sin\beta\,\sin\Theta\sin(\alpha-\Phi) = 0 \quad \text{(C52)}$$

$$\alpha_s = N\pi + \Phi \quad \text{(C53)}$$

We are observing a wave propagating in $z < 0$, but remember the domain we are integrating the function in is:

$$\alpha_s = \Phi \quad \text{(C54)}$$

The first integration result is already known:

$$\vec{e}_{rad}(\vec{r}) \simeq -\frac{1}{8\pi^2}\frac{\zeta}{k_0}\int_0^{\frac{\pi}{2}}\sqrt{\frac{2\pi}{-jrsin\Theta}}\tilde{D}_{fs}^{ej}(k_0 sin\beta, \alpha_s)$$
$$\cdot\vec{\tilde{J}}_a(k_0 sin\beta, \alpha_s)\,e^{-jk_0 r(sin\beta\,\sin\Theta+cos\beta|cos\theta|)}\sqrt{k_0 sin\beta}\,d\beta \quad \text{(C55)}$$

This expression highlights the second saddle point:

$$\frac{\partial}{\partial\beta}\left(-jk_0r(cos\beta|cos\Theta|+sin\beta sin\Theta)\right)=0 \tag{C56}$$

Since:

$$z-z_c<0\rightarrow|cos\Theta|=-cos\Theta \tag{C57}$$

$$\frac{\partial}{\partial\beta}\left((cos\beta|cos\Theta|+sin\beta sin\Theta)\right)=-\frac{\partial}{\partial\beta}\left(cos(\beta+\Theta)\right) \tag{C58}$$

$$-\frac{\partial}{\partial\beta}\left(cos(\beta+\Theta)\right)=\sin(\beta+\Theta)=0 \tag{C59}$$

$$\beta_s=N\pi-\Theta \tag{C60}$$

Again, the only possible choice of the saddle point is:

$$\beta_s=\pi-\Theta \tag{C61}$$

$\beta\in[0,\pi/2]$ indeed, and in this hemisphere $\Theta\in[\pi/2,\pi]$. Now, again:

$$I(\beta)=\int_C F(z)e^{\beta f(z)}dz\simeq\sqrt{\frac{2\pi}{-\beta f''(z_s)}}F(z_s)e^{\beta f(z_s)} \tag{C62}$$

$$F(z)=\widetilde{D}_{fs}^{ej}(k_0sin\beta,\alpha_s)\vec{\tilde{J}}_a(k_0sin\beta,\alpha_s)\sqrt{k_0sin\beta} \tag{C63}$$

$$e^{\beta f(z_s)}=e^{-jk_0r(sin\beta\,\sin\Theta+cos\beta|cos\Theta|)} \tag{C64}$$

$$\beta=k_0r \tag{C65}$$

$$f(z)=-j(sin\beta\,\sin\Theta+cos\beta|cos\Theta|) \tag{C66}$$

$$f''(z)=-jk_0(-cos\beta|cos\Theta|-sin\beta sin\Theta) \tag{C67}$$

$$\begin{aligned}f(z_s)&=-j(\cos(\pi-\Theta)|cos\Theta|+\sin(\pi-\Theta)sin\Theta)\\&=-j(-\cos\Theta|cos\Theta|+\sin\Theta sin\Theta)=-j\end{aligned} \tag{C68}$$

$$\begin{aligned}f''(z_s)&=-j(-\cos(\pi-\Theta)|cos\Theta|-\sin(\pi-\Theta)sin\Theta)\\&=-j(\cos\Theta|cos\Theta|-\sin\Theta sin\Theta)=j\end{aligned} \tag{C69}$$

Substituting in (C48):

$$\vec{e}_{rad}(\vec{r})$$

$$\simeq -\frac{1}{8\pi^2}\frac{\zeta}{k_0}\sqrt{\frac{2\pi}{-jrsin\Theta}}\sqrt{\frac{2\pi}{-jk_0r}}\tilde{D}_{fs}^{ej}(k_0sin\beta_s,\alpha_s)\vec{\tilde{J}}_a(k_0sin\beta_s,\alpha_s)\sqrt{k_0sin\beta_s}e^{-jk_0r} \quad \text{(C70)}$$

$$= -\frac{1}{8\pi^2}\frac{\zeta}{k_0}\frac{2\pi}{r}\sqrt{\frac{sin\beta_s}{j^2sin\Theta}}\tilde{D}_{fs}^{ej}(k_0sin\beta_s,\alpha_s)\vec{\tilde{J}}_a(k_0sin\beta_s,\alpha_s)e^{-jk_0r}$$

$$\vec{e}_{rad}(\vec{r}) = -j\frac{\zeta}{k_0}\tilde{D}_{fs}^{ej}(k_0sin\beta_s,\alpha_s)\vec{\tilde{J}}_a(k_0sin\beta_s,\alpha_s)\frac{e^{-jk_0r}}{4\pi r} \quad \text{(C71)}$$

$$= -jk_z\,\tilde{G}_{fs}^{ej}(k_0sin\beta_s,\alpha_s)\vec{\tilde{J}}_a(k_0sin\beta_s,\alpha_s)\frac{e^{-jk_0r}}{2\pi r} = \vec{e}_s(\vec{r})$$

Note that the result here is different compared to the previous one, since the saddle point is different.

Subtracting and then adding again this term we eventually obtain the wanted result:

$$\vec{e}_{rad}^{tot}(\vec{r})$$

$$= \frac{1}{4\pi^2}\int_0^{+\infty}\int_0^{2\pi}\tilde{G}_{fs}^{ej}(k_x,k_y,z,z')\vec{\tilde{J}}_{id}(k_\rho,a)e^{-jk_\rho\rho\cos(\alpha-\phi)}e^{-jk_z|z|}k_\rho dk_\rho d\alpha \quad \text{(C72)}$$

$$-\vec{e}_s(\vec{r}) + \vec{e}_s(\vec{r})$$

$$\vec{e}_{rad}^{tot}(\vec{r}_\infty) = \vec{e}_{osc}(\vec{r}_\infty) + \vec{e}_s(\vec{r}_\infty) \simeq \vec{e}_s(\vec{r}_\infty) \quad \text{(C73)}$$

Indeed, $\vec{e}_{osc}(\vec{r}_\infty) \to 0$, since it's characterized only by highly oscillating terms

Appendix D

This appendix shows how to make asymptotical considerations regarding the dimension of the antenna we're analyzing whether it is small, or large, in terms of the wavelength. In these situations either the Airy or the Huygens pattern tend to be dominant. The far field pattern can be expressed as in (A32):

$$\vec{E}_{rad}(\vec{r}) = C_{amp}\frac{jk}{4\pi}\{Airy(\vec{k})\}\left(\hat{r}\times\left(\vec{E}_{inc}\times(\hat{r}+\hat{z})\right)\right) = C_{amp}V_{PO}^{outw}\left(a,\vec{r},\vec{k}_{in}\right) \quad \text{(D1)}$$

$$V_{PO}^{outw}\left(a,\vec{r},\vec{k}_{in}\right) = Airy(ksin\theta,a)\vec{H}(\vec{r}_{\infty},\vec{k}_{in}) \quad \text{(D2)}$$

This is the result for a single incoming plane wave. However, the following derivations are already generalized for the case of multiple impinging plane waves.

Small antennas:

In this case the portion of the incident field the antenna can interact with is defined by the antenna itself and its properties, rather than the sources. If the ratio $a/\lambda \to 0$ the Airy pattern turns out to behave essentially as a constant as a function of $\vec{k}$:

$$\lim_{a\to 0} Airy\left(\hat{r}_{in},\vec{k}\right) = \pi a^2 \quad \text{(D3)}$$

This means that $V_{PO}^{outw}\left(a,\vec{r},\vec{k}_{in}\right)$ is essentially characterized by an averaging integral over $\vec{H}_{in}\left(\hat{r}_{in},\vec{k}\right)$. The result turns out to be:

$$\lim_{a\to 0}\vec{e}_{rad}(\vec{r}_{\infty}) = \frac{e^{-jkr_{\infty}}}{r_{\infty}}C_{amp}\int_0^{2\pi}\int_0^{\pi}\lim_{a\to 0}V_{PO}^{outw}\left(a,\vec{r},\vec{k}_{in}\right)sin\beta_{in}d\beta_{in}d\alpha_{in} \quad \text{(D4)}$$

$$\lim_{a\to 0}V_{PO}^{outw}\left(a,\vec{r},\vec{k}_{in}\right) = \lim_{a\to 0}\frac{A_{eff}}{A_{phys}}Airy\left(\hat{r}_{in},\vec{k}\right)\vec{H}_{in}\left(\hat{r}_{in},\vec{k}\right) \quad \text{(D5)}$$

$$\lim_{a\to 0}A_{eff} = \frac{3}{4\pi}\lambda^2 \quad \text{(D6)}$$

$$\lim_{a\to 0}V_{PO}^{outw}\left(a,\vec{r},\vec{k}_{in}\right) = \frac{3}{4\pi}\lambda^2\vec{H}_{in}\left(\hat{r}_{in},\vec{k}\right) \quad \text{(D7)}$$

Expressing as β_{in},α_{in} the direction of incidence of each impinging plane wave:

$$\lim_{a\to 0}\vec{e}_{rad}(\vec{r}_\infty)$$
$$=\left[\frac{3}{4\pi}\lambda^2\frac{jk}{4\pi}\right]\int_0^{2\pi}\int_0^{\pi}\hat{k}\times\left[\vec{E}_{in}(\beta_{in},\alpha_{in})\times\left(\hat{k}-\hat{r}_{in}\right)\right]sin\beta_{in}d\beta_{in}d\alpha_{in}\frac{e^{-jkr_\infty}}{r_\infty}$$
$$=\left[j\frac{3}{4k}\right]\int_0^{2\pi}\int_0^{\pi}\hat{k}\times\left[\vec{E}_{in}(\beta_{in},\alpha_{in})\times\left(\hat{k}-\hat{r}_{in}\right)\right]sin\beta_{in}d\beta_{in}d\alpha_{in}\frac{e^{-jkr_\infty}}{r_\infty} \quad \text{(D8)}$$

This last expression underlines two different contributes to the radiated electric field: one from the electric source and the other one from the magnetic one. The total field can thus be expressed as the superposition of two integrals:

$$\lim_{a\to 0}\vec{e}_{rad}(\vec{r}_\infty)=j\frac{3}{4k}\left(\vec{F}_{el}(\vec{k})-\vec{F}_{mag}(\vec{k})\right)\frac{e^{-jkr_\infty}}{r_\infty} \quad \text{(D9)}$$

$$\vec{F}_{el}(\vec{k})=\hat{k}\times\left(\int_0^{2\pi}\int_0^{\pi}\vec{E}_{in}(\beta_{in},\alpha_{in})sin\beta_{in}d\beta_{in}d\alpha_{in}\times\hat{k}\right) \quad \text{(D10)}$$

$$\vec{F}_{mag}(\vec{k})=\hat{k}\times\left(\int_0^{2\pi}\int_0^{\pi}\vec{E}_{in}(\beta_{in},\alpha_{in})sin\beta_{in}d\beta_{in}d\alpha_{in}\times\hat{r}_{in}\right) \quad \text{(D11)}$$

Looking at:

$$\vec{e}_{inc}(\vec{r})$$
$$=\int_0^{2\pi}\int_0^{\pi}\vec{e}_{in}(\beta_{in},\alpha_{in})e^{-kr(sin\beta_{in}cos\alpha_{in}\cos(\alpha_{in}-\Phi)+cos\beta_{in}cos\Theta)}\,sin\beta_{in}d\beta_{in}d\alpha_{in} \quad \text{(D12)}$$

It is apparent that the two contribution are just:

$$\vec{F}_{el}(\vec{k})=\vec{e}_{inc}(\vec{r}=0) \quad \text{(D13)}$$

$$\vec{F}_{mag}(\vec{k}) = \hat{k} \times \left(\int_0^{2\pi} \int_0^{\pi} \vec{E}_{in}(\beta_{in}, \alpha_{in}) sin\beta_{in} d\beta_{in} d\alpha_{in} \times \hat{r}_{in} \right)$$
$$= \hat{k} \times \left(\int_0^{2\pi} \int_0^{\pi} \hat{k}_{in} \times \vec{E}_{in}(\beta_{in}, \alpha_{in}) sin\beta_{in} d\beta_{in} d\alpha_{in} \right)$$
$$= \zeta \hat{k} \times \vec{h}_{inc}(\vec{r} = 0) \tag{D14}$$

Without considering the spherical spreading it results:

$$\lim_{a \to 0} V_{PO}^{outw}(a, \vec{r}, \vec{k}_{in}) = j \frac{3}{4k} \left(\vec{F}_{el}(\vec{k}) - \vec{F}_{mag}(\vec{k}) \right)$$
$$= j \frac{3}{4k} \left(\vec{e}_{in}(\vec{r} = 0) - \zeta \hat{k} \times \vec{h}_{in}(\vec{r} = 0) \right)$$
$$= j \frac{3}{4k} \left(\hat{k} \times \vec{e}_{in}(\vec{r} = 0) \times \hat{k} - \hat{k} \times \hat{k}_{in} \times \vec{e}_{in}(\vec{r} = 0) \right)$$
$$= j \frac{3}{4k} \hat{k} \left(\vec{e}_{in}(\vec{r} = 0) \times \left(\hat{k} + \hat{k}_{in} \right) \right) \tag{D15}$$

Note that in the end, for the case of electrically really small antennas excited by a bunch of plane waves with generalized incidence direction, the outward propagating wave results as it was radiated by a couple of electric and magnetic dipoles with an intensity that is directly proportional to the intensity of the incident field itself in the origin of the reference system (the antenna domain). Attention has to be paid to the fact that the radiated field does not correspond to a pure Huygens' source anymore, but to a superposition of multiple Huygens' sources instead. However, the small dipole radiation pattern is characterized by a relatively small directivity, and so is the superposition of the fields radiated by more dipoles, thus the radiated field would not present steep angular transitions, even if the incident field amplitude $\vec{E}_{in}(\beta_{in}, \alpha_{in})$ is a rapidly varying function of β_{in}, α_{in}. Small antennas are thus not able to observe this kind of fields, but only an angular average of them.

LARGE ANTENNAS:

For what concerns large antennas in terms of wavelength ($a/\lambda \gg 1$) other considerations and assumptions can be made to simplify the radiated (or the observable) field expression. First of all the effective area tends to value really close to the physical one, so that:

$$A_{eff} \to A_{phys}; \quad C_{amp} \to 1 \tag{D16}$$

The Airy pattern becomes more and more directive (not just a constant anymore), and significantly different from zero only when observing it at directions opposite to the ones of the incident wave vector $\hat{k} \simeq -\hat{r}_{in} \to \Theta \simeq \beta_{in}$. Now, let us expand the expression of the Huygens' pattern using the following vector property: $\boldsymbol{A \times (B \times C) = (AC)B - (AB)C.}$

$$\begin{aligned}\vec{H}_{in}(a, \hat{r}_{in}, \vec{k}) &= \frac{jk}{4\pi}\hat{k} \times \left[\vec{E}_{in}(\beta_{in}, \alpha_{in}) \times (\hat{k} - \hat{r}_{in})\right] \\ &= \frac{j}{2\lambda}\vec{E}_{in}(\beta_{in}, \alpha_{in})\left(\hat{k}(\hat{k} - \hat{r}_{in})\right) \\ &- \frac{j}{2\lambda}(\hat{k} - \hat{r}_{in})\left(\hat{k}\vec{E}_{in}(\beta_{in}, \alpha_{in})\right)\end{aligned} \tag{D17}$$

Since the Huygens' source pattern will be multiplied by the Airy pattern, which we said is different from zero only around the direction of incidence of every single wave, the expression can be written as:

$$\begin{aligned}&\vec{H}_{in}(a, \hat{r}_{in}, \vec{k}, \Theta \simeq \beta_{in}) \\ &= \frac{j}{2\lambda}\vec{E}_{in}(\beta_{in}, \alpha_{in})(-\hat{r}_{in}(-\hat{r}_{in} - \hat{r}_{in})) \\ &- \frac{j}{2\lambda}(-\hat{r}_{in} - \hat{r}_{in})\left(-\hat{r}_{in}\vec{E}_{in}(\beta_{in}, \alpha_{in})\right)\end{aligned} \tag{D18}$$

Obviously the incident plane wave electric field polarization is always orthogonal to its propagation direction, so the second term of the right hand side of the equation is equal to zero, thus:

$$\vec{H}_{in}(a, \hat{r}_{in}, \vec{k}, \Theta \simeq \beta_{in}) = \frac{j}{\lambda}\vec{E}_{in}(\beta_{in}, \alpha_{in}) \tag{D19}$$

$$V_{PO}^{outw}(a, \hat{r}_{in}, \vec{k}, \Theta \simeq \beta_{in}) = \frac{j}{\lambda}\vec{E}_{in}(\beta_{in}, \alpha_{in})Airy(\vec{k}_{in}, \vec{k}, \Theta \simeq \beta_{in}) \tag{D20}$$

Consequently, the integral of the outward-going observable total field can be simplified

$$\vec{e}_{rad}(r,\vec{k}) = \int_0^{2\pi}\int_0^{\pi} V_{PO}^{outw}(a,\vec{r},\vec{k}_{in}) sin\beta_{in} d\beta_{in} d\alpha_{in} \frac{e^{-jkr_\infty}}{r_\infty}$$

$$= \frac{j}{\lambda} 2\pi a^2 \int_0^{2\pi}\int_0^{\pi} \frac{J_1(k'_\rho a)}{k'_\rho a} \vec{E}_{in}(\beta_{in},\alpha_{in}) sin\beta_{in} d\beta_{in} d\alpha_{in} \frac{e^{-jkr_\infty}}{r_\infty} \quad \text{(D21)}$$

This integral is in general of difficult evaluation, because of the geometrical dependence of k'_ρ. However, for the present case, other approximations can be made. We know that $\vec{k}_{in} = -k\hat{r}_{in}$, and being γ the angle between $\hat{r}_{in}$ and $\hat{k}$ in the 'primed' reference system described by $\hat{z}' = -\hat{r}_{in}$ it is easy to appreciate that:

$$\hat{k}\hat{z}' = \hat{k}(-\hat{r}_{in}) = -cos\gamma \quad \text{(D22)}$$

$$\gamma = arcos(-\hat{k}\hat{r}_{in}) \quad \text{(D23)}$$

Looking at $\vec{k}\vec{k}_{in} = k^2 cos\gamma$ suggests to express $k'_\rho = ksin\gamma$ in terms of $|\vec{k} - \vec{k}_{in}|$, so:

$$|\vec{k} - \vec{k}_{in}|^2 = (\vec{k} - \vec{k}_{in})(\vec{k} - \vec{k}_{in}) = 2k^2(1 - cos\gamma)\hat{k}\hat{z}' = \hat{k}(-\hat{r}_{in}) = -cos\gamma \quad \text{(D24)}$$

$$cos\gamma^2 = \left(\frac{|\vec{k} - \vec{k}_{in}|^2}{2k^2} - 1\right)^2 \quad \text{(D25)}$$

Expanding the right hand side of the equation we obtain:

$$cos\gamma^2 = \left(\frac{|\vec{k} - \vec{k}_{in}|^2}{2k^2}\right)^2 - \frac{|\vec{k} - \vec{k}_{in}|^2}{k^2} + 1 \quad \text{(D26)}$$

$$sin\gamma^2 = \frac{|\vec{k} - \vec{k}_{in}|^2}{k^2} - \left(\frac{|\vec{k} - \vec{k}_{in}|^2}{2k^2}\right)^2 \quad \text{(D27)}$$

$$sin\gamma^2 = \frac{|\vec{k} - \vec{k}_{in}|^2}{k^2}\left(1 - \frac{|\vec{k} - \vec{k}_{in}|^2}{4k^2}\right) \quad \text{(D28)}$$

Remember that in this particular case, the only significant contribution comes from observation points such that $|\vec{k} - \vec{k}_{in}| \to 0$, so we can expand $sin\gamma$ around that point:

$$sin\gamma = \frac{\left|\vec{k}-\vec{k}_{in}\right|}{k}\sqrt{1-\frac{\left|\vec{k}-\vec{k}_{in}\right|^2}{4k^2}} \simeq \frac{\left|\vec{k}-\vec{k}_{in}\right|}{k}\left(1-\frac{\left|\vec{k}-\vec{k}_{in}\right|^2}{8k^2}\right) \quad \text{(D29)}$$

So that, for very large antenna, where $\left|\vec{k}-\vec{k}_{in}\right| \to 0$ one can consider $sin\gamma \simeq \left|\vec{k}-\vec{k}_{in}\right|$, which renders the equation:

$$\vec{e}_{rad}(\vec{r}) \simeq \frac{j}{\lambda}2\pi a^2 \int_0^{2\pi}\int_0^{\pi} \frac{J_1\left(\left|\vec{k}-\vec{k}_{in}\right|a\right)}{\left|\vec{k}-\vec{k}_{in}\right|a}\vec{E}_{in}(\beta_{in},\alpha_{in})sin\beta_{in}d\beta_{in}d\alpha_{in}\frac{e^{-jkr_\infty}}{r_\infty} \quad \text{(D30)}$$

As already stated, the Airy pattern is significantly different than zero only towards $\hat{r}_{in}$. Let us call $[0-\Theta_m]$ the Θ integration range, where Θ_m is an angle much larger than $\Theta_0 = \beta'$, so that the integral in that point is already zero. Let us parametrize the equation defining $[\beta',\alpha']$ as the angles that describe the observation point with respect to the squinted reference system $[x',y',z']$, and calling $\left|\vec{k}-\vec{k}_{in}\right| = |k'| = ksin\beta'$. The integral is different from zero only around $\beta' \to 0$. Besides, $\vec{E}_{in}(\beta',\alpha')$ variations as a function of $[\beta',\alpha']$ are much slower with respect to the ones of the Airy pattern, they can be considered constant around this region, and then extracted from the integral.

$$\begin{aligned}\vec{e}_{rad}(\vec{r}) &\simeq \frac{j}{\lambda}2\pi a^2\vec{E}_{in}(\beta'\to 0,\alpha')\int_0^{2\pi}\int_0^{\Theta_m}\frac{J_1(ksin\beta' a)}{ksin\beta' a}sin\beta' d\beta' d\alpha'\frac{e^{-jkr_\infty}}{r_\infty} \\ &= \frac{j}{\lambda ka}2\pi a^2\vec{E}_{in}(\to 0,\alpha')\int_0^{2\pi}\int_0^{\Theta_m}J_1(ksin\beta' a)d\beta' d\alpha'\frac{e^{-jkr_\infty}}{r_\infty}\end{aligned} \quad \text{(D31)}$$

The integral can be now closed analytically in α'

$$\begin{aligned}\vec{e}_{rad}(\vec{r}) &= \frac{j}{\lambda ka}(2\pi a)^2\vec{E}_{in}(\beta'\to 0,\alpha')\int_0^{\Theta_m}J_1(ksin\beta' a)d\beta'\frac{e^{-jkr_\infty}}{r_\infty} \\ &= j2\pi a\vec{E}_{in}(\beta'\to 0,\alpha')\int_0^{\Theta_m}J_1(ksin\beta' a)d\beta'\frac{e^{-jkr_\infty}}{r_\infty}\end{aligned} \quad \text{(D32)}$$

Remember that we are performing the integration in $d\beta' d\alpha'$, so $\Theta_m \to \beta' \to 0$ due to the high directivity of the Airy pattern, so $sin\beta' \to \beta'$

$$\vec{e}_{rad}(\vec{r}) = j2\pi a\vec{E}_{in}(\beta' \to 0, \alpha') \int_0^{\Theta_m} J_1(k\beta' a) d\beta' \frac{e^{-jkr_\infty}}{r_\infty} \tag{D33}$$

Applying the following change of variable $k\beta' a = x \to d\beta' = \frac{dx}{ka}$ allows us to perform the last integration analytically

$$\vec{e}_{rad}(\vec{r}) = j\frac{2\pi a}{ka}\vec{E}_{in}(\beta' \to 0, \alpha') \int_0^{\Theta_m ka} J_1(x) dx \frac{e^{-jkr_\infty}}{r_\infty} \tag{D34}$$

$$\vec{e}_{rad}(\vec{r}) = j\lambda\vec{E}_{in}(\beta' \to 0, \alpha') \int_0^{\Theta_m ka} J_1(x) dx \frac{e^{-jkr_\infty}}{r_\infty} \tag{D35}$$

$$\vec{e}_{rad}(\vec{r}) = j\lambda\vec{E}_{in}(\beta' \to 0, \alpha')[1 - J_0(\Theta_m ka)] \tag{D36}$$

$$\vec{e}_{rad}(\vec{r}) \simeq j\lambda\vec{E}_{in}(\Theta, \Phi)\lambda \tag{D37}$$

Appendix E

This appendix shows how to analytically close the radiation integrals, when expressed in cylindrical coordinates (k_ρ, α), in α in order to reduce the numerical evaluation to only one variable, decreasing a lot the computational time. Let us first recall the integral, considering now only the electric field given by the electric currents:

$$\vec{e}_{rad}(\vec{r}) = \frac{1}{4\pi^2}\int_0^{+\infty}\int_0^{2\pi} \tilde{G}_{fs}^{ej}(k_x, k_y, z, z')\vec{\tilde{J}}_{id}(k_\rho, a)e^{-jk_\rho\rho\cos(\alpha-\phi)}e^{-jk_z|z|}k_\rho dk_\rho d\alpha \quad \text{(E1)}$$

Since the Fourier transform of the current distribution is independent on α, the only dependence of the integrand function on α lays in the Green's function dyad and in the exponential terms. These are all oscillating terms, which means that the integral can be analytically closed, using Bessel's functions, with the following expression already listed in Chapter IV.a:

$$CC = \int_0^{2\pi} \cos^2\alpha\, e^{-jk_\rho\rho\cos(\alpha-\Phi)}d\alpha = \frac{1}{2}\int_0^{2\pi}(1+\cos(2\alpha))e^{-jk_\rho\rho\cos(\alpha-\Phi)}d\alpha \quad \text{(E2)}$$

$$SS = \int_0^{2\pi} \sin^2\alpha\, e^{-jk_\rho\rho\cos(\alpha-\Phi)}d\alpha = \frac{1}{2}\int_0^{2\pi}(1-\cos(2\alpha))e^{-jk_\rho\rho\cos(\alpha-\Phi)}d\alpha \quad \text{(E3)}$$

$$SC = \int_0^{2\pi} sin\alpha\, cos\alpha\, e^{-jk_\rho\rho\cos(\alpha-\Phi)}d\alpha = \frac{1}{2}\int_0^{2\pi}\sin(2\alpha)\, e^{-jk_\rho\rho\cos(\alpha-\Phi)}d\alpha \quad \text{(E4)}$$

$$C = \int_0^{2\pi} cos\alpha\, e^{-jk_\rho\rho\cos(\alpha-\Phi)}d\alpha \quad \text{(E5)}$$

$$S = \int_0^{2\pi} sin\alpha\, e^{-jk_\rho\rho\cos(\alpha-\Phi)}d\alpha \quad \text{(E6)}$$

The integral expressions at the right hand side have analytical results, with the form:

$$\int_0^{2\pi} \begin{matrix} cos \\ sin \end{matrix}(N\alpha)\, e^{-jk_\rho\rho\cos(\alpha-\Phi)}d\alpha = j^{-N}2\pi \begin{matrix} cos \\ sin \end{matrix}(N\Phi)J_N(k_\rho\rho) \quad \text{(E7)}$$

And the results are:

$$CC = \pi\left(J_0(k_\rho\rho) - \cos(2\Phi)\,J_2(k_\rho\rho)\right) \tag{E8}$$

$$SS = \pi\left(J_0(k_\rho\rho) + \cos(2\Phi)\,J_2(k_\rho\rho)\right) \tag{E9}$$

$$SC = -\pi\sin(2\Phi)\,J_2(k_\rho\rho) \tag{E10}$$

$$C = -j2\pi\,cos\Phi\,J_1(k_\rho\rho) \tag{E11}$$

$$S = -j2\pi\,sin\Phi\,J_1(k_\rho\rho) \tag{E12}$$

Where J_N are the Bessel function of integer order N. Let us have a look at the specific field components. Starting from (E1), and recalling the spectral Green's function expression:

$$\tilde{G}_{fs}^{ej}(k_x,k_y,z,z') = \frac{-\zeta}{2k_0k_z}\begin{bmatrix} k_0^2 - k_\rho^2\cos^2\alpha & -k_\rho^2 sin\alpha cos\alpha & -k_\rho cos\alpha(\pm k_z) \\ -k_\rho^2 sin\alpha cos\alpha & k_0^2 - k_\rho^2\sin^2\alpha & -k_\rho sin\alpha(\pm k_z) \\ -k_\rho cos\alpha(\pm k_z) & -k_\rho sin\alpha(\pm k_z) & k_0^2 - k_z^2 \end{bmatrix} \tag{E13}$$

The components result:

xx Component:

$$\begin{aligned}
&\vec{e}_{xx}^{ej}(\vec{r}) \\
&= -\frac{1}{8\pi^2}\frac{\zeta}{k_0}\int_0^{\infty}\int_0^{2\pi}\frac{k_0^2 - k_\rho^2\cos^2\alpha}{k_z}\vec{\tilde{J}}_{id,x}(\vec{k}_\rho)e^{-jk_\rho\rho\cos(\alpha-\Phi)}e^{-jk_z|z|}k_\rho dk_\rho d\alpha \\
&= -\frac{1}{8\pi^2}\frac{\zeta}{k_0}\left\{\int_0^{\infty}\frac{k_0^2}{k_z}\vec{\tilde{J}}_{id,x}(\vec{k}_\rho)e^{-jk_z|z|}k_\rho\int_0^{2\pi}e^{-jk_\rho\rho\cos(\alpha-\Phi)}d\alpha dk_\rho\right. \\
&\left. - \int_0^{\infty}\frac{k_\rho^2}{k_z}\vec{\tilde{J}}_{id-x}(\vec{k}_\rho)e^{-jk_z|z|}k_\rho\int_0^{2\pi}\cos^2\alpha\, e^{-jk_\rho\rho\cos(\alpha-\Phi)}d\alpha dk_\rho\right\} \\
&= -\frac{1}{8\pi^2}\frac{\zeta}{k_0}\left\{2\pi\int_0^{+\infty}\frac{k_0^2}{k_z}\vec{\tilde{J}}_{id,x}(\vec{k}_\rho)J_0(k_\rho\rho)e^{-jk_z|z|}k_\rho dk_\rho\right. \\
&\left. - \pi\int_0^{+\infty}\frac{k_\rho^2}{k_z}\vec{\tilde{J}}_{id,x}(\vec{k}_\rho)\left[J_0(k_\rho\rho) - \cos(2\Phi)\,J_2(k_\rho\rho)\right]e^{-jk_z|z|}k_\rho dk_\rho\right\} \\
&= -\frac{1}{8\pi}\frac{\zeta}{k_0}\left\{\int_0^{+\infty}\frac{1}{k_z}\vec{\tilde{J}}_{id,x}(\vec{k}_\rho)\left[2k_0^2J_0(k_\rho\rho)\right.\right. \\
&\left.\left. - k_\rho^2\left(J_0(k_\rho\rho) - \cos(2\Phi)\,J_2(k_\rho\rho)\right)\right]e^{-jk_z|z|}k_\rho dk_\rho\right\}
\end{aligned} \tag{E14}$$

xy Component:

$$\begin{aligned}
&\vec{e}_{xy}^{ej}(\vec{r}) \\
&= -\frac{1}{8\pi^2}\frac{\zeta}{k_0}\int_0^{\infty}\int_0^{2\pi}\frac{-k_\rho^2 sin\alpha cos\alpha}{k_z}\vec{\tilde{J}}_{id,y}(\vec{k}_\rho)e^{-jk_\rho\rho\cos(\alpha-\Phi)}e^{-jk_z|z|}k_\rho dk_\rho d\alpha \\
&= \frac{1}{8\pi^2}\frac{\zeta}{k_0}\int_0^{\infty}\frac{k_\rho^2}{k_z}\vec{\tilde{J}}_{id,y}(\vec{k}_\rho)e^{-jk_z|z|}k_\rho\int_0^{2\pi}sin\alpha cos\alpha e^{-jk_\rho\rho\cos(\alpha-\Phi)}d\alpha\, dk_\rho \\
&= -\frac{1}{8\pi}\frac{\zeta}{k_0}\int_0^{\infty}\frac{k_\rho^2}{k_z}\vec{\tilde{J}}_{id,y}(\vec{k}_\rho)\sin(2\Phi)J_2(k_\rho\rho)e^{-jk_z|z|}k_\rho dk_\rho
\end{aligned} \tag{E15}$$

xz Component:

$$\begin{aligned}
&\vec{e}_{xz}^{ej}(\vec{r}) \\
&= -\frac{1}{8\pi^2}\frac{\zeta}{k_0}\int_0^{\infty}\int_0^{2\pi}\frac{-k_\rho cos\alpha(\pm k_z)}{k_z}\vec{\tilde{J}}_{id,z}(\vec{k}_\rho)e^{-jk_\rho\rho\cos(\alpha-\Phi)}e^{-jk_z|z|}k_\rho dk_\rho d\alpha \\
&= -\frac{1}{8\pi^2}\frac{\zeta}{k_0}\int_0^{\infty}\frac{-k_\rho(\pm k_z)}{k_z}\vec{\tilde{J}}_{id,z}(\vec{k}_\rho)e^{-jk_z|z|}k_\rho\int_0^{2\pi}cos\alpha e^{-jk_\rho\rho\cos(\alpha-\Phi)}d\alpha dk_\rho \\
&= -j\frac{1}{4\pi}\frac{\zeta}{k_0}\int_0^{\infty}\pm k_\rho\vec{\tilde{J}}_{id,z}(\vec{k}_\rho)\,cos\Phi\,J_1(k_\rho\rho)e^{-jk_z|z|}k_\rho dk_\rho
\end{aligned} \tag{E16}$$

yx Component:

$$\begin{aligned}
&\vec{e}_{yx}^{ej}(\vec{r}) \\
&= -\frac{1}{8\pi^2}\frac{\zeta}{k_0}\int_0^{\infty}\int_0^{2\pi}\frac{-k_\rho^2 sin\alpha cos\alpha}{k_z}\vec{\tilde{J}}_{id,x}(\vec{k}_\rho)e^{-jk_\rho\rho\cos(\alpha-\Phi)}\,e^{-jk_z|z|}k_\rho dk_\rho d\alpha \\
&= -\frac{1}{8\pi}\frac{\zeta}{k_0}\int_0^{\infty}\frac{k_\rho^2}{k_z}\vec{\tilde{J}}_{id,x}(\vec{k}_\rho)\sin(2\Phi)J_2(k_\rho\rho)e^{-jk_z|z|}k_\rho dk_\rho
\end{aligned} \tag{E17}$$

yy Component:

$$
\begin{aligned}
&\vec{e}_{yy}^{ej}(\vec{r}) \\
&= -\frac{1}{8\pi^2}\frac{\zeta}{k_0}\int_0^{\infty}\int_0^{2\pi}\frac{k_0^2 - k_\rho^2\sin^2\alpha}{k_z}\vec{\tilde{J}}_{id,y}(\vec{k}_\rho)e^{-jk_\rho\rho\cos(\alpha-\Phi)}\,e^{-jk_z|z|}k_\rho dk_\rho d\alpha \\
&= -\frac{1}{8\pi^2}\frac{\zeta}{k_0}\left\{\int_0^{\infty}\frac{k_0^2}{k_z}\vec{\tilde{J}}_{id,y}(\vec{k}_\rho)e^{-jk_z|z|}k_\rho\int_0^{2\pi}e^{-jk_\rho\rho\cos(\alpha-\Phi)}d\alpha dk_\rho\right. \\
&\left.-\int_0^{\infty}\frac{k_\rho^2}{k_z}\vec{\tilde{J}}_{id,y}(\vec{k}_\rho)e^{-jk_z|z|}k_\rho\int_0^{2\pi}\sin^2\alpha\,e^{-jk_\rho\rho\cos(\alpha-\Phi)}d\alpha dk_\rho\right\} \\
&= -\frac{1}{8\pi^2}\frac{\zeta}{k_0}\left\{2\pi\int_0^{+\infty}\frac{k_0^2}{k_z}\vec{\tilde{J}}_{id,y}(\vec{k}_\rho)J_0(k_\rho\rho)e^{-jk_z|z|}k_\rho dk_\rho\right. \\
&\left.-\pi\int_0^{+\infty}\frac{k_\rho^2}{k_z}\vec{\tilde{J}}_{id,y}(\vec{k}_\rho)\left[J_0(k_\rho\rho)+\cos(2\Phi)J_2(k_\rho\rho)\right]e^{-jk_z|z|}k_\rho dk_\rho\right\} \\
&= -\frac{1}{8\pi}\frac{\zeta}{k_0}\left\{\int_0^{+\infty}\frac{1}{k_z}\vec{\tilde{J}}_{id,y}(\vec{k}_\rho)\left[2k_0^2J_0(k_\rho\rho)\right.\right. \\
&\left.\left.-k_\rho^2\left(J_0(k_\rho\rho)+\cos(2\Phi)J_2(k_\rho\rho)\right)\right]e^{-jk_z|z|}k_\rho dk_\rho\right\}
\end{aligned}
\tag{E18}
$$

yz Component:

$$
\begin{aligned}
&\vec{e}_{yz}^{ej}(\vec{r}) \\
&= -\frac{1}{8\pi^2}\frac{\zeta}{k_0}\int_0^{\infty}\int_0^{2\pi}\frac{-k_\rho sin\alpha(\pm k_z)}{k_z}\vec{\tilde{J}}_{id,z}(\vec{k}_\rho)e^{-jk_\rho\rho\cos(\alpha-\Phi)}e^{-jk_z|z|}k_\rho dk_\rho d\alpha \\
&= -\frac{1}{8\pi^2}\frac{\zeta}{k_0}\int_0^{\infty}\frac{-k_\rho(\pm k_z)}{k_z}\vec{\tilde{J}}_{id,z}(\vec{k}_\rho)e^{-jk_z|z|}k_\rho\int_0^{2\pi}sin\alpha e^{-jk_\rho\rho\cos(\alpha-\Phi)}d\alpha\,dk_\rho \\
&= -j\frac{1}{4\pi}\frac{\zeta}{k_0}\int_0^{\infty}\pm k_\rho\vec{\tilde{J}}_{id,z}(\vec{k}_\rho)sin\Phi J_1(k_\rho\rho)e^{-jk_z|z|}k_\rho dk_\rho
\end{aligned}
\tag{E19}
$$

zx Component:

$$\begin{aligned}
&\vec{e}_{zx}^{ej}(\vec{r}) \\
&= -\frac{1}{8\pi^2}\frac{\zeta}{k_0}\int_0^{\infty}\int_0^{2\pi}\frac{-k_\rho cos\alpha(\pm k_z)}{k_z}\vec{\tilde{J}}_{id,x}(\vec{k}_\rho)e^{-jk_\rho\rho\cos(\alpha-\Phi)}\,e^{-jk_z|z|}k_\rho dk_\rho d\alpha \\
&= -j\frac{1}{4\pi}\frac{\zeta}{k_0}\int_0^{\infty}\frac{k_\rho(\pm k_z)}{k_z}\vec{\tilde{J}}_{id,x}(\vec{k}_\rho)\,cos\Phi\,J_1(k_\rho\rho)e^{-jk_z|z|}k_\rho dk_\rho \\
&= -j\frac{1}{4\pi}\frac{\zeta}{k_0}\int_0^{\infty}\pm k_\rho\vec{\tilde{J}}_{id,x}(\vec{k}_\rho)\,cos\Phi\,J_1(k_\rho\rho)e^{-jk_z|z|}k_\rho dk_\rho
\end{aligned} \tag{E20}$$

zy Component:

$$\begin{aligned}
&\vec{e}_{zy}^{ej}(\vec{r}) \\
&= -\frac{1}{8\pi^2}\frac{\zeta}{k_0}\int_0^{\infty}\int_0^{2\pi}\frac{-k_\rho sin\alpha(\pm k_z)}{k_z}\vec{\tilde{J}}_{id,y}(\vec{k}_\rho)e^{-jk_\rho\rho\cos(\alpha-\Phi)}\,e^{-jk_z|z|}k_\rho dk_\rho d\alpha \\
&= -j\frac{1}{4\pi}\frac{\zeta}{k_0}\int_0^{\infty}\frac{k_\rho(\pm k_z)}{k_z}\vec{\tilde{J}}_{id,y}(\vec{k}_\rho)sin\Phi J_1(k_\rho z)e^{-jk_z|z|}k_\rho dk_\rho \\
&= -j\frac{1}{4\pi}\frac{\zeta}{k_0}\int_0^{\infty}\pm k_\rho\vec{\tilde{J}}_{id,y}(\vec{k}_\rho)sin\Phi J_1(k_\rho\rho)e^{-jk_z|z|}k_\rho dk_\rho
\end{aligned} \tag{E21}$$

zz Component:

$$\begin{aligned}
\vec{e}_{zz}^{ej}(\vec{r}) &= -\frac{1}{8\pi^2}\frac{\zeta}{k_0}\int_0^{\infty}\frac{k_0^2-k_z^2}{k_z}\vec{\tilde{J}}_{id,z}(\vec{k}_\rho)e^{-jk_z|z|}k_\rho\int_0^{2\pi}e^{-jk_\rho\rho\cos(\alpha-\Phi)}\,d\alpha\,dk_\rho \\
&= -\frac{1}{4\pi}\frac{\zeta}{k_0}\int_0^{\infty}\frac{k_0^2-k_z^2}{k_z}\vec{\tilde{J}}_{id,z}(\vec{k}_\rho)J_0(k_\rho\rho)e^{-jk_z|z|}k_\rho dk_\rho
\end{aligned} \tag{E22}$$

Let us consider now the magnetic source contribution to the electric field. First of all, the spectral Green's function expression is:

$$\tilde{G}_{fs}^{em}(k_x,k_y,z,z') = -\frac{j}{2k_z}\begin{bmatrix} 0 & \pm jk_z & -jk_\rho sin\alpha \\ \mp jk_z & 0 & jk_\rho cos\alpha \\ jk_\rho sin\alpha & -jk_\rho cos\alpha & 0 \end{bmatrix} \tag{E23}$$

Now, closing the integral in α for every single dyad component:

xx Component:

$$\vec{e}_{xx}^{em}(\vec{r}) = 0 \tag{E24}$$

xy Component:

$$\begin{aligned}\vec{e}_{xy}^{em}(\vec{r}) &= -\frac{j}{8\pi^2}\int_0^{2\pi}\int_0^{+\infty}\frac{\pm jk_z}{k_z}\vec{\tilde{M}}_{id,y}(k_\rho,\alpha)e^{-jk_\rho\,\rho\cos(\alpha-\Phi)}e^{-jk_z|z|}k_\rho dk_\rho d\alpha \\ &= -\frac{j}{8\pi^2}\int_0^{+\infty}\frac{\pm jk_z}{k_z}\vec{\tilde{M}}_{id,y}(k_\rho,\alpha)e^{-jk_z|z|}k_\rho\int_0^{2\pi}e^{-jk_\rho\rho\cos(\alpha-\Phi)}d\alpha\, dk_\rho) \\ &= \frac{1}{4\pi}\int_0^{+\infty}\pm\vec{\tilde{M}}_{id,y}(k_\rho,\alpha)J_0(k_\rho\rho)e^{-jk_z|z|}k_\rho dk_\rho\end{aligned} \tag{E25}$$

xz Component:

$$\begin{aligned}\vec{e}_{xz}^{em}(\vec{r}) &= -\frac{j}{8\pi^2}\int_0^{2\pi}\int_0^{+\infty}\frac{-jk_\rho sin\alpha}{k_z}\vec{\tilde{M}}_{id,z}(k_\rho)e^{-jk_\rho\rho\,\cos(\alpha-\Phi)}e^{-jk_z|z|}k_\rho dk_\rho d\alpha \\ &= -\frac{1}{8\pi^2}\int_0^{+\infty}\frac{k_\rho}{k_z}\vec{\tilde{M}}_{id,z}(k_\rho)e^{-jk_z|z|}k_\rho\int_0^{2\pi}sin\alpha e^{-jk_\rho\rho\cos(\alpha-\Phi)}d\alpha\, dk_\rho \\ &= \frac{j}{4\pi}\int_0^{+\infty}\frac{k_\rho}{k_z}\vec{\tilde{M}}_{id,z}(k_\rho)\,sin\Phi\,J_1(k_\rho\rho)e^{-jk_z|z|}k_\rho dk_\rho\end{aligned} \tag{E26}$$

yx Component:

$$\begin{aligned}\vec{e}_{yx}^{em}(\vec{r}) &= -\frac{j}{8\pi^2}\int_0^{2\pi}\int_0^{+\infty}\frac{\mp jk_z}{k_z}\vec{\tilde{M}}_{id,x}(k_\rho)e^{-jk_\rho\rho\,\cos(\alpha-\Phi)}e^{-jk_z|z|}k_\rho dk_\rho d\alpha = \\ &= -\frac{j}{4\pi}\int_0^{+\infty}\frac{\mp jk_z}{k_z}\vec{\tilde{M}}_{id,x}(k_\rho)J_0(k_\rho\rho)e^{-jk_z|z|}k_\rho dk_\rho \\ &= \frac{1}{4\pi}\int_0^{+\infty}\mp\vec{\tilde{M}}_{id,x}(k_\rho)J_0(k_\rho\rho)e^{-jk_z|z|}k_\rho dk_\rho\end{aligned} \tag{E27}$$

yy Component:

$$\vec{e}_{yy}^{em}(\vec{r}) = 0 \tag{E28}$$

yz Component:

$$\begin{aligned}\vec{e}_{yx}^{em}(\vec{r}) &= -\frac{j}{8\pi^2}\int_0^{2\pi}\int_0^{+\infty}\frac{jk_\rho cos\alpha}{k_z}\vec{\widetilde{M}}_{id,z}(k_\rho)e^{-jk_\rho\rho\cos(\alpha-\Phi)}e^{-jk_z|z|}k_\rho dk_\rho d\alpha \\ &= \frac{1}{8\pi^2}\int_0^{+\infty}\frac{k_\rho}{k_z}\vec{\widetilde{M}}_{id,z}(k_\rho)e^{-jk_z|z|}k_\rho\int_0^{2\pi}cos\alpha e^{-jk_\rho\rho\cos(\alpha-\Phi)}d\alpha\ dk_\rho \\ &= -\frac{j}{4\pi}\int_0^{+\infty}\frac{k_\rho}{k_z}\vec{\widetilde{M}}_{id,z}(k_\rho)cos\Phi\, J_1(k_\rho\rho)e^{-jk_z|z|}k_\rho\, dk_\rho\vec{E}_{yy}(\vec{r}) = 0\end{aligned} \tag{E29}$$

zx Component:

$$\begin{aligned}\vec{e}_{zx}^{em}(\vec{r}) &= -\frac{j}{8\pi^2}\int_0^{2\pi}\int_0^{+\infty}\frac{jk_\rho sin\alpha}{k_z}\vec{\widetilde{M}}_{id,x}(k_\rho)e^{-jk_\rho\rho\cos(\alpha-\Phi)}e^{-jk_z|z|}k_\rho dk_\rho d\alpha \\ &= -j\frac{1}{4\pi}\int_0^{+\infty}\frac{k_\rho}{k_z}\vec{\widetilde{M}}_{id,x}(k_\rho)\, sin\Phi\, J_1(k_\rho\rho)e^{-jk_z|z|}k_\rho dk_\rho\end{aligned} \tag{E30}$$

zy Component:

$$\begin{aligned}\vec{e}_{zy}^{em}(\vec{r}) &= -\frac{j}{8\pi^2}\int_0^{2\pi}\int_0^{+\infty}\frac{-jk_\rho cos\alpha}{k_z}\vec{\widetilde{M}}_{id,y}(k_\rho)e^{-jk_\rho\rho\cos(\alpha-\Phi)}e^{-jk_z|z|}k_\rho dk_\rho d\alpha \\ &= \frac{j}{4\pi}\int_0^{+\infty}\frac{k_\rho}{k_z}\vec{\widetilde{M}}_{id,y}(k_\rho)cos\Phi\, J_1(k_\rho\rho)e^{-jk_z|z|}k_\rho\, dk_\rho\end{aligned} \tag{E31}$$

zz Component:

$$\vec{e}_{zz}^{em}(\vec{r}) = 0 \tag{E32}$$

Appendix E

As far as the magnetic field is concerned, it is sufficient to substitute the proper constants in the spectral Green's functions in (4.18), (4.19), (4.20), (4.21), the operations are the same.

Appendix F

This appendix explains how to derive the steepest descent path given a certain exponential dependence in the integral function. This path ensures the fastest convergence of the integrand function, increasing the speed of its numerical evaluation. Let us analyze the expression:

$$e^{-jk_0 r\cos(\beta-\Theta)} \quad where \quad \beta = \beta_r + j\beta_i \tag{F1}$$

With a few straight forward mathematical identities one obtains:

$$e^{-jk_0 r\cos(\beta-\Theta)} = e^{-jk_0 r\cos(\beta_r-\Theta)\frac{e^{\beta_i}+e^{-\beta_i}}{2}} e^{-k_0 r\sin(\beta_r-\Theta)\frac{e^{\beta_i}-e^{-\beta_i}}{2}} \tag{F2}$$

In order to have a convergent integrand function the second part of this expression must be finite, which means :

$$\sin(\beta_r-\Theta)\frac{e^{\beta_i}-e^{-\beta_i}}{2} > 0 \tag{F3}$$

This defines the integral convergence zones:

$$if\ \beta_i > 0 \quad \rightarrow \quad \frac{e^{\beta_i}-e^{-\beta_i}}{2} > 0 \quad \rightarrow \quad \sin(\beta_r-\Theta) > 0 \rightarrow \quad \Theta < \beta_r < \pi + \Theta \tag{F4}$$

$$if\ \beta_i < 0 \quad \rightarrow \quad \frac{e^{\beta_i}-e^{-\beta_i}}{2} < 0 \quad \rightarrow \quad \sin(\beta_r-\Theta) < 0 \rightarrow \quad \Theta - \pi < \beta_r < \Theta \tag{F5}$$

This highlights the path that guarantees the fastest convergence:

$$\cos(\beta_r-\Theta)\frac{e^{\beta_i}+e^{-\beta_i}}{2} = 1 \tag{F6}$$

On this path the exponential is always decaying and non-oscillating as a function of β, and it presents a saddle point for $\beta = \Theta$, where its value is $e^{-jk_0 r}$. Let us define the integral:

$$I = \int_{SDP(\Theta)} e^{-jk_0 r cos(\beta-\Theta)} d\beta \tag{F7}$$

Let us perform a well suited change of variable:

$$-jk_0 r cos(\beta-\Theta) = -jk_0 r - k_0 r sin(\beta_r - \Theta)\frac{e^{\beta_i} - e^{-\beta_i}}{2} = -jk_0 r - k_0 r\tau^2 \tag{F8}$$

$$I = \int_{SDP(\Theta)} e^{-jk_0 r} e^{-k_0 r\tau^2} \frac{d\beta}{d\tau} d\tau \tag{F9}$$

To calculate the derivative it is convenient to express τ as:

$$-jk_0 r cos(\beta-\Theta) = -jk_0 r\left(1 - 2\sin^2\left(\frac{\beta-\Theta}{2}\right)\right) = -jk_0 r - k_0 r\tau^2 \tag{F10}$$

$$\tau^2 = -j2\sin^2\left(\frac{\beta-\Theta}{2}\right) \tag{F11}$$

$$\tau = \pm e^{-\frac{j\pi}{4}}\sqrt{2} sin\left(\frac{\beta-\Theta}{2}\right) \tag{F12}$$

$$\frac{d\beta}{d\tau} = \left(\frac{d\tau}{d\beta}\right)^{-1} = \left(\frac{d}{d\beta}\left(\pm e^{-\frac{j\pi}{4}}\sqrt{2} sin\left(\frac{\beta-\Theta}{2}\right)\right)\right)^{-1} = \frac{\pm e^{\frac{j\pi}{4}}\sqrt{2}}{cos\left(\frac{\beta-\Theta}{2}\right)} \tag{F13}$$

It is convenient to express everything as a function of τ:

$$cos\left(\frac{\beta-\Theta}{2}\right) = \sqrt{1 - \sin^2\left(\frac{\beta-\Theta}{2}\right)} = \sqrt{1 - \frac{j}{2}\tau^2} \tag{F14}$$

$$\frac{d\beta}{d\tau} = \frac{\pm e^{\frac{j\pi}{4}}\sqrt{2}}{\sqrt{1 - \frac{j}{2}\tau^2}} \tag{F15}$$

The anomaly introduced by the square root is solved looking at the fact that on the integration path $\tau = (-\infty, +\infty)$ the differential $d\tau$ is always positive; thus $\frac{d\beta}{d\tau}$ is a complex function with the same phase of $d\beta$. Let us analyze a point in the integration path, possibly easy to simplify the calculation, as $\beta = \Theta$:

$$\frac{d\beta}{d\tau}(\beta = \Theta) = \pm e^{\frac{j\pi}{4}}\sqrt{2} \tag{F16}$$

$$\arg\left(\frac{d\beta}{d\tau}(\beta = \Theta)\right) = \frac{\pi}{4} \quad Vel \quad \frac{5\pi}{4} \tag{F17}$$

However, since $d\beta = d\beta_r + jd\beta_i$ then $d\beta(\beta = \Theta) = d\beta_r + jd\beta_r$, and thus:

$$\arg\big(d\beta(\beta = \Theta)\big) = \frac{\pi}{4} \rightarrow \arg\left(\frac{d\beta}{d\tau}(\beta = \Theta)\right) = \frac{\pi}{4} \rightarrow \frac{d\beta}{d\tau}(\beta = \Theta) = +e^{\frac{j\pi}{4}}\sqrt{2} \tag{F18}$$

The integral eventually turns into:

$$I = \int_{SDP(\Theta)} e^{-jk_0 r\cos(\beta-\Theta)}d\beta = e^{\frac{j\pi}{4}}\sqrt{2}e^{-jk_0 r}\int_{-\infty}^{+\infty}\frac{e^{-kr\tau^2}}{\sqrt{1-\frac{j}{2}\tau^2}}d\tau \tag{F19}$$

Whose convergent behavior is ensured by $e^{-kr\tau^2}$, which is extremely fast decaying.
This deformation can also be applied in some of the radiation expressions where the integral is expressed as:

$$I = \int_{SDP(\Theta)} f(\beta)e^{-jk_0 r\cos(\beta-\Theta)}d\beta \tag{F20}$$

Provided that $f(\beta)$ is a slowly varying function. Attention must be payed whether the deformed path makes any singularity of $f(\beta)$ arise; however, in free space this is not the case. The final expression is then:

$$I = e^{\frac{j\pi}{4}}\sqrt{2}e^{-jk_0 r}\int_{-\infty}^{+\infty} f(\tau)\frac{e^{-kr\tau^2}}{\sqrt{1-\frac{j}{2}\tau^2}}d\tau \tag{F21}$$

Appendix G

This appendix shows how to perform a reaction integral on the antenna domain; this procedure allows to obtain the power available to the antenna retaining only the visible component of the Poynting vector. Let us calculate the power radiated by the ideal current distribution starting from the Poynting theorem in case of a lossless antenna:

$$\frac{1}{2}Re\left\{\iint_S (\vec{e}\times\vec{h}^*)\cdot d\vec{S}\right\} = -\frac{1}{2}Re\left\{\iiint_V (\vec{e}\cdot\vec{j}^* + \vec{h}^*\cdot\vec{m})dV\right\} \tag{G1}$$

$$P_{rad} = -\frac{1}{2}Re\left\{\iiint_V (\vec{e}\cdot\vec{j}^* + \vec{h}^*\cdot\vec{m})dV\right\} = P_{rad}^{el} + P_{rad}^{mag} \tag{G2}$$

$$P_{rad}^{el} = -Real\left(\frac{1}{2}\int_0^{2\pi}\int_0^{a}\vec{e}(\rho,\phi)\cdot\vec{j}_{PO}{}^*(\rho,\phi)\rho d\rho d\phi\right) \tag{G3}$$

$$P_{rad}^{mag} = -Real\left(\frac{1}{2}\int_0^{2\pi}\int_0^{a}\vec{h}^*(\rho,\phi)\cdot\vec{m}_{PO}(\rho,\phi)\rho d\rho d\phi\right) \tag{G4}$$

The fact that we're taking the real part means that we are accounting only for the real part of the power, and not for the reactive one. Now, explicitly expressing the electric and magnetic fields as in (4.43), (4.44) and substituting them in (G2) it is possible to observe that each one of $P_{rad}^{el}, P_{rad}^{mag}$ is given by two different contributes: one given by the electric source, and one given by the magnetic one. Let us analyze them separately, start from the reaction between the electric field and electric source:

$$\vec{e}(\rho,\phi) = \tilde{g}^{ej}(\rho,\phi,\rho',\phi') * \vec{j}_{id}(\rho',\phi') + \tilde{g}^{em}(\rho,\phi,\rho',\phi') * \vec{m}_{id}(\rho',\phi') \tag{G5}$$

$$P_{rad}^{el} = P_{rad}^{el,j} + P_{rad}^{el,m} \tag{G6}$$

$$P_{rad}^{el,j} = -\frac{1}{2}Re\int_0^{2\pi}\int_0^{a}\left(\tilde{g}^{ej}(\rho,\phi,\rho',\phi') * \vec{j}_{id}(\rho',\phi')\right)\cdot\vec{j}_{id}{}^*(\rho,\phi)\rho d\rho d\phi \tag{G7}$$

$$P_{rad}^{el,m} = -\frac{1}{2}Re\int_0^{2\pi}\int_0^{a}\left(\tilde{g}^{em}(\rho,\phi,\rho',\phi') * \vec{m}_{id}(\rho',\phi')\right)^*\cdot\vec{m}_{id}(\rho,\phi)\rho d\rho d\phi \tag{G8}$$

Power radiated by the electric current:

$$\left(\tilde{g}^{ej}(\rho,\phi,\rho',\phi') * \vec{J}_{id}(\rho',\phi')\right) = \int_0^{2\pi}\int_0^{a}\left(\tilde{g}^{ej}(\rho,\phi,\rho',\phi')\cdot\vec{J}_{id}(\rho',\phi')\right)\rho' d\rho' d\phi' \quad \text{(G9)}$$

$$P_{rad}^{el,j} = -\frac{1}{2}Re\int_0^{2\pi}\int_0^{a}\left(\int_0^{2\pi}\int_0^{a}\left(\vec{g}^{ej}(\rho,\rho',\phi,\phi')\cdot\vec{J}_{id}(\rho',\phi')\right)\rho' d\rho' d\phi'\right)\vec{J}_{id}{}^{*}(\rho,\phi)\rho d\rho d\phi \quad \text{(G10)}$$

Let us express the spatial Green's function through its spectral representation

$$\vec{g}^{ej}(\rho,\rho',\phi,\phi') = \frac{1}{4\pi^2}\iint_{-\infty}^{\infty} G_{xx}^{ej}(k_x,k_y)e^{-jk_x x}e^{jk_x x'}\, e^{-jk_y y}e^{jk_y y'}dk_x dk_y \quad \text{(G11)}$$

Following the same steps explained in Appendix C, imaging to have a plane wave coming from broadside and the electric field oriented along $\vec{J}_{id}(\rho',\phi') = j_{id}(\rho',\phi')\hat{x}$:

$$P_{rad}^{el,j} = -\frac{1}{2}Re\int_0^{2\pi}\int_0^{a}\left(\iint_{-\infty}^{\infty}\tilde{G}_{xx}^{ej}(k_x,k_y)e^{-jk_x x}e^{-jk_y y}\cdot\frac{1}{4\pi^2}\vec{\tilde{J}}_x(k_x,k_y)dk_x dk_y\right)\vec{J}_{id}{}^{*}(\rho,\phi)\rho d\rho d\phi \quad \text{(G12)}$$

$$P_{rad}^{el,j} = -\frac{1}{2}\frac{1}{4\pi^2}Re\iint_{-\infty}^{\infty}\tilde{G}_{xx}^{ej}(k_x,k_y)\vec{\tilde{J}}_{id,x}(k_x,k_y)\cdot\int_0^{2\pi}\int_0^{a}\vec{J}_{id}{}^{*}(\rho,\phi)e^{-jk_x x}e^{-jk_y y}\,\rho d\rho d\phi\, dk_x dk_y \quad \text{(G13)}$$

$$P_{rad}^{el,j} = -\frac{1}{2}\frac{1}{4\pi^2}Re\iint_{-\infty}^{\infty}\tilde{G}_{xx}^{ej}(k_x,k_y)\vec{\tilde{J}}_{id,x}(k_x,k_y)\vec{\tilde{J}}_{id,x}^{*}(-k_x,-k_y)dk_x dk_y \quad \text{(G14)}$$

Where:

$$\vec{\tilde{J}}_{id,x}(k_x,k_y)=\int_0^{2\pi}\int_0^{a}\left(\vec{J}_{id,x}(\rho',\phi')\right)e^{jk_x x'}e^{jk_y y'}\,\rho' d\rho' d\phi' \tag{G15}$$

$$\vec{\tilde{J}}^{*}_{id,x}(-k_x,-k_y)=\int_0^{2\pi}\int_0^{a}\vec{J}_{id,x}{}^{*}(\rho,\phi)\,e^{-jk_x x}\,e^{-jk_y y}\rho d\rho d\phi \tag{G16}$$

Let us now assume that the source is real (verified in our specific case), that is

$$j_x(\rho',\phi')=j_x^{*}(\rho',\phi') \tag{G17}$$

$$J^{*}_{id,x}(-k_x,-k_y)=J_{id,x}(-k_x,-k_y) \tag{G18}$$

$$P_{rad}^{el,j}=-\frac{1}{8\pi^2}Re\iint_{-\infty}^{\infty}\tilde{G}_{xx}^{ej}(k_x,k_y)\left|J_{id,x}(k_x,k_y)\right|^2 dk_x dk_y \tag{G19}$$

Let us analyze now the power associated to the magnetic source:

$$P_{rad}^{el,m}=-\frac{1}{2}Re\int_0^{2\pi}\int_0^{a}\left(\tilde{g}^{em}(\rho,\phi,\rho',\phi')*\vec{m}_{id}(\rho',\phi')\right)\cdot\vec{j}_{id}{}^{*}(\rho,\phi)\,\rho d\rho d\phi \tag{G20}$$

Expressing the Green's function by means of its spectral representation, and performing the same operations as before, and having the magnetic source oriented along $\vec{m}_{id}(\rho',\phi')=m_{id}(\rho',\phi')\hat{y}$, eventually one obtains:

$$P_{rad}^{el,m}=-\frac{1}{8\pi^2}Re\iint_{-\infty}^{\infty}\tilde{G}_{xy}^{em}(k_x,k_y)\vec{\tilde{M}}_{id,y}(k_x,k_y)\vec{\tilde{J}}_{id,x}(-k_x,-k_y)dk_x dk_y\;=0 \tag{G21}$$

Power radiated by the magnetic current:

$$P_{rad}^{mag,m}=-\frac{1}{2}Re\int_0^{2\pi}\int_0^{a}\vec{h}^{*}(\rho,\phi)\cdot\vec{m}_{id}(\rho,\phi)\rho d\rho d\phi \tag{G22}$$

$$P_{rad}^{mag,m} = -\frac{1}{2} Re \int_0^{2\pi} \int_0^{a} \left(\int_0^{2\pi} \int_0^{a} \left(\tilde{g}^{hm}(\rho, \rho', \phi, \phi') \cdot \vec{m}_{id}(\rho', \phi') \right) \rho' d\rho' d\phi' \right)^{*} \vec{m}_{id}(\rho, \phi) \rho d\rho d\phi \tag{G23}$$

$$\tilde{g}^{hm}(\rho, \rho', \phi, \phi') = \frac{1}{4\pi^2} \iint_{-\infty}^{\infty} \tilde{G}_{yy}^{hm}(k_x, k_y) e^{-jk_x x} e^{jk_x x'} \, e^{-jk_y y} e^{jk_y y'} dk_x dk_y \tag{G24}$$

$$P_{rad}^{mag,m} = -\frac{1}{8\pi^2} Re \int_0^{2\pi} \int_0^{a} \left(\iint_{-\infty}^{\infty} \tilde{G}_{yy}^{hm}(k_x, k_y) e^{-jk_x x} e^{jk_x x'} \cdot \int_0^{2\pi} \int_0^{a} \vec{m}_{id,y}(\rho', \phi') e^{-jk_y y} e^{jk_y y'} \rho' d\rho' d\phi' \, dk_x dk_y \right)^{*} \vec{m}_{id,y}(\rho, \phi) \rho d\rho d\phi \tag{G25}$$

$$P_{rad}^{mag,m} = -\frac{1}{8\pi^2} Re \left(\iint_{-\infty}^{\infty} \tilde{G}_{yy}^{hm}(k_x, k_y) \vec{\tilde{M}}_{id,y}(k_x, k_y) \cdot \int_0^{2\pi} \int_0^{a} \vec{m}_{id,y}(\rho, \phi) \, e^{-jk_x x} e^{jk_x x} \rho d\rho d\phi \, dk_x dk_y \right)^{*} \tag{G26}$$

$$P_{rad}^{mag,m} = -\frac{1}{8\pi^2} Re \left(\iint_{-\infty}^{\infty} \tilde{G}_{yy}^{hm}(k_x, k_y) \, \vec{\tilde{M}}_{id,y}(k_x, k_y) \, \vec{\tilde{M}}_{id,y}(-k_x, -k_y) dk_x dk_y \right)^{*} \tag{G27}$$

$$P_{rad}^{mag,m} = -\frac{1}{2} \frac{1}{4\pi^2} Re \iint_{-\infty}^{\infty} \left(G_{yy}^{hm}(k_x, k_y) \right)^{*} \left| M_{id,y}(k_x, k_y) \right|^2 dk_x dk_y \tag{G28}$$

Let us analyze now the power associated to the electric source:

$$P_{rad}^{mag,j} = -\frac{1}{2} Re \int_0^{2\pi} \int_0^{a} \vec{h}^{*}(\rho, \phi) \cdot \vec{j}_{id}(\rho, \phi) \rho d\rho d\phi \tag{G29}$$

$$P_{rad}^{mag,j} = -\frac{1}{2} Re \int_0^{2\pi} \int_0^{a} \left(\int_0^{2\pi} \int_0^{a} \left(\tilde{g}^{hj}(\rho, \rho', \phi, \phi') \cdot \vec{J}_{id}(\rho', \phi') \right) \rho' d\rho' d\phi' \right)^* \vec{m}_{id}(\rho, \phi) \rho d\rho d\phi \tag{G30}$$

$$\tilde{g}^{hj}(\rho, \rho', \phi, \phi') = \frac{1}{4\pi^2} \iint_{-\infty}^{\infty} \tilde{G}_{yx}^{hj}(k_x, k_y) e^{-jk_x x} e^{jk_x x'} e^{-jk_y y} e^{jk_y y'} dk_x dk_y \tag{G31}$$

$$P_{rad}^{mag,j} = -\frac{1}{2} \frac{1}{4\pi^2} Re \left[\int_0^{2\pi} \int_0^{a} \left(\iint_{-\infty}^{\infty} \tilde{G}_{yx}^{hj}(k_x, k_y) e^{-jk_x x} e^{-jk_y y} dk_x dk_y \cdot \int_0^{2\pi} \int_0^{a} \vec{J}_{id,x}(\rho', \phi') e^{jk_x x'} e^{jk_y y'} \rho' d\rho' d\phi' \right)^* \vec{m}_{id,y}(\rho, \phi) \rho d\rho d\phi \right] \tag{G32}$$

$$P_{rad}^{mag,j} = -\frac{1}{8\pi^2} Re \left(\iint_{-\infty}^{\infty} \tilde{G}_{yx}^{hj}(k_x, k_y) \, \vec{\tilde{J}}_{id,x}(k_x, k_y) \cdot \int_0^{2\pi} \int_0^{a} \vec{m}_{id,y}(\rho, \phi) \, e^{-jk_x x} e^{-jk_y y} \rho d\rho d\phi \, dk_x dk_y \right)^* \tag{G33}$$

$$P_{rad}^{mag,j} = 0 \tag{G34}$$

Now, the total radiated power is given by:

$$P_{rad} = P_{rad}^{el} + P_{rad}^{mag} = -\frac{1}{2} \frac{1}{4\pi^2} Re \iint_{-\infty}^{\infty} \left(G_{xx}^{ej}(k_x, k_y) \left| \vec{\tilde{J}}_{id,x}(k_x, k_y) \right|^2 + \left(G_{yy}^{hm}(k_x, k_y) \right)^* \left| \vec{\tilde{M}}_{id,y}(k_x, k_y) \right|^2 \right) dk_x dk_y \tag{G35}$$

Where the FT's of the sources are:

$$\begin{aligned}\vec{m}_{id}(\hat{k}_{in},\vec{r}) &= C_{amp}\left[\vec{E}_i^{pw}(\vec{r})\times\hat{k}_{in}\right]\\ \vec{J}_{id}(\hat{k}_{in},\vec{r}) &= C_{amp}\left[\hat{k}_{in}\times\vec{H}_i^{pw}(\vec{r})\right]\end{aligned}\quad \forall\vec{r}\in S_{in}(\hat{k}_{in}) \tag{G36}$$

$$\vec{E}_i^{pw}(\vec{r}) = C_{amp}E_x^{pw}(\vec{r})\hat{x};\quad \hat{k}_{in} = -\hat{z};\quad \vec{H}_i^{pw}(\vec{r}) = \frac{1}{\zeta}\hat{k}\times\vec{E}_i^{pw}(\vec{r}) \tag{G37}$$

$$\vec{m}_{id}(\hat{k}_{in},\vec{r}) = C_{amp}E_x^{pw}\hat{y} \tag{G38}$$

$$E_x(k_x,k_y) = \iint_{A_{ph}} E_{pw}e^{jk_xx}e^{jk_yy}dxdy \tag{G39}$$

$$\vec{J}_{id}(\hat{k}_{in},\vec{r}) = -C_{amp}\frac{E_x}{\zeta}\hat{x} = -C_{amp}\frac{E_x(k_x,k_y)}{\zeta}\hat{x} \tag{G40}$$

$$J_{id,x}(k_x,k_y) = -C_{amp}\frac{E_x(k_x,k_y)}{\zeta};\quad M_{id,y}(k_x,k_y) = C_{amp}E_x(k_x,k_y) \tag{G41}$$

And the total radiated power results:

$$\begin{aligned}P_{rad} &= P_{rad}^{el} + P_{rad}^{mag}\\ &= -\frac{C_{amp}^2}{8\pi^2}Re\left[\iint_{-\infty}^{\infty}\left(\tilde{G}_{xx}^{ej}(k_x,k_y)\left|\frac{E_x(k_x,k_y)}{\zeta}\right|^2\right.\right.\\ &\left.\left.+\left(\tilde{G}_{yy}^{hm}(k_x,k_y)\right)^*\left|E_x(k_x,k_y)\right|^2\right)dk_xdk_y\right]\\ &= -\frac{C_{amp}^2}{8\pi^2}Re\left[\iint_{-\infty}^{\infty}\left(\frac{\tilde{G}_{xx}^{ej}(k_x,k_y)}{\zeta}\right.\right.\\ &\left.\left.+\zeta\left(\tilde{G}_{yy}^{hm}(k_x,k_y)\right)^*\right)\frac{1}{\zeta}\left|E_x(k_x,k_y)\right|^2dk_xdk_y\right]\end{aligned} \tag{G42}$$

The Green's functions components are:

$$\tilde{G}_{xx}^{ej}(k_x,k_y) = -\frac{\zeta}{2k}\frac{k^2-k_x^2}{k_z} \tag{G43}$$

$$\tilde{G}_{yy}^{hm}(k_x,k_y) = -\frac{1}{2k\zeta}\frac{k^2-k_y^2}{k_z} \tag{G44}$$

$$\frac{\tilde{G}_{xx}^{ej}(k_x,k_y)}{\zeta} + \zeta\left(\tilde{G}_{yy}^{hm}(k_x,k_y)\right)^* = -\frac{1}{2k}\frac{2k^2-k_x^2-k_y^2}{k_z} \tag{G45}$$

Substituting in (G42):

$$P_{rad} = -\frac{C_{amp}^2}{8\pi^2} Re \iint_{-\infty}^{\infty} \left(-\frac{1}{2k}\frac{2k^2 - k_x^2 - k_y^2}{k_z}\right)\frac{1}{\zeta}\left|E_x(k_x, k_y)\right|^2 dk_x dk_y \tag{G46}$$

$$P_{rad} = \frac{C_{amp}^2}{4\pi^2} Re \iint_{-\infty}^{\infty} \left(\frac{1}{2k}\frac{2k^2 - k_\rho^2}{k_z}\right)\frac{1}{2\zeta}\left|E_x(k_x, k_y)\right|^2 dk_x dk_y \tag{G47}$$

Expressing the integrand function in cylindrical coordinates:

$$\begin{aligned} P_{rad} &= \frac{C_{amp}^2}{4\pi^2} Re \int_0^{2\pi}\int_0^{\infty} \left(\frac{1}{2k}\frac{2k^2 - k_\rho^2}{k_z}\right)\frac{1}{2\zeta}\left|E_x(k_\rho, \alpha)\right|^2 k_\rho dk_\rho d\alpha \\ &= \frac{C_{amp}^2}{2\pi} Re \int_0^{\infty} \left(\frac{1}{2k}\frac{2k^2 - k_\rho^2}{k_z}\right)\frac{1}{2\zeta}\left|E_x(k_\rho)\right|^2 k_\rho dk_\rho \end{aligned} \tag{G48}$$

Please, note that the Green's function was considered real, so that $G^{fc}(k_x, k_y)^* = G^{fc}(k_x, k_y)$; also the observation point and the source were taken at $z, z' = 0$; thus the exponential dependence in z of the Green's function was not taken into account, simplifying the calculations.

Thanks to the complex conjugate products we performed any exponential dependence of the integrand function is disappeared. Thus, considering the real part of the whole spectrum in dk_ρ simply means that only the visible part of the Poynting vector has to be accounted for, cropping the integral for $k_\rho = [0 \rightarrow k_0]$. The expression is then:

$$P_{rad} = \frac{C_{amp}^2}{2\pi} \int_0^{k_0} \left(\frac{1}{2k}\frac{2k^2 - k_\rho^2}{k_z}\right)\frac{1}{2\zeta}\left|E_x(k_\rho)\right|^2 k_\rho dk_\rho \tag{G49}$$

Finally, assumptions can be made depending on the antenna dimension; let us start working on (G46):

$$P_{rad} = \frac{C_{amp}^2}{4\pi^2} Re\left(\iint_{-\infty}^{\infty} \left(\frac{k}{k_z}\right) \frac{1}{2\zeta} \left|E_x(k_x, k_y)\right|^2 dk_x dk_y - \iint_{-\infty}^{\infty} \left(\frac{k_\rho^2}{2kk_z}\right) \frac{1}{2\zeta} \left|E_x(k_x, k_y)\right|^2 dk_x dk_y \right) \tag{G50}$$

$$k_\rho = ksin\beta, \quad k_z = kcos\beta; \quad dk_\rho = \frac{dk_\rho}{d\beta} d\beta = kcos\beta d\beta \tag{G51}$$

$$P_{rad} = \frac{C_{amp}^2}{4\pi^2} \left(2\pi \int_0^{\frac{\pi}{2}} \left(\frac{k}{kcos\beta}\right) \frac{1}{2\zeta} |E_x(ksin\beta)|^2 ksin\beta kcos\beta d\beta - 2\pi \int_0^{\frac{\pi}{2}} \left(\frac{k_\rho^2}{2kkcos\beta}\right) \frac{1}{2\zeta} \left|E_x((ksin\beta))\right|^2 ksin\beta kcos\beta d\beta \right) \tag{G52}$$

$$P_{rad} = \frac{1}{2\zeta} \frac{C_{amp}^2}{2\pi} k^2 \left(\int_0^{\frac{\pi}{2}} |E_x(ksin\beta)|^2 sin\beta d\beta - \frac{1}{2} \int_0^{\frac{\pi}{2}} \left|E_x((ksin\beta))\right|^2 sin^3\beta d\beta \right) \tag{G53}$$

Small antenna in terms of wavelength:

$$E_x(k_x, k_y) \approx E_x(k_x = 0, k_y = 0) = \iint_{A_{ph}} E_{pw} dxdy = E_{pw} A_{ph} \tag{G54}$$

$$P_{rad} = \frac{1}{2\zeta} \frac{C_{amp}^2}{2\pi} k^2 \left|E_{pw}\right|^2 A_{ph}^2 \left(\int_0^{\frac{\pi}{2}} sin\beta d\beta - \frac{1}{2} \int_0^{\frac{\pi}{2}} sin^3\beta d\beta \right) \tag{G55}$$

$$P_{rad} = \frac{1}{2\zeta} \frac{C_{amp}^2}{2\pi} k^2 \left|E_{pw}\right|^2 A_{ph}^2 \left(1 - \frac{1}{3}\right) \tag{G56}$$

$$P_{rad} = C_{amp}^2 \frac{1}{2\zeta} \frac{4\pi}{3\lambda^2} A_{ph}^2 \left|E_{pw}\right|^2 \tag{G57}$$

$$P_{rad} = C_{amp}^2 \frac{A_{ph}^2}{A_{huy}} \frac{1}{2\zeta} \left|E_{pw}\right|^2 \tag{G58}$$

Large antenna in terms of wavelength:

$$P_{rad} = \frac{C_{amp}^2}{4\pi^2} Re \iint_{-\infty}^{\infty} \left(\frac{1}{2k}\frac{2k^2 - k_\rho^2}{k_z}\right)\frac{1}{2\zeta}\left|E_x(k_x, k_y)\right|^2 dk_x dk_y \quad \text{(G59)}$$

$$\left|E_x(k_x, k_y)\right|^2 \approx 0 \; for k_\rho > k_{min} \quad \text{(G60)}$$

$$k_z = \sqrt{k^2 - k_\rho^2} = k^2\sqrt{1 - \frac{k_\rho^2}{k^2}} \approx k - \frac{k_\rho^2}{2k} \quad \text{(G61)}$$

$$\left(\frac{1}{2k}\frac{2k^2 - k_\rho^2}{k_z}\right) \rightarrow \left(\frac{1}{2k}\frac{2k^2 - k_\rho^2}{k - \frac{k_\rho^2}{2k}}\right) = 1 \quad \text{(G62)}$$

$$P_{rad} = \frac{C_{amp}^2}{4\pi^2} Re \iint_{\substack{around \\ origin}} \frac{1}{2\zeta}\left|E_x(k_x, k_y)\right|^2 dk_x dk_y$$

$$= C_{amp}^2 \iint \frac{1}{2\zeta}|\vec{e}_x(x, y)|^2 dx dy \quad \text{(G63)}$$

Finally, from (G58) it is possible to derive the value of the amplifying factor used for the definition of the ideal currents. The expression is valid for antennae that are electrically really small, so it is necessary to substitute A_{huy}, that corresponds to the effective area of an Huygens' source, with the general A_{eff}. The expression turns into:

$$P_{rad} = C_{amp}^2 \frac{A_{ph}^2}{A_{eff}}\frac{1}{2\zeta}\left|E_{pw}\right|^2 \quad \text{(G64)}$$

The power received from the ideal antenna can be related to its effective area as:

$$P_{rec}^{id} = \frac{1}{2\zeta}|E^{pw}|^2 A_{eff} \quad \text{(G65)}$$

Equating (G64) and (G65), which means that the field scattered by a uniform distribution of Huygens' source has to be equal to the power received by the ideal antenna, justifies the value adopted for the ideal current procedure:

$$P_{rad} = C_{amp}^2 \frac{A_{ph}^2}{A_{eff}}\frac{1}{2\zeta}\left|E_{pw}\right|^2 = \frac{1}{2\zeta}|E^{pw}|^2 A_{eff} = P_{rec}^{id} \quad \text{(G66)}$$

$$C_{amp} = \frac{A_{eff}}{A_{ph}} \tag{G67}$$

Appendix H

This appendix shows how to extend the ideal current procedure to more generalized cases where the incident field can be described as a superposition of multiple plane waves. This is one of the most important aspect of the technique, since it can easily address the absorbed power when multiple plane waves are incoming with different directions. The procedure is similar to the previous one, since we can apply the 'superposition of the effects' principle being the whole system linear. Each wave is travelling towards the center of the reference system, where the antenna lies, with a direction that is defined by β_{in}, α_{in}. Through the equivalence theorem a set of currents (ideal currents) is defined, for every single wave, in a circular surface of radius a lying on the plane orthogonal to the wave propagating direction $\hat{k}_{in}$; then the currents will be made radiate to calculate the ideal scattered field, equal and opposite to the portion of the total incoming field the antenna can actually interacts with.
Let us start defining the total incident field (under the assumption of coherent waves), considering for now just 2 waves:

$$\vec{e}(\vec{r}) = \vec{E}_1(\beta_1, \alpha_1)e^{-j\vec{k}_1\vec{r}} + \vec{E}_2(\beta_1, \alpha_1)e^{-j\vec{k}_2\vec{r}} \tag{H1}$$

Explicitly

$$\begin{aligned}\vec{k}_i\vec{r} = -kr(&sin\beta_{in}cos\alpha_{in}\hat{x} + sin\beta_{in}sin\alpha_{in}\hat{y} + cos\beta_{in}\hat{z})(sin\Theta cos\Phi\hat{x} \\ &+ sin\Theta sin\Phi\hat{y} + cos\Theta\hat{z}) \\ &= -kr(sin\beta_{in}cos\alpha_{in}sin\Theta cos\Phi + sin\beta_{in}sin\alpha_{in}sin\Theta sin\Phi \\ &+ cos\beta_{in}cos\Theta)) \\ &= -kr(sin\beta_{in}cos\alpha_{in}\cos(\alpha_{in} - \Phi) + cos\beta_{in}cos\Theta)\end{aligned} \tag{H2}$$

So that

$$\begin{aligned}\vec{e}(\vec{r}) = \vec{E}_1(\beta_1, \alpha_1)&e^{-kr(sin\beta_1 cos\alpha_1\cos(\alpha_1 - \Phi) + cos\beta_2 cos\Theta)} \\ &+ \vec{E}_2(\beta_2, \alpha_2)e^{-kr(sin\beta_2 cos\alpha_2\cos(\alpha_2 - \Phi) + cos\beta_2 cos\Theta)}\end{aligned} \tag{H3}$$

Extending this to an integral on the whole solid angle:

$$\vec{e}(\vec{r}) = \int_0^{2\pi}\int_0^{pi} \vec{E}_{in}(\beta_{in},\alpha_{in}) e^{-kr(sin\beta_{in}cos\alpha_{in}\cos(\alpha_{in}-\Phi)+cos\beta_{in}cos\Theta)}\, sin\beta_{in} d\beta_{in} d\alpha_{in} \quad \text{(H4)}$$

Each one of these plane waves will induce a well-defined set of electric and magnetic currents on the antenna domain, which is orthogonal to the incident direction.
The electric current are defined as (keep in mind that $\hat{n} = \hat{z}' = -\hat{r}_{in}$):

$$\vec{j}(\vec{r}) = -C_{amp}\hat{r}_{in} \times \vec{h}_{in}(\vec{r}) \quad \text{(H5)}$$

$$\vec{m}(\vec{r}) = C_{amp}\hat{r}_{in} \times \vec{e}_{in}(\vec{r}) \quad \text{(H6)}$$

$$C_{amp} = \frac{A_{eff}}{A_{phys}} \quad \text{(H7)}$$

$$\vec{J}_{eq}(\vec{r}) = -\vec{j}(\vec{r})\chi(\hat{r}_{in}, a) \quad \text{(H8)}$$

$$\vec{m}_{eq}(\vec{r}) = -\vec{m}(\vec{r})\chi(\hat{r}_{in}, a) \quad \text{(H9)}$$

It is convenient to define an alternative reference system for each plane wave such that the incidence direction results always orthogonal to the antenna domain itself. This system is defined by $\hat{z}' = -\hat{r}_{in}$, and the antenna planar domain will be called $S_{in} = \pi a^2$.
This way the ideal currents turn into:

$$\vec{J}_{eq}(\hat{r}_{in}, \vec{r}) = C_{amp}\hat{z}' \times \vec{h}(\vec{r}) = \frac{C_{amp}}{\zeta}\hat{z}' \times \hat{k}_{in} \times \vec{e}(\vec{r}) \quad \text{(H10)}$$

$$\vec{m}_{eq}(\hat{r}_{in}, \vec{r}) = C_{amp}\vec{e}(\vec{r}) \times \hat{z}' \quad \text{(H11)}$$

Now, the field radiated in the far field region by this set of currents, is in general defined as an outward propagating wave:

$$\vec{e}^{id}_{scat}(\vec{r}_\infty, \vec{r}_{in}) = \iint_{S_{in}} \left[\tilde{\tilde{g}}^{ej}_{fs}(\vec{r}_\infty, \vec{r}')\vec{J}_{id}(\hat{r}_{in}, \vec{r}) + \tilde{\tilde{g}}^{em}_{fs}(\vec{r}_\infty, \vec{r}')\vec{m}_{id}(\hat{r}_{in}, \vec{r})\right] d\vec{r}' \quad \text{(H12)}$$

Note that S_{in} can in general change for every plane wave used to represent the incident field. It is clear from Appendix A, that in the far field region asymptotical consideration on the

spatial Green's function can lead to a very simple and useful expression for the radiated field, which is:

$$\vec{e}_{scat}^{id}(\vec{r}_\infty, \vec{r}_{in}) = V_{id}^{outw}\left(a, \vec{r}, \vec{k}_{in}\right)\frac{e^{-jkr_\infty}}{r_\infty} \tag{H13}$$

Where using the V just indicates the fact that it is a Voltage quantity, which is:

$$V_{id}^{outw}\left(a, \vec{r}, \vec{k}_{in}\right) = -\frac{jk}{4\pi}\left\{\zeta\left(\tilde{\bar{I}} - \hat{k}\hat{k}\right)\vec{J}(\hat{r}_{in}, \vec{k}) - \hat{k} \times \vec{M}(\vec{r}_{in}, \vec{k})\right\} \tag{H14}$$

The Fourier transform of the equivalent currents has to be evaluated over the squinted domain of the antenna:

$$\vec{J}(\hat{r}_{in}, \vec{k}) = \iint_{S_{in}} \vec{j}(\hat{r}_{in}, \vec{r})e^{j\vec{k}\vec{r}}d\vec{r} \tag{H15}$$

$$\vec{M}(\hat{r}_{in}, \vec{k}) = \iint_{S_{in}} \vec{m}(\hat{r}_{in}, \vec{r})e^{j\vec{k}\vec{r}}d\vec{r} \tag{H16}$$

Note that in the region the Fourier transform is performed the incoming plane wave does not present any variation ($\vec{r}_{in} = 0 \in S_{in}$). This renders $\vec{j}(\hat{r}_{in}, \vec{r}), \vec{m}(\hat{r}_{in}, \vec{r})$ constant (see previous definition), thus:

$$\vec{J}(\vec{r}_{in} = 0, \vec{k}, \vec{k}_{in}) = \vec{j}(\vec{r}_{in} = 0, \vec{r})Airy_{in}(\vec{k}_{in}, \vec{k}) \tag{H17}$$

$$\vec{M}(\vec{r}_{in} = 0, \vec{k}, \vec{k}_{in}) = \vec{m}(\vec{r}_{in} = 0, \vec{r})Airy_{in}(\vec{k}_{in}, \vec{k}) \tag{H18}$$

$$Airy_{in}(\vec{k}_{in}, \vec{k}) = 2\pi a^2\frac{J_1(k'_\rho a)}{k'_\rho a} \tag{H19}$$

Now, we express $\vec{k}$ in terms of the local coordinates, defining as (β', α') the angles that describe the observation point highlighted by $\vec{k}$. Do not confuse this parametrization with the one performed in the previous chapters and in this one. These sets of $([\beta', \alpha'], [\rho', \Theta', \Phi'])$ change for every single plane wave, and so for each single squinted domain, we are evaluating. In particular, $[\beta', \alpha']$ represent the observation points starting from the squinted

reference system, and they're different from $[\beta_{in}, \alpha_{in}]$. The difference with respect to the broadside incidence case is that now we have to express k'_ρ in terms of $\hat{r}_{in}, \vec{k}$. Also, in order to calculate the Airy pattern already as a function of the standard reference system, thus avoiding the complex Matlab implementation of the rotation of the squinted one, we can note that:

$$\hat{k}\hat{z}' = \hat{k}(-\hat{r}_{in}) = -cos\gamma \tag{H20}$$

$$\gamma = arccos(-\hat{k}\hat{r}_{in}) = arccos(\hat{k}\hat{k}_{in}) \tag{H21}$$

So that now:

$$k_\rho = ksin\gamma \tag{H23}$$

Note that $k_\rho \neq k'_\rho$ since the first one is expressed with respect to the standard reference system, while the second one is expressed with respect to the squinted reference system. Let us now improve the V_{obs}^{outw} expression:

$$\begin{aligned} V_{id}^{outw}(a, \hat{r}_{in}, \vec{k}) &= -\frac{jk}{4\pi}\left\{\zeta\left(\tilde{\tilde{I}} - \hat{k}\hat{k}\right)\vec{J}(\hat{r}_{in}, \vec{k}) - \hat{k} \times \vec{M}(\vec{r}_{in}, \vec{k})\right\} \\ &= -\frac{jk}{4\pi}\left\{\zeta\left(\tilde{\tilde{I}} - \hat{k}\hat{k}\right)\vec{J}_{eq}(\hat{r}_{in}, \vec{r}) - \hat{k}\right. \\ &\left. \times \vec{m}_{eq}(\hat{r}_{in}, \vec{r})\right\} Airy_{in}(\vec{k}_{in}, \vec{k}) \end{aligned} \tag{H24}$$

$$\begin{aligned} \vec{J}_{eq}(\vec{r}_{in} = 0, \vec{r}) &= \frac{C_{amp}}{\zeta}\hat{z}' \times \left[\hat{k}_{in} \times \vec{E}_{in}(\beta_{in}, \alpha_{in})\right] \\ &= \frac{C_{amp}}{\zeta}\hat{z}' \times \left[-\hat{r}_{in} \times \vec{E}_{in}(\beta_{in}, \alpha_{in})\right] \\ &= \frac{C_{amp}}{\zeta}\hat{z}' \times \left[\hat{z}' \times \vec{E}_{in}(\beta_{in}, \alpha_{in})\right] \\ &= \frac{C_{amp}}{\zeta}\hat{r}_{in} \times \left[\hat{r}_{in} \times \vec{E}_{in}(\beta_{in}, \alpha_{in})\right] \end{aligned} \tag{H25}$$

Expressing the field in local (either spherical or Cartesian, according to the vector product) coordinates, and applying the vector identity $\boldsymbol{A} \times (\boldsymbol{B} \times \boldsymbol{C}) = (\boldsymbol{AC})\boldsymbol{B} - (\boldsymbol{AB})\boldsymbol{C}$ we obtain:

$$\vec{j}_{eq}(\vec{r}_{in}=0,\vec{r})=-\frac{C_{amp}}{\zeta}\vec{E}_{in}(\beta_{in},\alpha_{in}) \tag{H26}$$

In the same way:

$$\vec{m}_{eq}(\vec{r}_{in}=0,\vec{r})=-C_{amp}\vec{E}_{in}(\beta_{in},\alpha_{in})\times\hat{z}'=C_{amp}\vec{E}_{in}(\beta_{in},\alpha_{in})\times\hat{r}_{in} \tag{H27}$$

Thus:

$$\begin{aligned} V_{id}^{outw}(a,\hat{r}_{in},\vec{k}) &= -\frac{jk}{4\pi}\left\{\zeta\left(\tilde{\tilde{I}}-\hat{k}\hat{k}\right)\vec{j}_{eq}(\hat{r}_{in},\vec{r})-\hat{k}\right. \\ &\left.\times\vec{m}_{eq}(\hat{r}_{in},\vec{r})\right\}Airy_{in}(\vec{k}_{in},\vec{k}) \end{aligned} \tag{H28}$$

$$\begin{aligned} V_{id}^{outw}(\hat{r}_{in},\vec{k}) &= C_{amp}\frac{jk}{4\pi}\left\{\left(\tilde{\tilde{I}}-\hat{k}\hat{k}\right)\vec{E}_{in}(\beta_{in},\alpha_{in})-\hat{k}\right. \\ &\left.\times\left(\vec{E}_{in}(\beta_{in},\alpha_{in})\times\hat{r}_{in}\right)\right\}Airy_{in}(\vec{k}_{in},\vec{k}) \end{aligned} \tag{H29}$$

It is simple to demonstrate that:

$$\left(\tilde{\tilde{I}}-\hat{k}\hat{k}\right)\vec{E}_{in}(\beta_{in},\alpha_{in})=\hat{k}\times\left(\vec{E}_{in}(\beta_{in},\alpha_{in})\times\hat{k}\right) \tag{H30}$$

$$\begin{aligned} V_{id}^{outw}(\hat{r}_{in},\vec{k}) &= C_{amp}\frac{jk}{4\pi}\left\{\hat{k}\times\left(\vec{E}_{in}(\beta_{in},\alpha_{in})\times\hat{k}\right)-\hat{k}\right. \\ &\left.\times\left(\vec{E}_{in}(\beta_{in},\alpha_{in})\times\hat{r}_{in}\right)\right\}Airy_{in}(\vec{k}_{in},\vec{k}) \end{aligned} \tag{H31}$$

$$V_{id}^{outw}(a,\hat{r}_{in},\vec{k})=C_{amp}\frac{jk}{4\pi}\hat{k}\times\left[\vec{E}_{in}(\beta_{in},\alpha_{in})\times\left(\hat{k}-\hat{r}_{in}\right)\right]Airy_{in}(\vec{k}_{in},\vec{k}) \tag{H32}$$

Defining now the Huygens' pattern:

$$\vec{H}_{in}(\hat{r}_{in},\vec{k})=\frac{jk}{4\pi}\hat{k}\times\left[\vec{E}_{in}(\beta_{in},\alpha_{in})\times\left(\hat{k}-\hat{r}_{in}\right)\right] \tag{H33}$$

We obtain the final definition for the outward observable field amplitude:

$$V_{id}^{outw}(a, \hat{r}_{in}, \vec{k}) = C_{amp} Airy_{in}(\vec{k}_{in}, \vec{k}) \vec{H}_{in}(\hat{r}_{in}, \vec{k}) \tag{H34}$$

The total observable field in the far field region is the superposition of every single outward propagating wave induced by the incoming plane waves; so for every direction $\vec{k}$:

$$\vec{e}_{obs}^{outw}(r, \vec{k}) = \int_0^{2\pi} \int_0^{\pi} V_{id}^{outw}(a, \hat{r}_{in}, \vec{k}) sin\beta_{in} d\beta_{in} d\alpha_{in} \frac{e^{-jkr_\infty}}{r_\infty} \tag{H35}$$

Table of Figures

Table of Figures